HIGHWAY RESEARCH RECORD

Number 116

Culverts and Storm Drains
4 Reports

Presented at the
44th ANNUAL MEETING
January 11-15, 1965

SUBJECT CLASSIFICATION
23 Highway Drainage
34 General Materials

HIGHWAY RESEARCH BOARD
of the
Division of Engineering and Industrial Research
National Academy of Sciences—National Research Council
Washington, D. C.
1966

Department of Design

W. B. Drake, Chairman
Assistant State Highway Engineer
Kentucky Department of Highways, Lexington

HIGHWAY RESEARCH BOARD STAFF

F. N. Wray, Engineer of Design
R. C. Edgerton, Assistant Engineer of Design

GENERAL DESIGN DIVISION

W. L. Warren, Chairman
Engineer of Design
California Division of Highways, Sacramento

COMMITTEE ON SURFACE DRAINAGE OF HIGHWAYS
(As of December 31, 1964)

Carl F. Izzard, Chairman
Chief, Hydraulic Research Division, Office of Research and Development
U. S. Bureau of Public Roads, Washington, D. C.

C. R. Edgerton, Hydrographic Engineer, North Carolina State Highway Commission, Raleigh,
Kenneth S. Eff, Chief, Hydraulic Section, Civil Engineering Branch, Office, Chief of Engineers, Department of the Army, Washington, D. C.
Kenneth M. Fenwick, Assistant Engineer of Design, California Division of Highways, Sacramento
John G. Hendrickson, Jr., Director of Engineering Research, American Concrete Pipe Association, Chicago, Illinois
S. W. Jens, Consulting Engineer, St. Louis, Missouri
Frank L. Johnson, Hydraulic Engineer, Region 6, U. S. Bureau of Public Roads, Fort Worth, Texas
A. H. Koepf, Manager, Field Engineering—Highway Products, Kaiser Aluminum and Chemical Sales, Inc., Oakland, California
Frank Leonard, Design Engineer, Idaho Department of Highways, Boise
Robert A. Norton, Engineer of Hydraulics and Bridge Maintenance, Connecticut State Highway Department, Wethersfield
Ralph M. Peterson, Chief, Branch of Management Studies and Systems Planning, U. S. Forest Service, Washington, D. C
A. L. Pond, Jr., Hydraulic Engineer, Virginia Department of Highways, Richmond
W. O. Ree, Agricultural Research Service, Stillwater, Oklahoma
James K. Searcy, Hydraulic Engineer, Hydraulic Branch, Bridge Division, U. S. Bureau of Public Roads, Washington, D. C.
E. P. Sellner, Manager, Water Resources Bureau, Portland Cement Association, Chicago, Illinois
Roy E. Smith, Managing Director, National Corrugated Steel Pipe Association, Chicago, Illinois
F. W. Thorstenson, Assistant Road Design Engineer, Minnesota Department of Highways, St. Paul
Mainard Wacker, Chief Highway Designer (Hydraulics), Hydraulics Section, Advance Plans Division, Wyoming Highway Department, Cheyenne

Department of Materials and Construction

R. L. Peyton, Chairman
Assistant State Highway Engineer
State Highway Commission of Kansas, Topeka

HIGHWAY RESEARCH BOARD STAFF

R. E. Bollen, Engineer of Materials and Construction
W. G. Gunderman, Assistant Engineer of Materials and Construction

GENERAL MATERIALS DIVISION

John L. Beaton, Chairman
Materials and Research Engineer
Materials and Research Department
California Division of Highways, Sacramento

COMMITTEE ON CULVERTS AND CULVERT PIPE
(As of December 31, 1964)

Reynold K. Watkins, Chairman
Professor and Head
Mechanical Engineering Department
Utah State University, Logan

T. F. DeCapiteau, Drainage Products Engineer, Manufacturing Division, Republic Steel Corporation, Youngstown, Ohio
W. B. Drake, Assistant State Highway Engineer, Kentucky Department of Highways, Lexington
Kenneth S. Eff, Chief, Hydraulic Section, Civil Engineering Branch, Office, Chief of Engineers, Department of the Army, Washington, D. C.
C. J. Francis, Director, Engineering Division, Soil Conservation Service, U. S. Department of Agriculture, Washington, D. C.
R. T. Healy, Executive Secretary, Connecticut Concrete Pipe Association, Inc., South Windham
John G. Hendrickson, Jr., Director of Engineering Research, American Concrete Pipe Association, Chicago, Illinois
A. H. Koepf, Manager, Field Engineering—Highway Products, Kaiser Aluminum and Chemical Sales, Inc., Oakland, California
J. Alan Myers, Manager, Highway Construction Marketing, United States Steel Corporation, Pittsburgh, Pennsylvania
Eric Nordlin, Supervising Highway Engineer, Materials and Research Department, California Division of Highways, Sacramento
C. E. Proudley, Materials Consultant, Raleigh, North Carolina
E. P. Sellner, Manager, Water Resources Bureau, Portland Cement Association, Chicago, Illinois
Rockwell Smith, Research Engineer—Roadway, Association of American Railroads, Chicago, Illinois
M. G. Spangler, Civil Engineering Department, Iowa State University, Ames
Harold A. Swanson, Manager, Civil Engineering, International Pipe and Ceramics Corporation, East Orange, New Jersey
H. L. White, Chief Engineer, Armco Metal Products Division, Middletown, Ohio

Contents

Foreword

The four papers in this Highway Research Record cover subjects related to highway culverts. Engineers involved in drainage design and in the structural design, selection, and installation of culverts should find useful information in these papers.

The paper by Leach and Kittle demonstrates the economies that can be effected by the use of ponded storage in a storm drainage system.

John L. Grace, Jr., offers recommendations of friction factors for the commonly used corrugations of annular corrugated pipe including the 2- × 6-in. corrugations of structural plate pipe and the 1- × 3-in. corrugations used in some larger riveted sizes. The recommendations are based on model test results extended by analytical methods.

In the third paper, Robert C. Deen describes a simplified method for predicting the required camber in highway culvert installations. Fairly close agreement between predicted and observed settlements is reported.

Jurgen Demmin reports on a series of load tests on a large structural plate pipe arch. The author interprets the results as a substantial verification of the Ring Compression Method of conduit design.

Hydraulic Design of the Fort Campbell Storm Drainage System

LAURENCE G. LEACH, Chief, Hydraulic Section, and
BENJAMIN L. KITTLE, Hydraulic Engineer, U. S. Army Engineer Division, South Atlantic, Atlanta, Georgia

The Corps of Engineers, U. S. Army, awarded a contract in June 1963 for construction of a storm drainage system to serve a major portion of the cantonment area of Fort Campbell, Kentucky. A total of 31,000 lineal feet of pipe, ranging in size from 12- to 84-in. diameter, was required to drain 2,000 acres of land in the main post area. The cost of this drainage system was approximately $2,000,000.

While the project is unusual, based on pipe quantities and construction costs involved, it is also somewhat unique in that the original estimated cost of $5,500,000 was drastically lowered by the use of temporary ponding to reduce peak discharges in the main trunk sewer. The hydraulic design of the system permits a limited amount of ponding (at the majority of storm drainage inlets) as a result of a 10-yr frequency design storm. This relatively small amount of temporary storage capacity reduced required pipe sizes considerably, but the largest percentage of cost savings was effected by enlarging two major ponding areas in the upstream portion of the project. These two excavated temporary retention basins permitted large reductions in pipe diameters for nearly three miles of trunk sewer.

•FORT CAMPBELL is located on the Kentucky-Tennessee state line about 50 miles northwest of Nashville, Tennessee. The region is characterised by gently rolling terrain having a thick clay overburden underlain by a cavernous limestone formation. The development of solution channels in the underlying limestone, with accompanying erosion of the overburden due to circulating groundwater, has resulted in the formation of a typical Karst topography with saucer-shaped depressions on the ground surface and, in some instances, open sinkholes. The cantonment area comprises about 6,000 acres located in the eastern part of the base adjacent to US 41A. Figure 1 is a map of the main post area of Fort Campbell.

The central and western portions of the cantonment area occupy higher ground, containing fewer sinkholes, than the eastern section. The central portion of the built-up area was constructed on a low ridge which runs generally north and south. Because this higher ground is relatively well drained, with few sinkholes, it was developed before the lower land to the east. The later development of Fort Campbell into a permanent army facility, however, necessitated the expansion of the cantonment to the east. The eastern section had very few drainage lines and contained numerous large sinks. The natural drainage provided by the sinkholes was not satisfactory. Following a heavy rainstorm, water would stand for days or weeks in some sinks, would be readily drained from others, and would remain ponded in others almost indefinitely. Dating from World War II, attempts were made to drain the sinks by constructing vertical drainage wells through the clay overburden into the underlying weathered limestone. These wells were only moderately successful, since only a few would handle the runoff from a storm of normal intensity without ponding, and all presented a continuing maintenance problem to keep them functioning. When postwar expansion of the main

Paper sponsored by Committee on Surface Drainage of Highways.

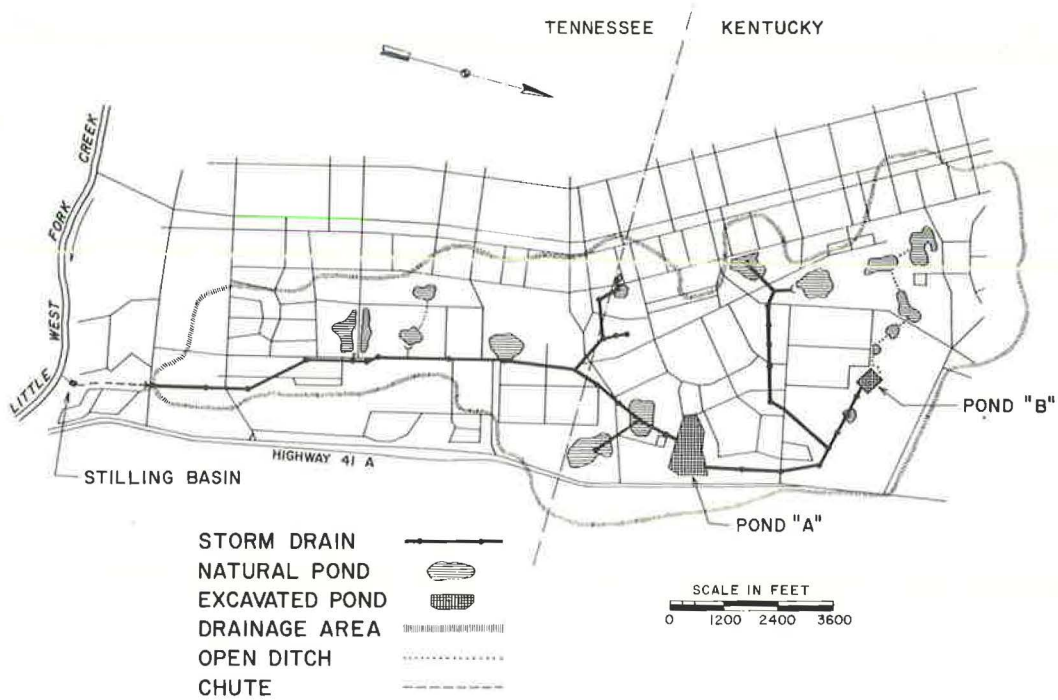

Figure 1. Layout of storm drainage system.

post began to infringe upon the sink areas, it became apparent that a positive drainage system would have to be provided for Fort Campbell.

COMPARISON OF DRAINAGE SCHEMES CONSIDERED

Early in 1955 a drainage study was prepared for the Nashville District (of the Corps of Engineers) by a private consulting engineer firm. This study proposed a system of underground conduits to remove the storm runoff as fast as it was collected. The system involved reinforced concrete box conduits having cross-sectional dimensions as large as 17 by 14 feet and as much as 45 feet below the ground surface at the downstream end of the project. The enormity of such a project is reflected in its estimated cost of $5,500,000.

The Nashville District, in an attempt to devise a satisfactory drainage system that was economically feasible, prepared and submitted a drainage report in 1957 to the Chief of Engineers. Five possible plans were considered in this study. Plan A was essentially a refinement of the original consulting engineer report and provided for immediate removal of storm runoff. The estimated cost of this plan was $4,600,000. Plan B permitted a minor amount of ponding in the existing sink areas which reduced the cost estimate considerably. Plans C and D were alternates to Plans A and B and involved disposing of a major portion of the runoff into an existing large open sinkhole. While both of these plans were probably feasible, the uncertainties involved with underground disposal of storm runoff ruled out their use. Plan E was essentially the same as Plan B except for the use of certain open ditches instead of pipe to reduce costs. The estimated cost of this plan was $3,370,000.

In addition to these five plans, consideration was also given to the use of a storm water pumping station at a strategic location to reduce pipe sizes and to the construction of an unlined drainage tunnel driven through rock in the lower portion of the system. Neither of these schemes proved to be economically feasible.

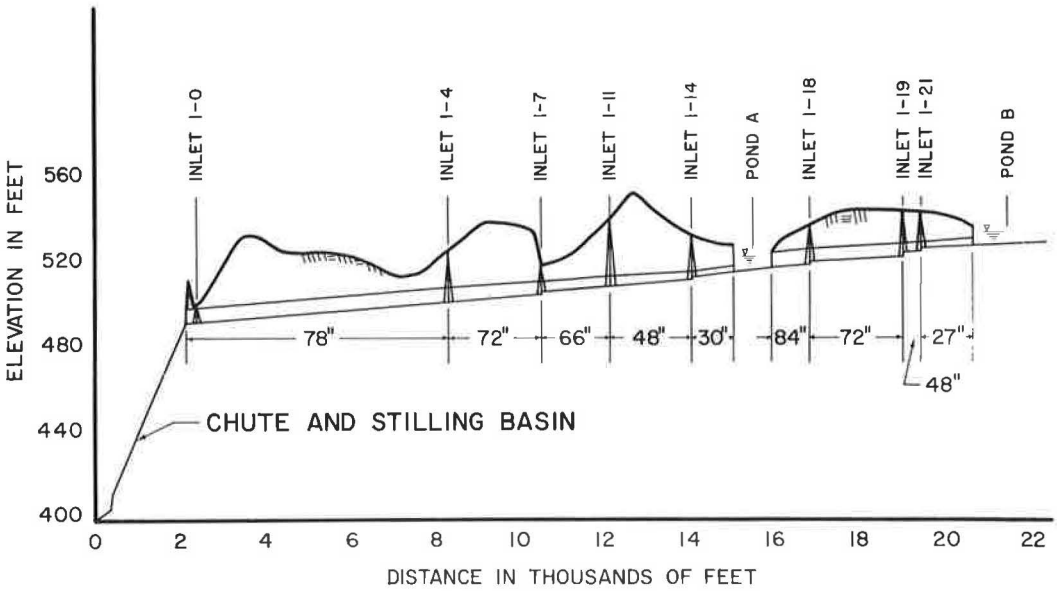

Figure 2. Profile of main trunk sewer.

Based on a preliminary design prepared by the South Atlantic Division, the Nashville District submitted a revised drainage report in 1960 which provided additional storage capacity by enlarging two key ponding areas by excavation. This was essentially Plan E with the addition of two major ponding areas. The estimated construction cost of this plan was $2,000,000. This was the scheme that was later adopted for construction.

DESCRIPTION OF ADOPTED SCHEME

Superimposed on the street layout, shown in Figure 1, is the storm drainage system including drainage area limits, open ditches, ponding areas, pipe, discharge chute, and stilling basin. The cross hatching indicates the approximate limits of ponding for a 10-yr frequency storm. All ponding occurs in natural sink areas except for excavated Ponds A and B. Beginning at the upstream end of the system, the pipe sizes increase progressively until an 84-in. diameter pipe is required to handle the flow entering Pond A. Sufficient storage capacity is provided in Pond A to limit the outlet pipe size to 30-in. diameter. Progressing downstream, pipe diameters increase again until the required outfall pipe diameter is 78 inches. The flow discharging from the outlet pipe enters a 6.5-ft wide concrete chute, approximately 1,800 feet long, which terminates in a stilling basin at the elevation of the creek. Figure 2 is a profile of the main trunk sewer.

OUTLINE OF THE HYDRAULIC DESIGN

The design rainfall used for the Fort Campbell drainage project has an expected frequency of recurrence of once in ten years and a maximum hourly intensity of 1.95 inches. Rainfall intensity-duration data for the Fort Campbell area were obtained from U. S. Weather Bureau publications. Accumulative volumes of rainfall were computed by use of the developed intensity-duration curve. Rainfall excess values were then obtained by applying estimated infiltration rates. The relationships between duration and rainfall intensity, volume, loss, and excess are shown in Figure 3.

Drainage areas to be served by the system were delineated on topographical maps and the times of concentration computed based on length of overland flow, slope of terrain, and type of vegetive cover. Peak inflow rates were determined by use of the Rational Formula using a runoff coefficient of 0.90 for impervious areas and 0.3 for

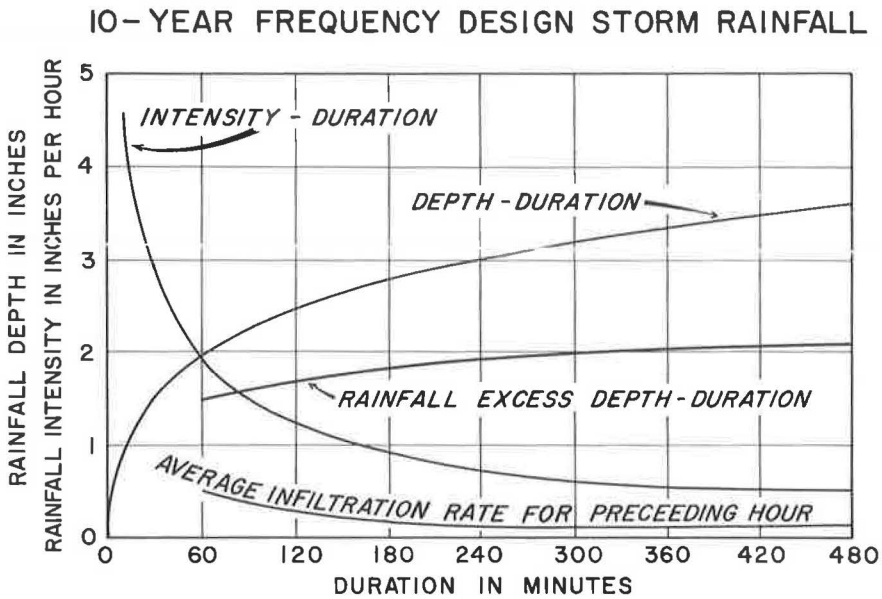

Figure 3. Rainfall relationships for design storm.

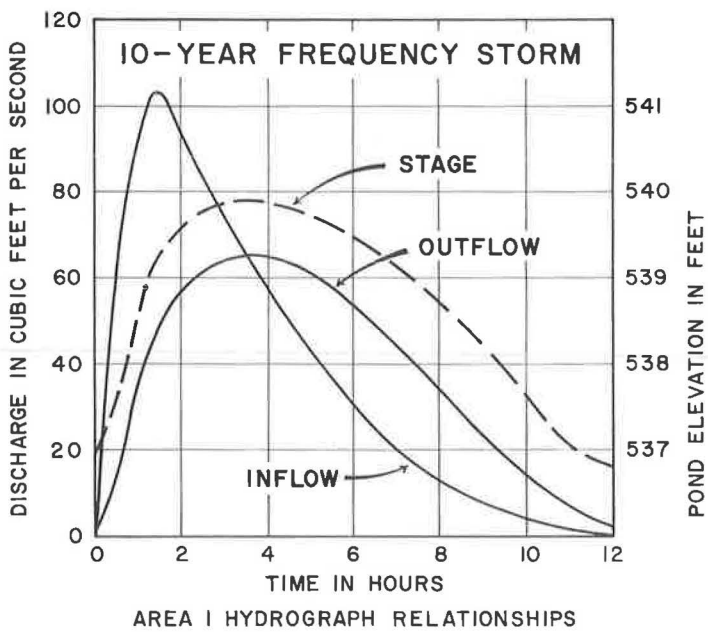

Figure 4. Inflow outflow hydrograph for area 1.

pervious areas. Inflow hydrographs were developed for each drainage area by using the peak rate of runoff and the time of concentration to define the crest and the rising portion of the hydrograph and then drawing the recession side in such a manner as to balance the total runoff (2.1 inches in 8 hours). Figure 4 shows the inflow hydrograph for drainage area No. 1, which is the area tributary to the northernmost natural pond

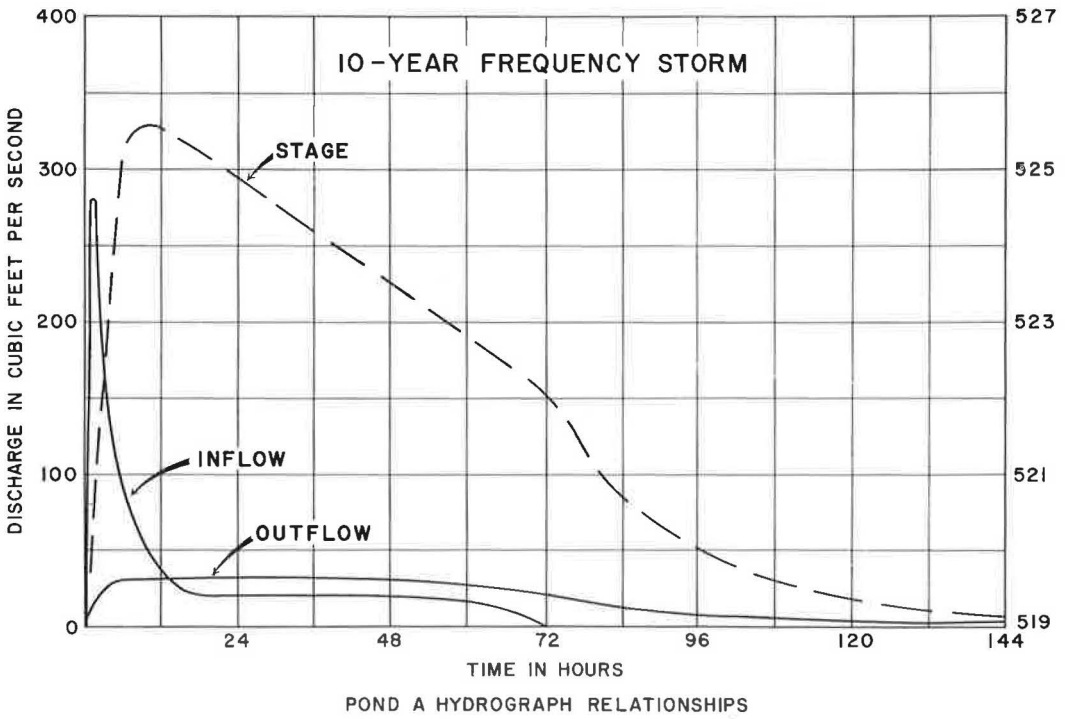

Figure 5. Inflow-outflow hydrograph for Pond A.

shown in Figure 1. For clarity, the limits of the individual drainage areas have not been shown in Figure 1.

In addition to the numerous natural ponding areas, two large ponds were excavated at hydraulically critical points. Pond B is approximately 600 feet long and 500 feet wide. Pond A is approximately 1,200 feet long and varies in width from 400 to 800 feet. Each of the two excavated ponds provides approximately 130 acre-feet of temporary storage capacity. To obtain this ponding volume, it was necessary to excavate 250,000 cubic yards of earth (total for both ponds). The surplus material from the excavation was used to fill and grade small sink areas throughout the cantonment area.

The runoff from each drainage area was routed through storage, where available, to determine the outflow hydrograph or rate of contribution to the drainage system. Figure 4 shows the routing for the natural pond serving drainage area No. 1. This routing is typical for all natural ponds in the system. To induce temporary storage and restrict the rate of runoff entering the drainage system, most of the inlets were equipped with a short control pipe. When flowing partially full, critical flow with inlet control was assumed. After the pipe was flowing full, the discharge was computed by the conventional orifice formula. The long pipe lines draining Ponds A and B were rated assuming friction control and an entrance loss of one-tenth of a velocity head.

The outflow hydrographs, separated by the travel time between design points, were added to obtain the maximum rate of contribution to the drainage system. Figure 5 shows the inflow-outflow relationship for Pond A which receives inflow from drainage areas 1 through 13. It will be noted that the peak discharge entering Pond A is 280 cfs while the outflow is limited to 32 cfs. This reduction in peak discharge entering the downstream system, together with a similar reduction upstream at Pond B, reduced the cost of the project approximately $1,000,000. The reason for this large reduction in pipe cost is apparent when it is realized that 13,000 lin ft of trunk sewer lies between Pond A and the outfall. Provision of adequate storage capacity at Ponds A and B permitted the outlet pipe from Pond A to be reduced from 90- to 30- in. diameter.

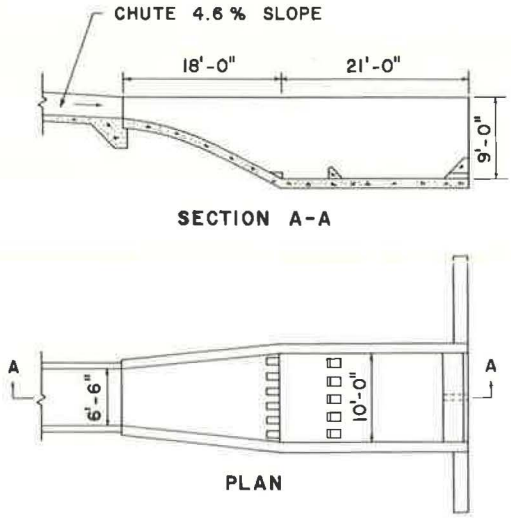

Figure 6. Stilling basin details.

The ground surface, downstream of the pipe outfall, falls rapidly (90 feet) to Little West Fork Creek, the ultimate disposal point for the storm drainage. To prevent erosion of the steep slope, a rectangular concrete chute 6.5 feet in width and 1,800 feet in length was provided. The required height of the side walls was determined by backwater computations beginning at critical depth near the pipe outlet and progressing downstream. Bulking of water due to air entrainment was computed and found to be negligible. Superelevation required at each of the horizontal curves in the chute was computed. It was found that it was significant at only one curve where a superelevation of 0.4 foot was provided. A freeboard of one foot over the computed water surface was provided throughout the length of the chute.

A stilling basin of conventional design was provided at the termination of the chute. As shown in Figure 6, the basin is 39 feet in length, 10 feet wide, and has two rows of baffle blocks and end sill of sufficient height to create the proper depth of tailwater for the formation of a hydraulic jump. Care was taken to locate the basin at the proper elevation to eliminate possible erosion in the ditch section between the stilling basin outlet and Little West Fork Creek. The design discharge for the stilling basin is 240 cfs. The velocity of the flow is reduced from 25 feet per second, at the entrance to the stilling basin, to 3.5 feet per second at the basin end sill.

TABLE 1

COMPARISON OF HYDROGRAPH DATA FOR STORMS OF VARIOUS FREQUENCIES

Area No.	Drainage Area (acres)	1-Year				10-Year				50-Year			
		Max. Inflow (cfs)	Max. Outflow (cfs)	Max. Pond Elev.	Pond. Time (hr)	Max. Inflow (cfs)	Max. Outflow (cfs)	Max. Pond Elev.	Pond. Time (hr)	Max. Inflow (cfs)	Max. Outflow (cfs)	Max. Pond Elev.	Pond. Time (hr)
1	198.6	63.5	40.0	539.0	6.5	103.5	63.6	539.9	12.5	137.5	77.0	540.7	13.0
6[a]	372.0	165.0	18.7	536.4	30.0	270.0	22.3	538.9	72.0	347.0	23.8	540.0	96.0
7	38.4	19.3	16.0	541.8	4.5	31.0	18.4	542.9	8.0	38.9	19.6	543.5	10.5
8	31.9	15.3	6.1	539.2	6.0	25.2	12.1	539.8	10.0	31.6	14.8	540.2	12.0
9	44.3	17.4	7.4	543.2	6.0	28.6	8.2	544.2	12.5	36.4	8.6	544.6	42.0
10	61.5	40.2	26.7	539.2	4.5	64.2	32.9	540.0	9.0	79.8	34.8	540.5	10.0
11	39.9	25.0	7.0	537.9	6.5	40.2	7.8	538.7	12.0	49.8	8.0	539.1	18.5
12	47.9	30.4	12.7	529.8	6.0	49.1	18.3	531.0	10.5	61.3	20.0	532.0	11.5
13[b]	244.7	180.0	19.6	521.8	137.0	270.0	32.0	525.6	192.0	333.0	36.0	528.2	219.0
14	100.0	40.8	12.5	539.3	10.0	66.3	20.6	540.4	17.5	85.0	23.0	540.8	21.0
15	66.2	26.2	7.9	537.9	6.5	42.6	9.0	538.6	18.5	54.6	9.0	539.4	25.0
16[c]	19.3	14.2	14.2	—	—	22.9	22.9	—	—	28.6	28.6	—	—
17	87.2	58.4	50.0	531.2	4.5	93.5	62.0	534.7	10.0	116.2	68.0	535.1	10.0
18[c]	24.9	17.3	17.3	—	—	27.8	27.8	—	—	35.0	35.0	—	—
19	257.0	79.8	26.2	521.0	13.5	132.5	37.0	523.9	21.0	172.9	41.0	525.4	33.0
20	5.4	3.7	1.9	520.8	3.5	5.9	2.6	521.0	5.5	7.2	3.3	521.5	8.5
21[b]	32.0	14.6	11.7	516.9	5.0	22.7	17.4	517.8	9.0	29.8	18.4	519.0	10.0
22[b]	32.7	22.2	9.8	511.1	10.0	37.1	19.9	512.2	13.0	49.7	22.5	513.4	16.5
23	208.0	87.6	26.2	512.1	18.5	144.7	39.0	513.6	19.0	185.0	46.2	514.7	25.0
24	54.6	30.4	7.7	522.6	6.0	50.0	8.8	523.9	15.5	62.3	9.2	524.3	21.0
25[c]	23.3	10.0	10.0	—	—	16.5	16.5	—	—	20.8	20.8	—	—

[a]Includes areas 2 thru 6. [b]Includes discharge from upstream area. [c]No ponding in these areas.

To insure that the drainage system was adequate to handle storms of infrequent occurrence, a 50-yr frequency flood was routed through the system. The computations indicated that the system was adequate to provide for this extreme storm without flooding of any facilities. A 1-yr frequency storm was also routed through the system to determine the depth and duration of ponding that would be expected to occur more frequently. Table 1 shows a comparison of ponding area hydrograph data for a 1-, a 10-, and a 50-yr frequency storm.

CONCLUSION

The Fort Campbell storm drainage system is, in essence, a hydraulically balanced network of temporary ponding areas connected by short control pipes to a main trunk sewer. The major portion of the runoff from the upstream third of the drainage basin is retained for a sufficient length of time, in the two major ponds, to reduce drastically peak downstream discharge rates. The large cost reduction that was accomplished by the judicious use of temporary ponding made the project economically feasible. While drainage projects on the scale of this one are unusual, a comparable percentage of cost savings can be realized on smaller projects by a similar use of temporary ponding. This project emphasizes that in this era of rising costs, the drainage engineer should always be mindful of the potential for drainage cost reductions that are afforded by relatively minor amounts of temporary ponding.

ACKNOWLEDGMENT

The authors, in the preparation of this paper, have made liberal use of reports, studies, and correspondence prepared by various Corps of Engineers offices concerned with the Fort Campbell project. Permission to use this material is gratefully acknowledged.

Friction Factors for Hydraulic Design of Corrugated Metal Pipe

JOHN L. GRACE, JR., U. S. Army Engineer Waterways Experiment Station

Results of model tests of two types of corrugated metal pipe including friction factor-Reynolds number diagrams and mean flow formulas developed from velocity distribution data are reported. Calculated maximum values of the friction factor due to the corrugations and the bolt nuts on the crests of the structural plate corrugations for various sizes of each type of pipe are compared with those of similar prototypes as reported by other investigators. Recommended design values of the friction factor for annular corrugated pipes with corrugation depth-spacing ratios of 1:3 and 1:5.33 are related to diameter, and simple empirical equations describing the relations are developed.

•STRUCTURAL PLATE PIPE, widely used in drainage systems, is made of corrugated metal sections bolted together in the field. These sections permit erection of pipe 5 ft in diameter or larger (in increments of 0.5 ft). Structural plate corrugations have a depth of 2 in. and a pitch of 6 in. In standard corrugated metal pipe the depth of the corrugations is only ½ in. and the pitch or spacing of the corrugations is 2⅔ in., crest-to-crest.

Tests to determine friction factors for standard corrugated metal pipe were made on pipes 3, 5, and 7 ft in diameter at the U. S. Army Engineer Bonneville Hydraulic Laboratory which published the results in 1955 (1, 8). Roughness coefficients determined in these tests are used generally in culvert design. However, extrapolation of these roughness coefficients to values applicable to structural plate pipe, which has corrugations four times as deep and a depth-pitch ratio of 1:3 rather than 1:5.33 was considered unreliable. The HRB Committee on Surface Drainage of Highways has long recognized the need for field or laboratory determination of hydraulic design coefficients for this commonly used drainage material.

Anticipating that full-scale tests would have been costly, and that it would have been feasible to test only the smaller sizes of structural plate pipe, the Bureau of Public Roads and the Office, Chief of Engineers, initiated in 1958 a hydraulic model investigation at the U. S. Army Engineer Waterways Experiment Station (WES) for the purpose of determining friction factors for structural plate pipe. One model simulating a 5-ft diameter standard corrugated pipe was tested to permit comparison of model and prototype results and to check the applicability of simulating corrugated metal pipes with corrugated fiber glass conduits. The good agreement obtained between results of the WES model and the Bonneville Hydraulic Laboratory prototype tests of 5-ft-diameter standard corrugated metal pipe warranted the use of the fiber glass models.

MODELS AND TEST PROCEDURES

Four models were constructed: a 1:4-scale model of 5-ft-diameter standard corrugated pipe and three simulating structural plate pipes 5, 10, and 20 ft in diameter at scales of 1:2.2, 1:8, and 1:16, respectively. The diameter between crests of corrugations of all models was 15 in. with the exception of the model simulating 5-ft-diameter

Paper sponsored by Committee on Surface Drainage of Highways.

Figure 1. Sections of models representing (left to right) 5-, 10-, and 20-ft-diameter structural plate pipes.

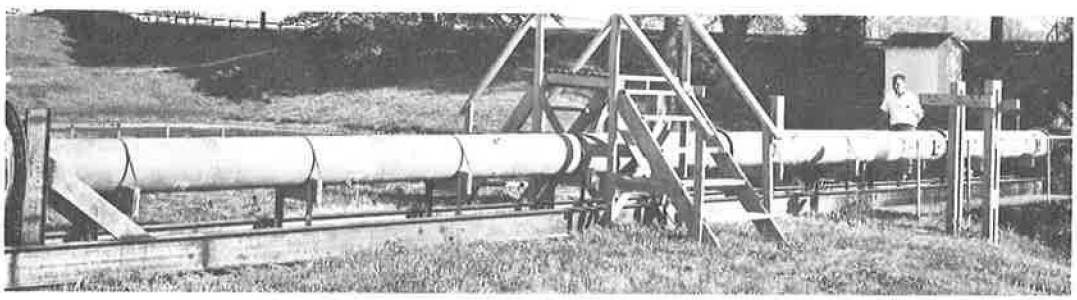

(a)

(b)

Figure 2. Structural plate pipe models of 40-diameter lengths; (a) 1:8-scale model of 10-ft-diameter pipe, and (b) 1:2.2-scale model of 5-ft-diameter pipe.

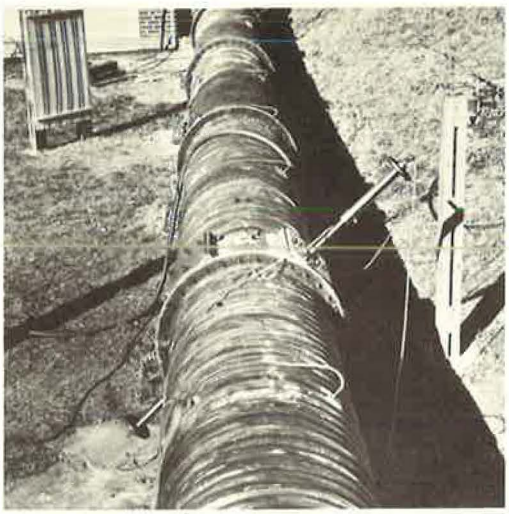

Figure 3. Piezometers and velocity probes.

Figure 4. Velocity probes.

structural plate pipe which utilized a diameter of 27.27 in. The crests of corrugations referred to throughout the paper are those nearest the axis of the pipe and the diameters quoted are the actual minimum inside diameters except in the cases where results are related to nominal pipe diameter. This unusual diameter (27.27 in.) and model scale (1:2.2) was calculated to be necessary to obtain flows with Reynolds numbers representative of prototype conditions using an available pumping system with a rated capacity of 100 cfs under a 55-ft head. Fabricated sections of the models simulating structural plate pipes are shown in Figure 1. The sections were assembled and tested in lengths ranging from 22 to 100 times the respective pipe diameter. Models of 5- and 10-ft-diameter structural plate pipes are shown in Figure 2.

Water used in the operation of the models was supplied by centrifugal pumps and measured by means of either a calibrated venturi meter or traverses of velocity across the pipes. Piezometers located on the crests of the corrugations (Fig. 3) were used to observe the hydraulic gradients. Velocity probes and traversing mechanisms (Fig. 4) were equipped with total pressure and static pressure tubes to obtain velocity and static pressure distribution data.

Before beginning a test, a discharge sufficient to remove air entrapped in the corrugations at the top of the pipe was set and instruments used to measure discharge, pressure, and velocity were primed. The test discharge was established, and all data desired at that discharge were obtained without interruption or modification of flow. The hydraulic gradient was observed. Traverses of total and static pressures across the pipe normal to the crest of a corrugation were obtained. The temperature of the water was measured during each test. Flow with a Reynolds number of 5×10^6 in the model simulating 5-ft-diameter structural plate pipe is illustrated in Figure 5.

Figure 5. Flow in model of 5-ft-diameter pipe, $\mathfrak{R} + 5 \times 10^6$.

In determining the slope of the hydraulic gradient, pressure readings near the entrance and exit of the test sections were neglected to eliminate the respective effects of boundary layer development and acceleration of flow. The average velocities, V, the slopes determined from the hydraulic gradients, S, and the actual diameter between crests of the corrugations, D, were used to determine values of the friction factor, f, by means of the Darcy-Weisbach equation. Values of the shear velocity, v, computed by means of the basic relation, $v^* = \sqrt{\frac{D}{4}}\,Sg$, were used to determine values of a parameter termed wall Reynolds number, $R_W = (v^*k/\nu)$. The symbols k and ν represent depth of corrugation in feet and kinematic viscosity, respectively.

STANDARD CORRUGATED PIPE

Although the relative roughness, K/D, of the model of 5-ft-diameter standard corrugated pipe was 0.00936 rather than the expected value of 0.0083, the resistance coefficient curve, f, versus wall Reynolds number, of the model was similar in shape to that of the prototype reported by Webster and Metcalf (8) for wall Reynolds numbers up to 1600 (Fig. 6). The maximum value of the resistance coefficient agreed most favorably with that interpolated based on the results of the 3- and 5-ft-diameter standard corrugated pipes. Thus, it was concluded that the material effect of fiber glass on the resistance coefficient was essentially the same as that of metal and that geometrically similar fiber glass models would adequately simulate corrugated metal pipes.

Analysis of the Bonneville Hydraulic Laboratory prototype test data indicated that the maximum value of the resistance coefficient of standard corrugated pipes occurs at flows with a common wall Reynolds number of 1300 (see Fig. 6). Therefore, appro-

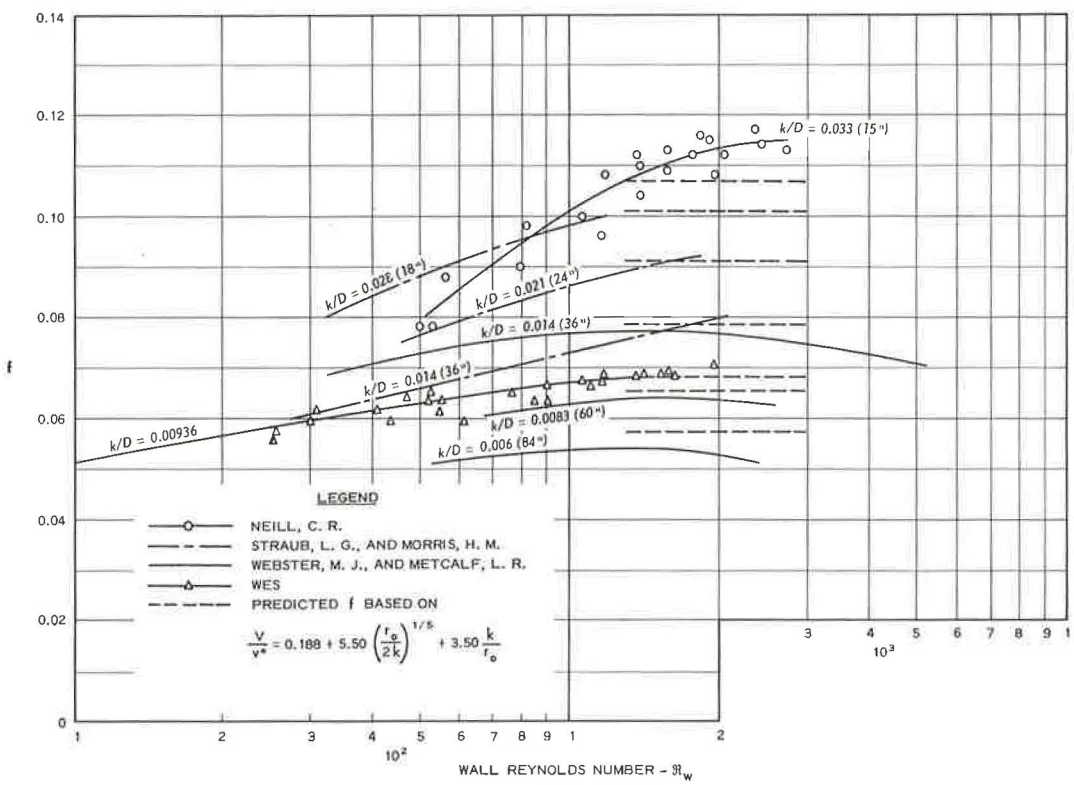

Figure 6. Resistance coefficients vs wall Reynolds number—standard corrugated metal pipe, full pipe flow.

priate velocity distribution data of both the WES model and the 5-ft-diameter prototype were used to develop the following mean flow formula which can be used to compute the maximum value of the resistance coefficient of any size of standard corrugated pipe.

$$\frac{V}{v^*} = \sqrt{\frac{8}{f}} = 0.188 + 5.50 \left(\frac{r_o}{2k}\right)^{1/5} + 3.50 \frac{k}{r_o}$$

Resistance coefficients computed by means of the mean flow formula agree most favorably with the maximum values reported by the Bonneville (1) and the Saint Anthony Falls (2) Hydraulic Laboratories but are approximately seven percent less than the maximum value reported by Neill (5) for 15-in.-diameter pipe and that reported by Garde (4) and Chamberlain (3) for 12-in.-diameter standard corrugated pipe. Admittedly, the mean flow formula for standard corrugated pipe was developed from limited velocity distribution data (especially in the region of threshold velocities) due to practical considera-

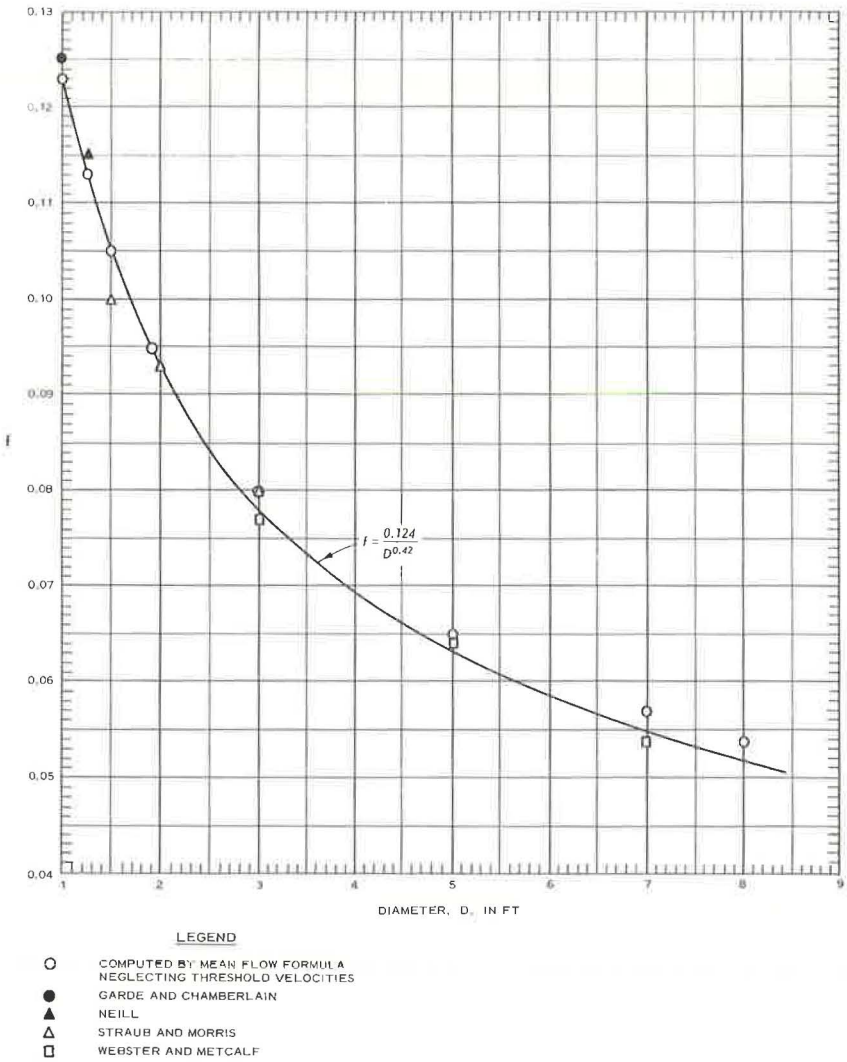

Figure 7. f vs pipe diameter—standard corrugated pipe.

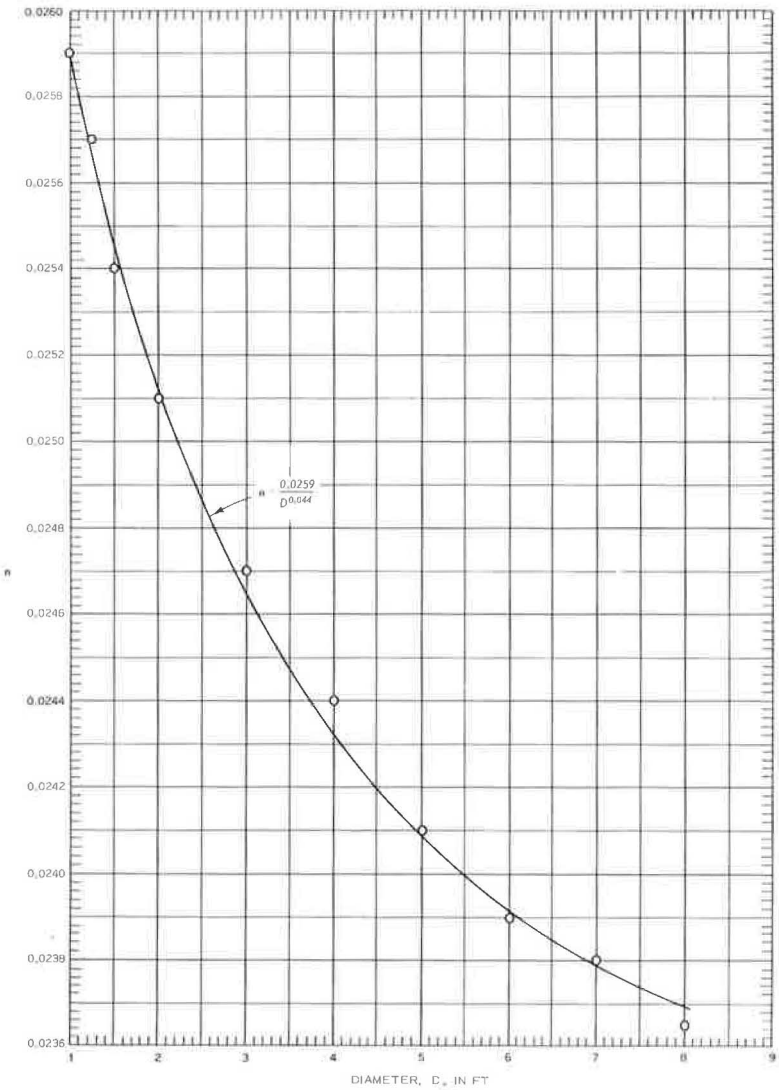

Figure 8. Manning's n vs pipe diameter—standard corrugated pipe.

tions and, therefore, the mathematical expression derived for the threshold velocities is questionable. If the term 3.50 (k/r_o) is neglected, the modified mean flow formula predicts maximum values of the resistance coefficients that agree favorably with those reported by other investigators for standard corrugated metal pipes ranging from 1 to 7 ft in diameter as shown in Figure 7. This does not imply that the threshold velocities do not exist in standard corrugated metal pipe but merely that the expression derived is not adequate and this was expected in view of the lack of appropriate data near the boundary of this type of pipe. Figure 7 indicates that the maximum or design value of the resistance coefficient of any size of standard corrugated pipe may be calculated by means of the empirical equation, $f = 0.124/D^{0.42}$, where D is pipe diameter in feet. Values of f were converted to Manning's n by means of basic relations and the relation between n and pipe diameter (Fig. 8) is satisfied by the empirical equation, $n = 0.0259/D^{0.044}$. These values of the resistance coefficient can be expected at flows with wall Reynolds numbers near 1300 and are considered applicable for design since values

of R_W, encountered in field installations of 12-, 60-, and 96-in.-diameter standard corrugated pipes flowing full with friction slopes of 0.5 to 8.0 percent and water temperatures ranging from 45 to 75 F, range from 550 to 3400, 1250 to 7550, and 1550 to 9550, respectively. There may be objections to the recommendation that the maximum values of the resistance coefficients observed in standard corrugated pipes be used as a basis for selection of design values for all conditions since prototype tests (1, 3, and 4) indicate that the resistance coefficients decrease with increasing wall Reynolds numbers greater than 1300. Certainly this appears to be merited for the cases where the R_w of flow in standard corrugated pipes is expected to be well above the value of 1300 (the range of R_W where a maximum value of the resistance coefficient is indicated). In such cases, it is recommended that the results of the Bonneville Hydraulic Laboratory prototype tests (1) as shown in Figure 6 be used in extrapolating the design values of the resistance coefficient.

STRUCTURAL PLATE CORRUGATED PIPE

The resistance coefficient curve determined from tests of the model simulating 5-ft-diameter structural plate pipe (Fig. 9) revealed that the resistance coefficient attained a maximum value of 0.111 at a R_W of about 8000 and that f remained constant for R_W up to 22,000. Values of wall Reynolds numbers, expected in field installations of 5-, 10-, and 20-ft-diameter structural plate pipes flowing full with friction slopes of 0.5 to 8.0 percent and water temperatures ranging from 45 to 75 F, range from 5,000 to 30,000, 7,000 to 43,000, and 10,000 to 60,000, respectively. Thus, the conditions investigated with the model of 5-ft-diameter structural plate pipe simulate anticipated field flow conditions adequately. Unfortunately, the limiting value of R_W (8000) was

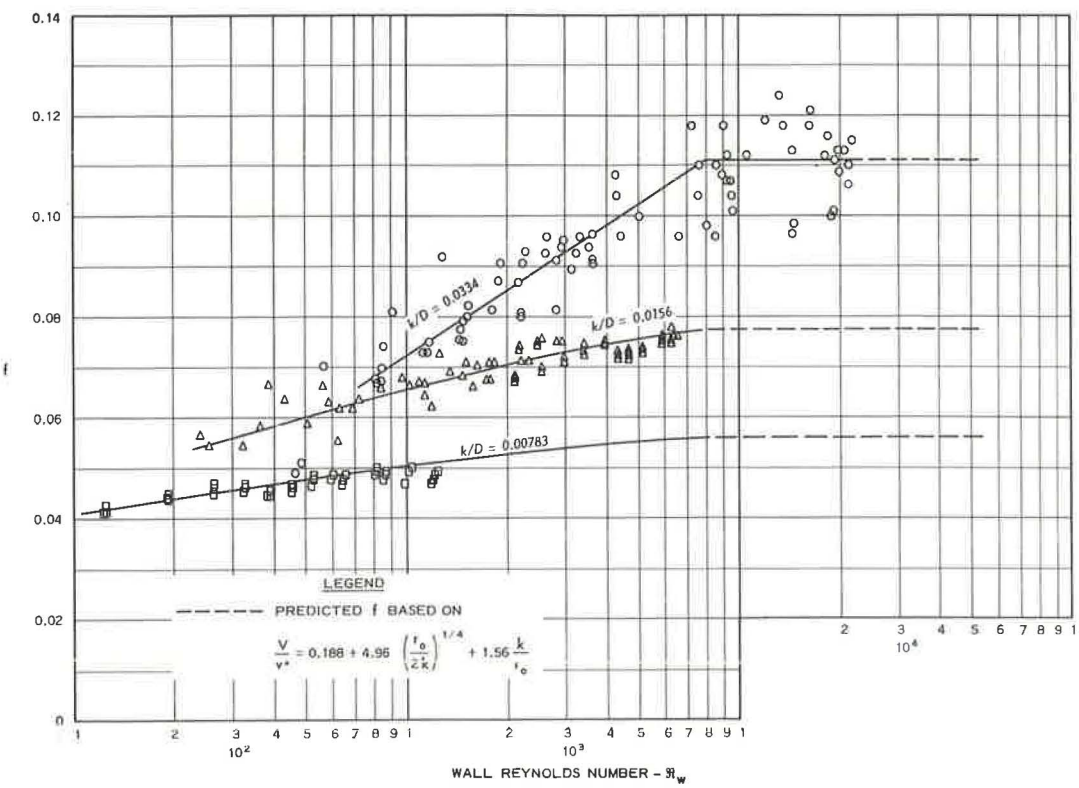

Figure 9. Resistance coefficient vs wall Reynolds number—structural plate pipe, full pipe flow.

greater than that anticipated initially; and consequently, flows with wall Reynolds numbers equal to or greater than 8000 were not possible with the selected models of 10- and 20-ft-diameter structural plate pipes and the available water supply systems. However, results obtained with the model of 10-ft-diameter structural plate pipe and wall Reynolds numbers just below this limit agreed most favorably with that of the model of 5-ft-diameter structural plate pipe, and it was concluded that the resistance coefficient of any size of this type of pipe approaches a maximum value and remains constant for flows with R_W equal to or greater than 8000. Since an analysis of the results of Webster and Metcalf (8) indicate that the maximum value of the resistance coefficient of standard corrugated pipes (3, 5, and 7 ft in diameter) occurred at flows with a common wall Reynolds number, it seems quite reasonable that a similar relation would exist for structural plate pipes.

Velocity distribution data of the model simulating 5-ft-diameter structural plate pipe in the range of wall Reynolds numbers, where the resistance coefficient was at its maximum and constant value, were used to develop the following mean flow formula.

$$\frac{V}{v^*} = \sqrt{\frac{8}{f}} = 0.188 + 4.96 \left(\frac{r_o}{2k}\right)^{1/4} + 1.56 \frac{k}{r_o}$$

Velocity distribution data of the model simulating 10-ft-diameter structural plate pipe within the range of R_W near 8000 are satisfied by the mean flow formula also. Thus, it is concluded that the mean flow formula can be used to compute the maximum value of the resistance coefficient due to the corrugations of any size of structural plate pipe.

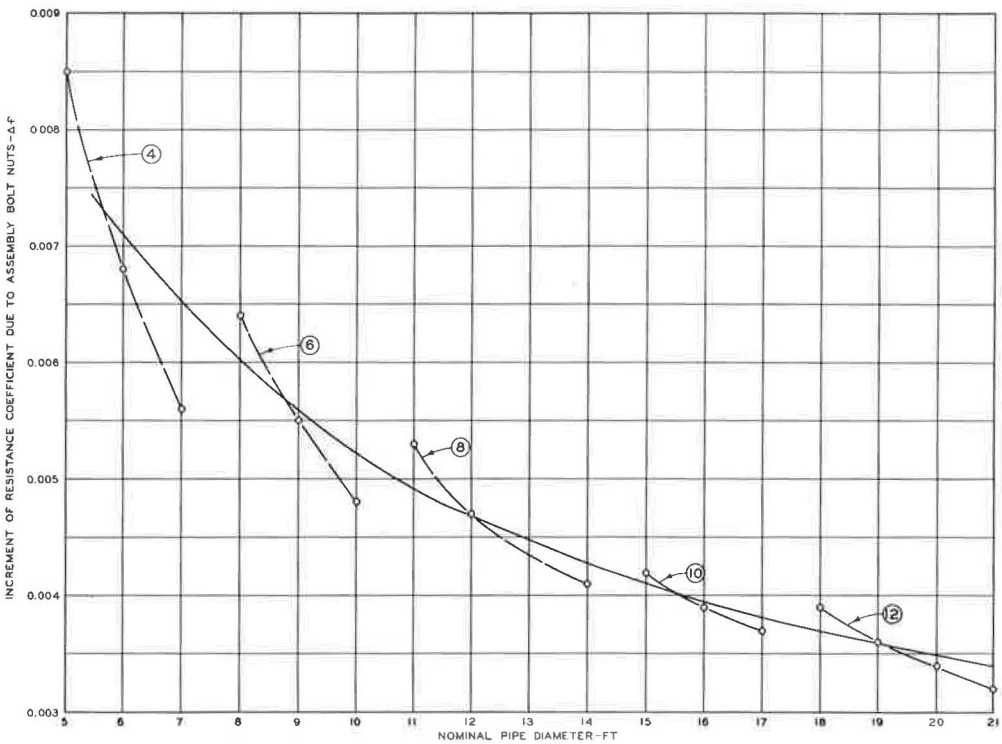

Figure 10. Resistance factor, Δf, attributable to assembly bolt nuts—structural plate pipe.

TABLE 1

BOLT-NUT RESISTANCE FACTOR, Δf, STRUCTURAL PLATE PIPE

$$\Delta f = \frac{C_D N a}{0.785 D^2}\left(\frac{v}{V}\right)^2$$

$C_D = 1.1$ a = 0.0070 sq ft

No. of Plates per Ring	Pipe Diameter		No. of Nuts per Diameter	$\frac{v}{V}$	Δf
	Nominal (in.)	Actual (ft)			
4	60	4.93	50	0.649	0.0085
	72	5.94	63	0.621	0.0068
	84	6.97	77	0.598	0.0056
6	96	7.98	123	0.580	0.0064
	108	9.00	143	0.564	0.0055
	120	10.02	164	0.549	0.0048
8	132	11.04	227	0.537	0.0053
	144	12.06	254	0.525	0.0047
	168	14.09	321	0.506	0.0041
10	180	15.11	398	0.498	0.0042
	192	16.13	434	0.490	0.0039
	204	17.15	470	0.483	0.0037
12	216	18.17	575	0.476	0.0039
	228	19.18	616	0.469	0.0036
	240	20.21	660	0.464	0.0034
	252	21.22	705	0.459	0.0032

Δf = increment of resistance coefficient attributable to bolt nuts.
C_D = coefficient of drag.
N = number of objects (bolt nuts) on crest of corrugations in a length of one pipe diameter.
a = projected area of object in a plane normal to direction of flow, sq ft.
D = actual diameter of pipe between crests of corrugations, ft.
v = local veolcity at midheight of object, fps.
V = mean velocity of flow, fps.

Assembly bolt nuts which are located on the crests of the corrugations in prototypes were not simulated in the models and, therefore, the mean flow formula does not reflect the added resistance they would entail. However, H. G. Bossy of the U. S. Bureau of Public Roads made a detailed review of literature concerned with the coefficient of drag of shapes similar to the bolt nuts and developed a method to determine the increment of resistance attributable to the assembly bolt nuts of structural plate pipe. The results of Bossy's analysis, presented in Table 1 and Figure 10, indicate that the increment of the resistance coefficient, Δf, which can be attributed to the bolt nuts varies with pipe diameter, and that a Δf of 0.0085 is reasonably applicable for the 5-ft-diameter structural plate pipe. Adding this increment to the f determined from the mean flow formula based on an actual diameter between corrugation crests of 59.1 in., that recommended by the manufacturer, gives an f of 0.12. The first and only reported prototype tests by Neill (5) of a 5-ft-diameter structural plate pipe (within this range of wall Reynolds numbers) indicate a maximum constant value of 0.13 for the resistance coefficient based on a diameter from crest to crest of corrugations of 59 in. (7). Thus, the maximum value of the resistance coefficient predicted from the WES model tests agrees favorably with that indicated by Neill's prototype tests. Additional friction-loss data of a small model of 5-ft-diameter structural plate pipe presented by Kellerhals (6) confirm the data of the WES model of 5-ft-diameter structural plate pipe in the lower range of central Reynolds number, VD/ν (2 to 5 × 10^5).

Resistance coefficients due to the corrugations of structural plate pipes with nominal diameters ranging from 5 to 20 ft were calculated by means of the mean flow formula and the actual inside diameters between crests of corrugations as given by the manufacturers. The increment of the resistance coefficient attributable to the assembly bolt nuts determined by Bossy (Fig. 10) was added to the value of the resistance coefficient due to the corrugations to determine the total resistance coefficient of each of the several sizes of structural plate pipe. The relation between total resistance coefficient and diameter of pipe (Fig. 11) is satisfied by the empirical equations, $f = 0.258/D^{0.482}$ and $f_n = 0.320/D_n^{0.576}$. It is noted that the equation based on nominal pipe diameter will yield a value of the resistance coefficient other than that determined by the equation based on actual pipe diameter. This is required in order that the head loss computed by the Darcy-Weisbach equation using the nominal diameter and a velocity based on the nominal diameter and design discharge will agree with that determined using actual diameter and velocity, i.e.,

$$h_l = f\frac{L}{D}\frac{V^2}{2g} = f_n\frac{L}{D_n}\frac{V_n^2}{2g} \text{ and } f_n = f\left(\frac{D_n}{D}\right)^5$$

The recommended design value of the total resistance coefficient obtained from the foregoing equations of Figure 11 is that expected to occur at flows with wall Reynolds numbers of 8000 or greater (the range of R_W in which f has attained a constant maximum value and also that to be expected in the field).

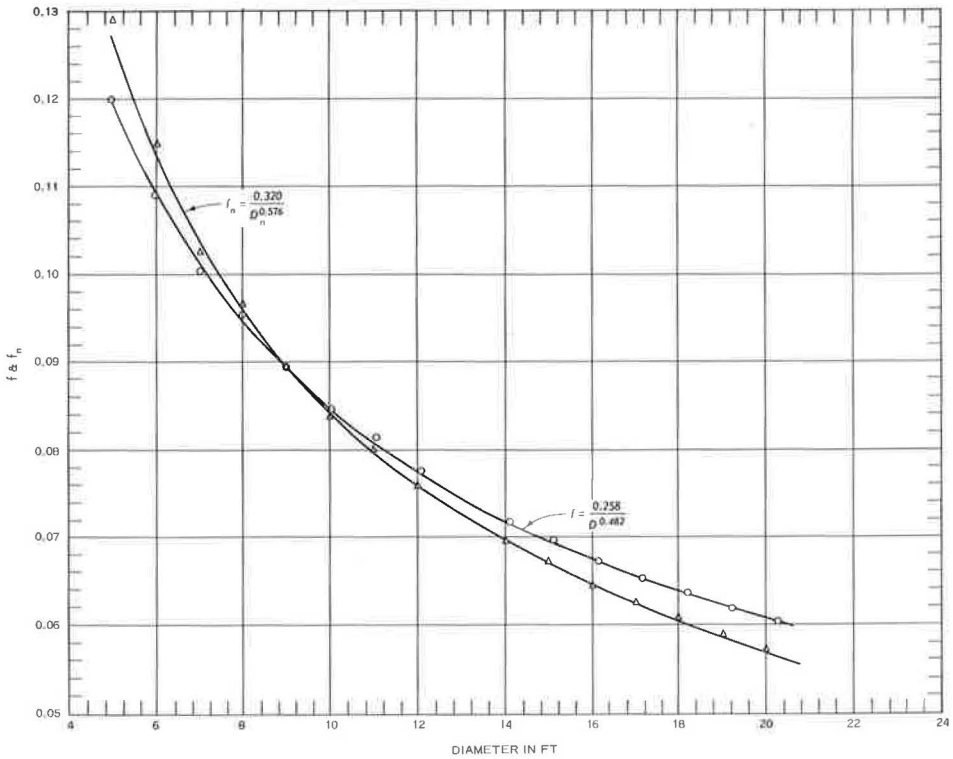

Figure 11. f and f_n vs pipe diameter—structural plate pipe.

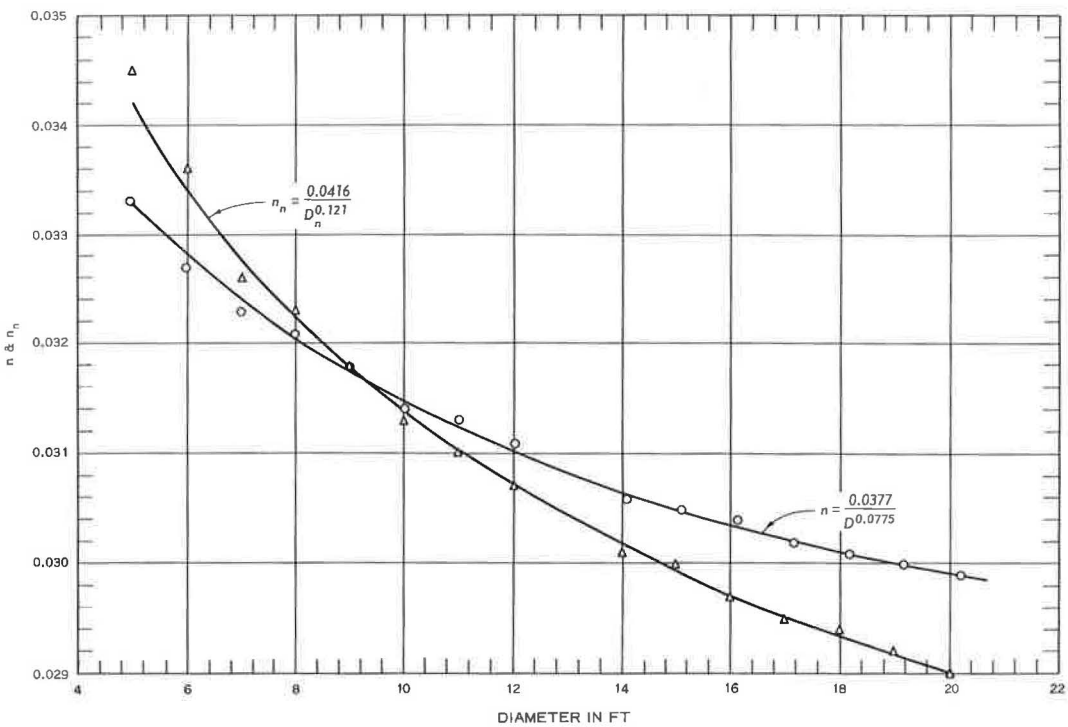

Figure 12. n and n_n vs pipe diameter—structural plate pipe.

Values of f were converted to Manning's n by means of basic relations. The relation of recommended design values of Manning's n to pipe diameter (Fig. 12) is satisfied by the empirical equations, $n = 0.037/D^{0.0775}$ and $n_n = 0.0416/D_n^{0.121}$

OTHER CORRUGATED PIPE

Since the depth-to-pitch ratio of corrugations 1 in. by 3 in. is the same as that of structural plate corrugations, 2 in. by 6 in., the mean flow formula for structural

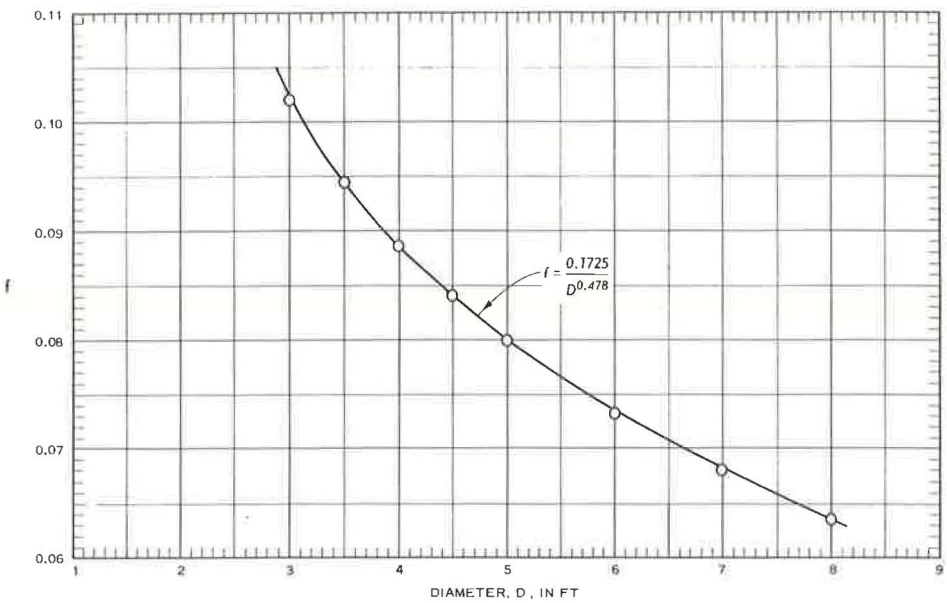

Figure 13. f vs pipe diameter—1- × 3-in. corrugations.

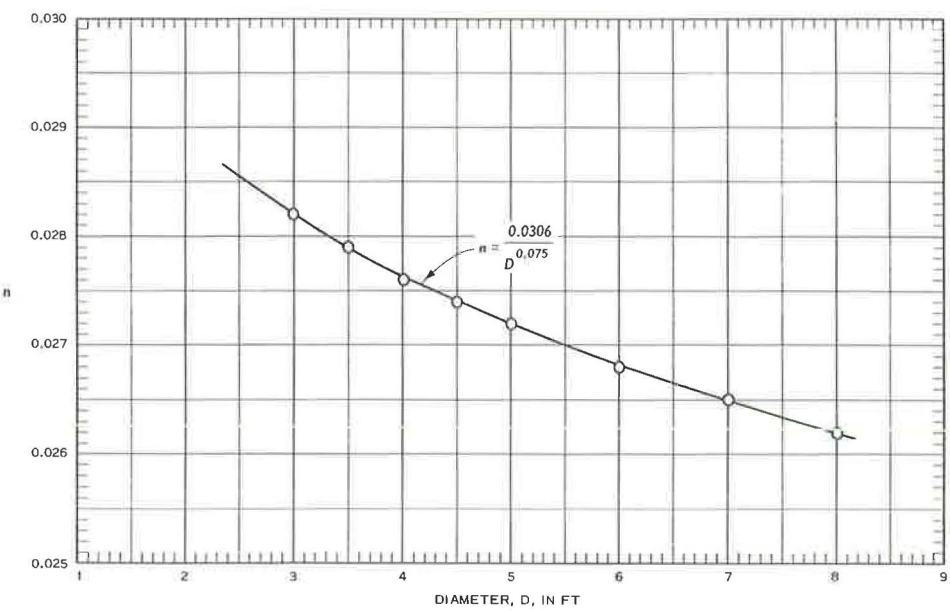

Figure 14. Manning's n vs pipe diameter—1- × 3-in. corrugations.

plate pipe is considered applicable to corrugated pipe with annular 1-in. by 3-in. corrugations. Values of f determined by means of the mean flow formula are related to pipe diameter in Figure 13 which indicates that the resistance coefficient of any size of this type of pipe can be calculated by the empirical equation, $f = 0.1725/D^{0.478}$. Manning's n may be computed directly by the equation, $n = 0.0306/D^{0.075}$ (see Fig. 14). Design values of Manning's n ranging from 0.0282 to 0.0262 are indicated for 3- to 8-ft-diameter pipes with annular 1-in. by 3-in. corrugations.

The results reported herein are believed to be most adequate for determining design values of the resistance coefficient for each type of corrugated pipe discussed. However, sufficient data are not available with which the effect of corrugation pitch or spacing, λ, can be determined. In addition, little is known of the effects of helical rather than annular corrugations on the resistance coefficient. It is believed that the need for tests to determine the resistance coefficient of various configurations, including both annular and helical, will arise in the near future and it is hoped that efforts will be directed to determine the importance of these geometric properties on velocity distribution in the range of maximum resistance, in order that a more complete understanding of the law of velocity distribution in corrugated pipe can be developed.

ACKNOWLEDGMENTS

The results reported herein are a summary of the research project sponsored jointly by the Bureau of Public Roads and the Office, Chief of Engineers and conducted at the U. S. Army Engineer Waterways Experiment Station for investigation of the hydraulic resistance of structural plate corrugated metal pipe. The author is indebted to K. S. Eff of the Office, Chief of Engineers, H. G. Bossy of the Bureau of Public Roads, T. E. Murphy of the Waterways Experiment Station, and G. H. Keulegan of the Bureau of Standards (now an employee of the Waterways Experiment Station) for many helpful discussions of the test results and review of the analytical methods employed. Special thanks are extended to Mr. Bossy for his analysis to determine the increase in the resistance coefficient attributable to the assembly bolt nuts of structural plate corrugated metal pipe and for invaluable review of the paper.

REFERENCES

1. Webster, M. J., and Metcalf, L. R. Friction Losses in Corrugated Metal Pipe. U. S. Army Engineer Bonneville Hydraulic Laboratory, Rept. 40-1, Bonneville, Oregon, July 1955.
2. Straub, L. G., and Morris, H. M. Hydraulic Data Comparison of Concrete and Corrugated Metal Culvert Pipes. St. Anthony Falls Hydraulic Laboratory, Univ. of Minnesota, Technical Paper 3B, Minneapolis, Minn., 1950.
3. Chamberlain, A. R. Effect of Boundary Form on Fine Sand Transport in Twelve-Inch Pipes. Colorado State Univ. Rept. CER No. 55, June 1955.
4. Garde, R. J. Sediment Transport Through Pipes. Colorado State Univ. Rept. CER No. 56, Oct. 1956.
5. Neill, C. R. Hydraulic Roughness of Corrugated Pipes. Proc., ASCE, Vol. 88, HY-3, New York, N. Y., pp. 23-44, May 1962.
6. Kellerhals, Rolf, and Bossy, H. G. Discussion of Hydraulic Roughness of Corrugated Pipes. Proc., ASCE, Vol. 89, HY-1, New York, N. Y., pp. 201-205, Jan. 1963.
7. Neill, C. R. Closure of Discussion of Hydraulic Roughness of Corrugated Pipes. Proc., ASCE, Vol. 89, HY-4, New York, N. Y., pp. 205-208, July 1963.
8. Webster, Morris J., and Metcalf, Lawrence R. Proc., ASCE, Hydraulics Division, Sept. 1959.

Camber Design Study for Concrete Pipe Culvert

ROBERT C. DEEN, Assistant Director of Research, Kentucky Department of Highways

When a pipe culvert is constructed on or near the natural ground surface and covered by a highway fill or embankment, the weight of the embankment compresses and consolidates the foundation soil, settlement occurs, and the culvert subsides and sags below the original grade line. Experience has shown that culverts which become clogged with silt and debris become disjointed and faulted, leak, become undermined, and endanger the stability of the embankment. These, and other damages attendant to settlement, restrict the flow of water, prevent adequate inspection of the structure, and may eventually require extensive maintenance or complete replacement of the structure. Some of this damage may be avoided by placing the culvert on cambered grades—that is, by installing the culvert with its flow line somewhat above its normal or desired elevation along the central portion of its length. This idea anticipates that settlement under the load of the embankment will, in time, lower the flow line to the desired straight grade.

The project reported in this paper was undertaken to develop a simplified criterion which would permit the inclusion of camber as a routine design feature in highway culvert installations. The work was based on the theory of consolidation and consisted of consolidation tests and prediction of settlement profiles under proposed embankments, the installation of these culverts cambered according to the predicted settlement profiles, and the observance of the settlements during and following the completion of the embankments. Fairly close agreement between the predicted and observed settlements invited serious speculation as to the possibility of estimating camber, within reasonable limitations, from typical void ratio-pressure curves obtained from typical or average soils.

•WHEN A pipe culvert is constructed on or near the natural ground surface and covered by a highway fill or embankment, the weight of the embankment compresses and consolidates the foundation soil, settlement occurs, and the culvert subsides or sags below the original line as illustrated in Figure 1. The amount of settlement depends, of course, on the fill height or load, the depth of foundation soil, and the susceptibility of the foundation soil to consolidation. In addition, and because there may be movement of the foundation soil outwardly and toward the toes of the embankment, the structure may tend to lengthen. It may also lengthen slightly, however, simply because the distance along the sag or settlement curve is greater than the straight grade distance. These movements are damaging to the drainage structure and should be minimized or otherwise compensated in design insofar as practicable.

Experience has shown that culverts which settle excessively below their original straight grade frequently become clogged with silt and debris, become disjointed and faulted, leak, become undermined, and endanger the stability of the embankment. These, and other damages attendant to settlement, restrict the flow of water, prevent adequate inspection of the structure, and may eventually require extensive maintenance or complete replacement of the structure. Some of this damage may be avoided by placing culverts on cambered grades—that is, by installing the culvert with its flow line somewhat above its normal or desired elevation along the central portion of its length (Fig. 2).

Paper sponsored by Committee on Culverts and Culvert Pipe.

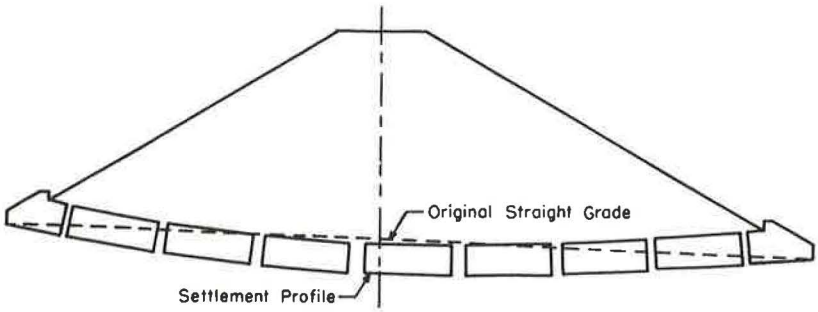

Figure 1. Settlement of culvert below straight grade.

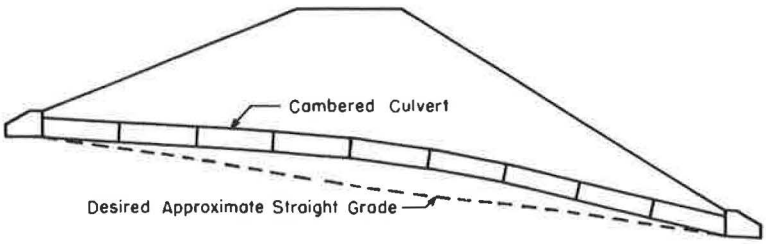

Figure 2. Cambered culvert and desired straight grade.

This idea anticipates that settlement under the load of the embankment will, in time, lower the culvert to approximately the desired straight grade.

Some engineering specifications (1), handbooks (2) and treatises suggest the desirability of cambering culvert pipe, but the literature which has been reviewed does not seem to offer any generally accepted criterion or formula for predicting even approximately the magnitude of the camber to be used. Spangler (3) suggests that the proper amount of camber could be determined rather precisely in advance of construction by application of some of the present knowledge of soil mechanics, such as the Terzaghi theory of consolidation (4), but favors a more empirical approach to the problem. While it is well recognized among soils engineers that extensive consolidation data and foundation settlement analyses are necessary in the design of large and costly structures, it would not be practical to require these analyses for each culvert installation on a highway. To avoid such an expensive and time-consuming procedure, a short, fairly accurate, simple method is desired, whether it be rational or empirical.

The ultimate objective of this investigation, therefore, was to develop a simplified criterion which would permit the inclusion of camber as a routine design feature in highway culvert installations. In reality, the work was founded on the theory of consolidation and consisted of consolidation tests and predictions of settlement profiles under proposed embankments, the installation of culverts cambered according to the predicted settlement profiles, and the observance of settlements during and following the completion of the embankments. Fairly close agreement between the predicted and observed settlements invited serious speculation as to the possibility of estimating camber, within reasonable limitations, of course, from typical void ratio-pressure curves obtained from typical or average soils.

PROJECT DESCRIPTION

Six locations on a section of I-64 near Simpsonville, Kentucky (Fig. 3), were selected for study. Plans for the proposed highway were inspected, auger borings were made, and the respective sites chosen on the basis of embankment heights and soil depths avail-

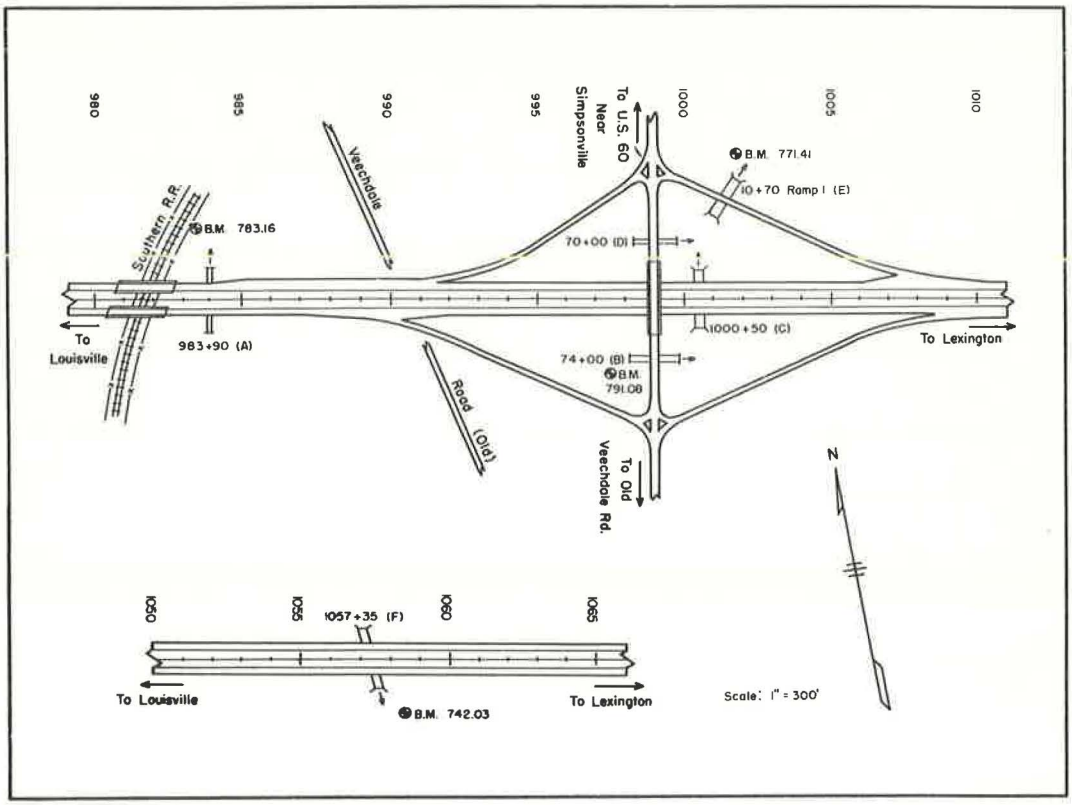

Figure 3. Culvert locations.

TABLE 1

CULVERT DIMENSIONS AND INSTALLATION DATA

Culvert Designation	Station No.	Diameter (in.)	Actual Length (ft)	Number of Pipe Sections	Slope (%)	Foundation Soil Depth (ft)	Embankment Height[a] (ft)	Max. Camber[b] (ft)
A	983 + 90 Interstate	18	227.25	56	1.89	3-11	23	0.19
B	74 + 00 Veechdale Rd.	24	169.75	42	0.60	0-5½	33	0.18
C	1000 + 50 Interstate	30	201.70	50	1.90	0-6	13½	0.14
D	70 + 00 Veechdale Rd.	18	150.05	37	4.39	0-5½	27	0.23
E	10 + 70 Ramp I	36	146.15	36	0.90	2-2½	28½	0.26
F	1057 + 35 Interstate	30	214.10	53	0.00	6-6½	19	0.43

[a]Represents average of values measured at center of each pair of lanes for 4-lane divided highway or value measured at center of roadway for undivided highway. Includes pavement thickness.
[b]Did not necessarily occur at point where embankment height was measured.

able. A summary of culvert dimensions and installation data is presented in Table 1. All the pipe culverts on this section of highway consisted of reinforced concrete pipe.

Every effort was made to avoid interference with the regular construction of the culverts and embankments other than to establish the cambered grade line elevations. Preliminary work began on the camber project in July 1958. Rough grading and embankments were completed in August 1959. The bituminous pavement on the undivided roadway which crosses the interstate route and which overlies Pipes B and D was constructed in the fall of 1959 while the mainline of I-64 was paved in the fall of 1960.

METHODS AND PROCEDURES

Soil samples were obtained with soil augers at various intervals along the centerline of each culvert site to establish soil profiles, depths to water table, and depths to bedrock. Undisturbed soil samples were obtained by the open-pit method near the centerline of survey at each culvert site. The pits were deepened until the desired layer of soil was encountered. In some cases, samples from different levels were obtained in the same pit. Pit depths ranged from approximately 3 to 7 feet. When the desired layer was reached, an undisturbed sample was carefully obtained and sealed, marked for identification, and transported to the laboratory for testing.

The specimens for consolidation testing were trimmed and fitted by hand directly into the consolidation rings. Trimming was performed in a moist room to maintain the original moisture contents as closely as possible. The finished specimens were 2.5 inches in diameter and 1-in. thick. Pressures beginning at $\frac{1}{4}$ tons per square foot were applied in increments, using a load-increment ratio of one. The pressure on any particular sample was increased until it was greater than the unit pressure to be applied by the weight of the embankment on the soil in the field. The maximum pressure for all tested samples was either 2 or 4 tons per square foot. The resulting void ratio-pressure curve from each consolidation test was used in the camber computations.

The foundation soil profiles were superimposed on the pipe culvert section sheets included in the highway plans. The depth of soil beneath the culvert flow line and the height of embankment above the flow line were determined at 24-ft intervals along each culvert site. This interval was selected because the construction crew chose to set their batter boards every 24 feet, which is the length of six pipe sections.

Using the respective void ratio-pressure curves and Eqs. 1 and 2, the expected settlement was calculated for each of the 24-ft intervals. All embankment material was assumed to have a unit weight of 120 pcf. Often, in settlement calculations, the distribution of the vertical stress within the foundation produced by the weight of the embankment is determined by use of influence charts, which are solutions of the Boussinesq, Westergaard or similar equations (5). However, the depths of foundation soils encountered in this project were so shallow in relation to the widths of the embankments at the base that stresses produced by the embankment weights diminished very little with depths of foundation soils. For this reason, the midplanes of the foundation soils were assumed to carry the full stresses produced by the embankment loads. Also, because the foundation soils were relatively thin, the pressure produced on the midplane of the foundation soil—due to its own weight—was neglected. Total settlements for Pipes A and F were based on two dominating layers of compressible soil in the profile. For the other pipes, the entire depth of soil beneath the flow line was assumed to be compressible. The straight-grade elevations originally shown on the plans were corrected to include the camber desired for each installation.

As construction of the culverts progressed, elevations were obtained at the 24-ft intervals within the culverts. Masonry nails were driven into the mortared joints in the culvert inverts. Elevations were obtained on the nail heads to check the accuracy to which the culverts were placed and also to provide initial readings before any settlement occurred. Where the culvert flow lines were sufficiently flat to permit a horizontal line of sight, elevations were determined with a level mounted on a special tripod as shown in Figure 4. Readings were obtained on a short section of a standard level rod as shown in Figure 5. A 6-v hunter's lantern served as means of illumination within the culverts. Where the grades were too steep to use this technique, the straight

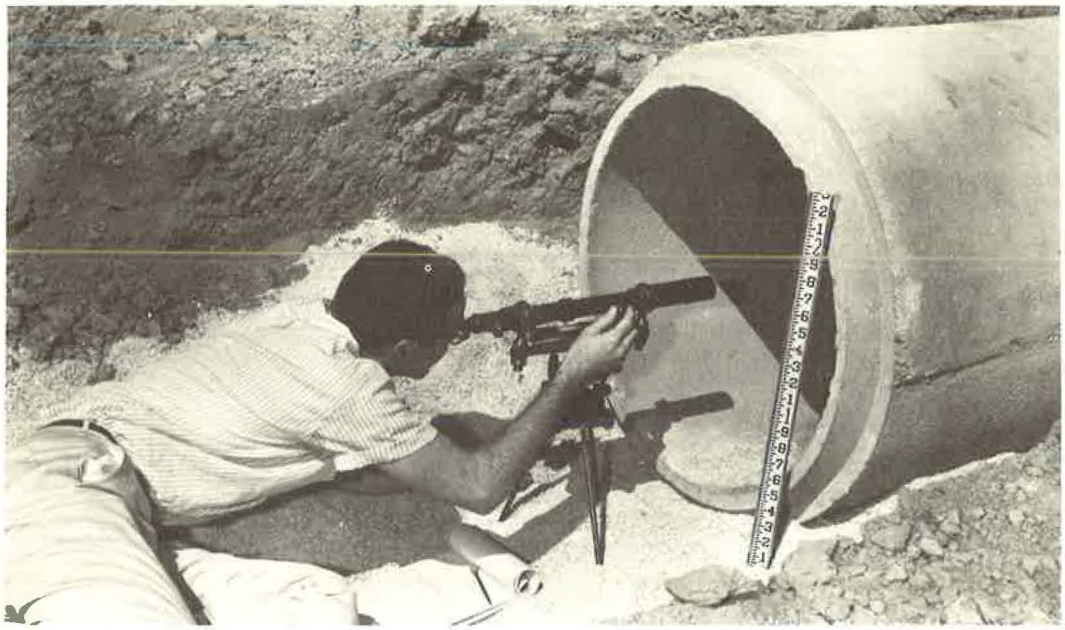

Figure 4. Use of level to obtain elevations within culverts laid on relatively flat grades.

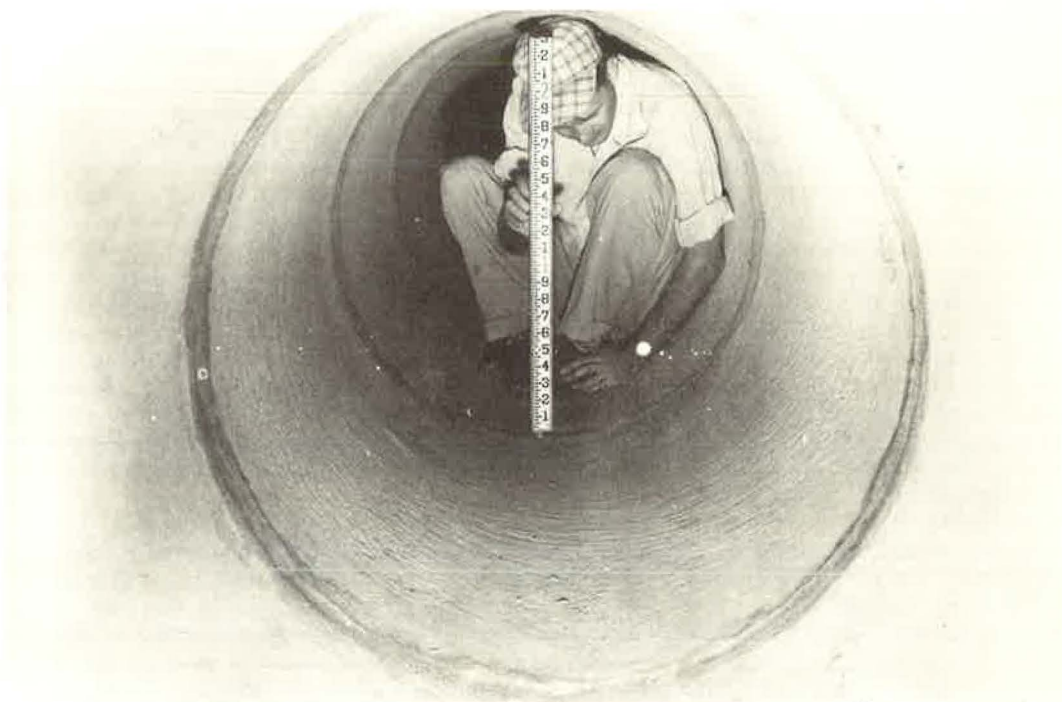

Figure 5. Section of standard level rod used in settlement measurements.

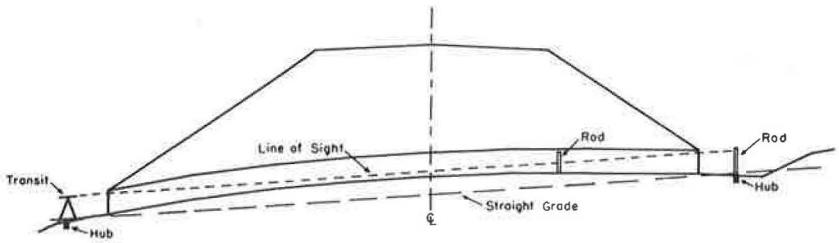

Figure 6. Sketch illustrating use of transit in measuring settlement within culverts laid on steep grades.

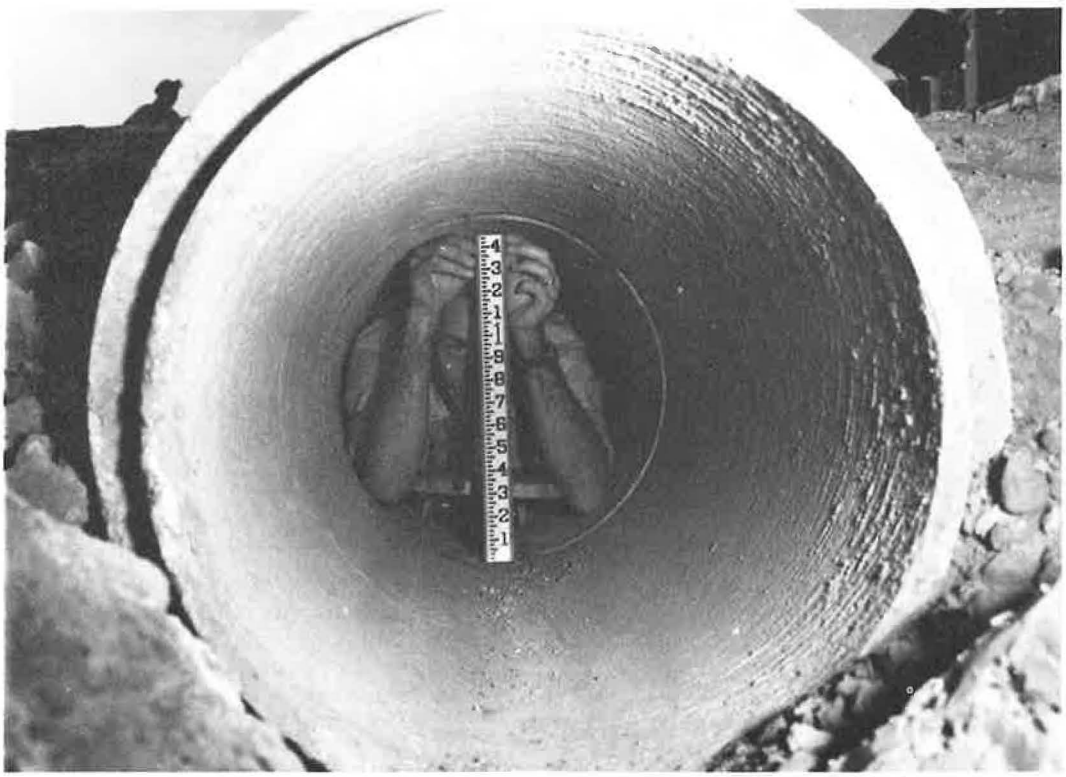

Figure 7. Short section of level rod used in conjunction with transit to measure culvert settlement.

grade line of the culvert was extended and a hub was driven 2 feet from each end of the culvert so that its top was on the grade-line extension. By using a transit, a line of sight could be obtained which was parallel to the straight grade line. A variation in a rod reading within the culvert from the height of the instrument above the straight grade line indicated the magnitude of camber or of settlement. This method is illustrated in Figures 6 and 7.

RESULTS AND DISCUSSION

From the 12 undisturbed samples obtained at the culvert sites, 10 fixed-ring and six floating-ring consolidation samples were trimmed and tested. It was not possible to perform the floating-ring consolidation test on Pipe E and F samples because they were

TABLE 2

VOID RATIOS DETERMINED BY CONSOLIDATION TESTS

Culvert Designation	Sample Number	Void Ratio					
		Pressure (T/sq ft)					
		0	¼	½	1	2	4
A	1 fixed	1.037	1.028	1.022	1.005	0.968	0.918
	1 floating	1.045	1.032	1.022	0.998	0.959	0.900
	2 fixed	0.672	0.659	0.651	0.640	0.625	0.610[a]
	2 floating	0.608	0.585	0.576	0.563	0.549	0.535[a]
B	1 fixed	0.722	0.712	0.702	0.684	0.653	0.620[a]
	1 floating	0.765	0.739	0.728	0.710	0.671	0.623
	2 fixed	0.680	0.673	0.665	0.651	0.629	0.598
	2 floating	0.720	0.708	0.697	0.679	0.650	0.610
C	1 fixed	1.058	1.009	0.985	0.932	0.864	0.799[a]
	2 fixed	0.933	0.922	0.907	0.859	0.791	0.727[a]
	2 floating	0.692	0.675	0.662	0.636	0.600	0.565[a]
D	2 floating	0.741	0.717	0.710	0.689	0.648	0.609[a]
E	1 fixed	0.783	0.753	0.736	0.702	0.653	0.607
	2 fixed	0.846	0.773	0.745	0.700	0.642	0.583
F	1 fixed	1.107	1.041	0.997	0.943	0.866	0.784[a]
	2 fixed	0.803	0.790	0.777	0.757	0.716	0.665
Average	—	0.826	0.801	0.786	0.760	0.718	0.672

[a]Extrapolated values from void ratio-pressure curves.

too soft to support the weight of the ring. Averages of the fixed- and floating-ring test values were used in settlement calculations when available for the same soil. Table 2 presents the void ratios and pressures obtained from each test.

To provide a simplified guide for estimating camber, a nomograph has been prepared. First, an average void ratio-pressure curve was plotted from the average of all consolidation data accumulated in this study. The void ratio scale was then converted to a settlement scale by use of

$$S = \frac{e_1 - e_2}{1 + e_1} \cdot D \qquad (1a)$$

$$S/D = \frac{e_1 - e_2}{1 + e_1} \qquad (1b)$$

where

S = total expected settlement,
D = thickness of compressible layer,
e_1 = initial void ratio, and
e_2 = final void ratio.

Because foundation soils at depths, the midplane in this case, are subjected to some pressure due to their own weight, a value for the initial void ratio, e_1, was arbitrarily selected as that value corresponding to a pressure of 0.18 ton/sq ft, which is equivalent

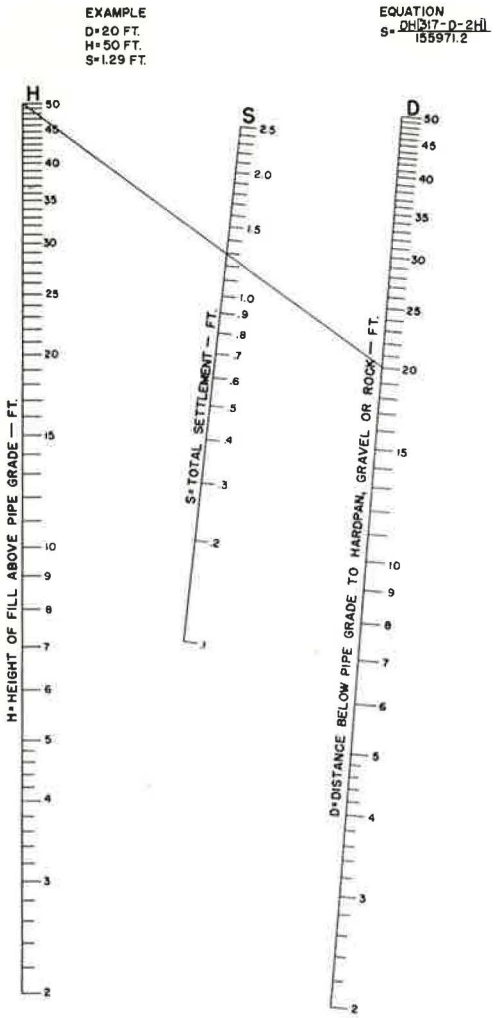

Figure 8. Nomograph for pipe settlement under fill.

to an embankment height of approximately 3 feet. The pressure scale was converted to a height-of-fill scale by determining the heights of fill material, weighing 120 pcf, corresponding to various pressures, or

$$H = \frac{2,000\ p}{120} = 16.67\ p \qquad (2)$$

where

p = pressure in tons/sq ft and
H = height of fill in feet.

Because the settlement versus height-of-fill curve did include the simplifying assumption that average foundation soils were loaded equally prior to constructing the embankment, a nomograph was prepared as shown in Figure 8. The nomograph was prepared by determining the best equation for the average void ratio-pressure curve and combining this equation with the more general equations previously given. This gave an equation in which height of fill and depth of foundation soil are necessarily known and settlement is the value sought. Examples of camber calculations are given in the Appendix.

The construction crew placed the culverts so that most of the elevation points were within a few hundredths of a foot of the correct values. The maximum error was a tenth of a foot for a very few scattered points.

As indicated in Figure 9, the cambered grade line for a pipe culvert placed beneath the 4-lane divided highway rose to some maximum value beneath the embankment for two lanes, dipped slightly due to the reduction in embankment height at the median strip, and then rose beneath the other two lanes before tapering to zero camber at the culvert outlet. Cambered grade lines for culverts beneath the undivided highways indicated the maximum values to be near the centers of the embankments and zero values at the culvert ends. No settlement was predicted for the culvert ends because they would carry very little load. However, some settlement, possibly due to a horizontal distribution of vertical stresses along the culvert or to disturbance caused by headwall construction, did occur at the ends.

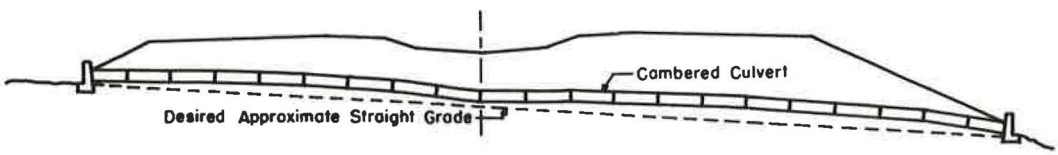

Figure 9. Typical cambered flow line for culvert beneath 4-lane divided highway.

In discussing the accuracy of the camber predictions, each culvert will be considered separately so that varying construction procedures and other factors which affected the study might be more clearly explained. Except for Pipe B, all embankment cross-sections shown in Figures 10 through 15 were obtained at the time of the last settlement measurements. The settlement curves do not necessarily indicate the total number of measurements obtained for a particular culvert, because many of them would

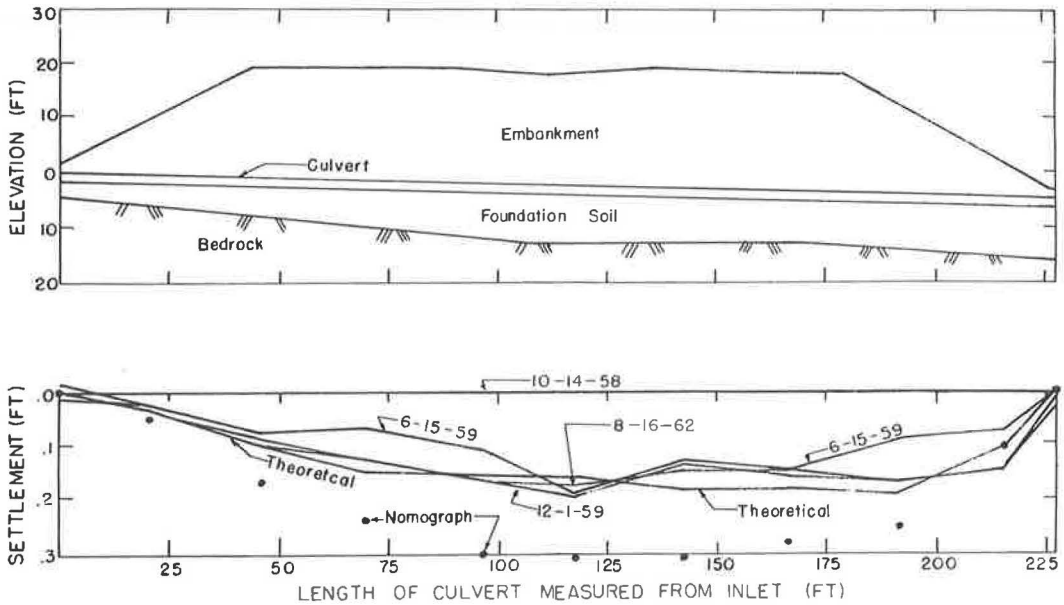

Figure 10. Actual and theoretical settlement curves for Pipe A.

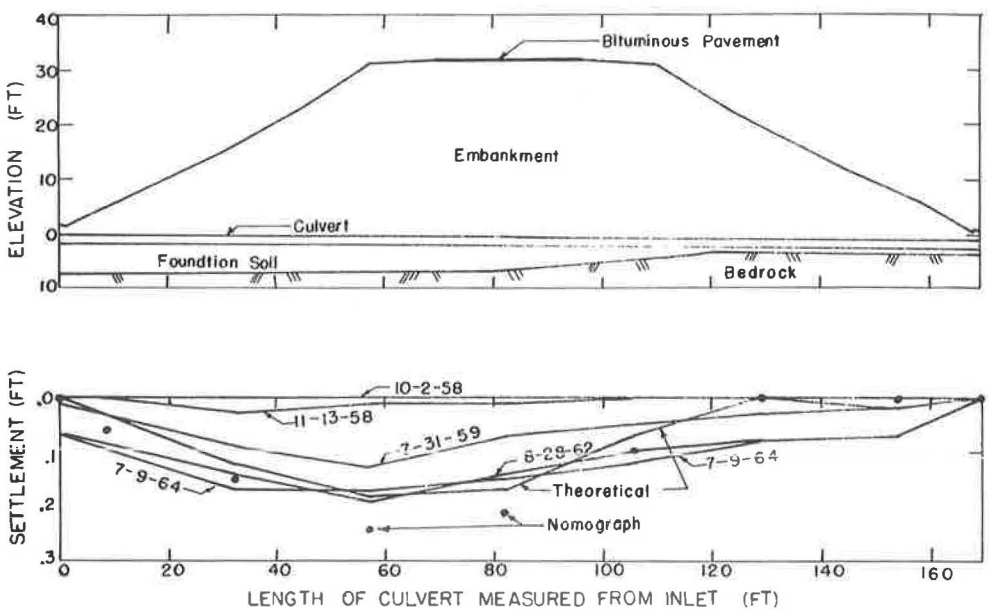

Figure 11. Actual and theoretical settlement curves for Pipe B.

almost coincide and would confuse the sketch. The settlement curve designated as "Theoretical" in Figures 10 through 15 were obtained by using the void ratio-pressure data for the soil sampled at each pipe location and applying Eqs. 1 and 2. The settlements marked "Nomograph" were obtained using Figure 8.

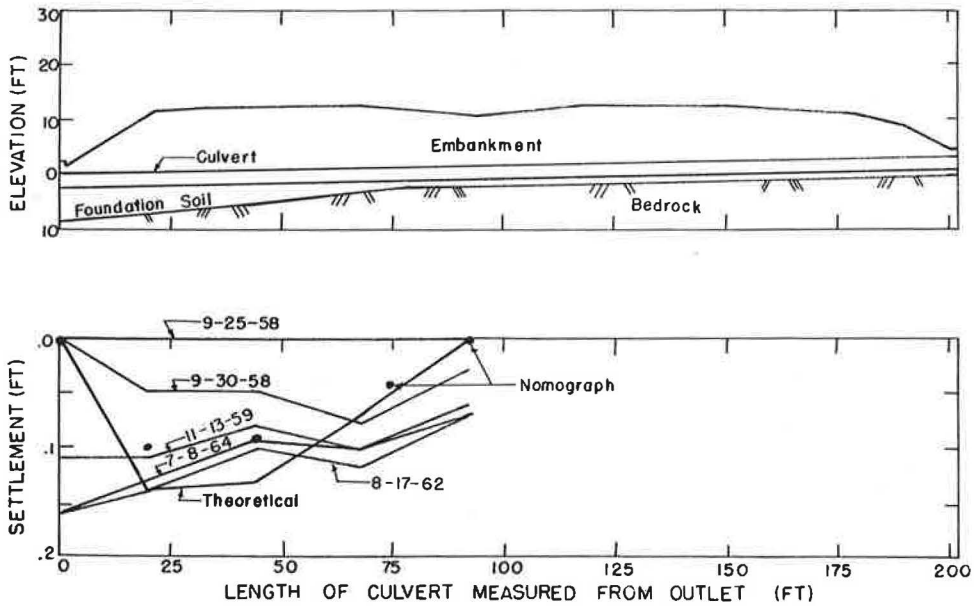

Figure 12. Actual and theoretical settlement curves for Pipe C.

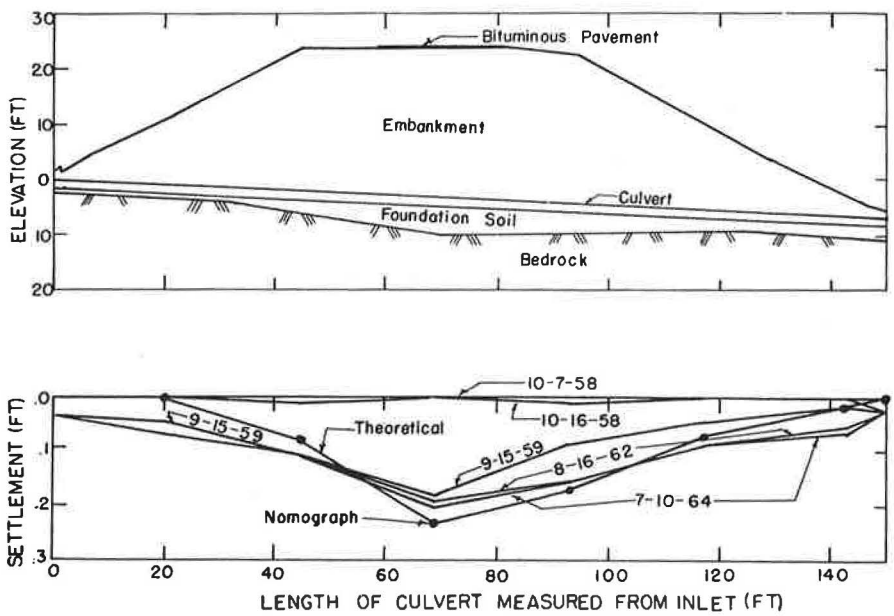

Figure 13. Actual and theoretical settlement curves for Pipe D.

Pipe A

Curves illustrating the predicted ultimate settlement and observed settlements at various time intervals are presented in Figure 10. It is noted that the maximum camber was required at a point near the shoulder of the highway over the outlet portion of the culvert where the combination of embankment height and depth of foundation soil

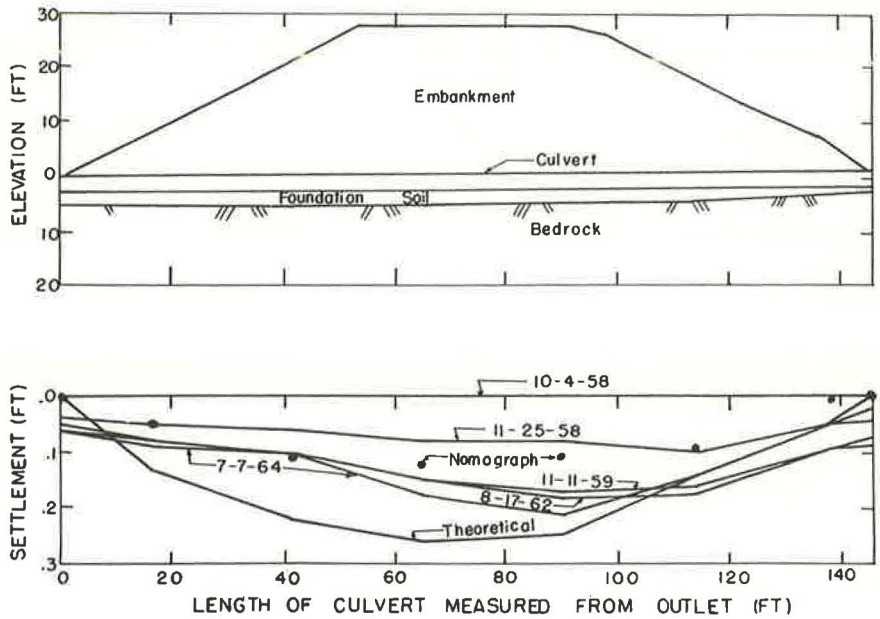

Figure 14. Actual and theoretical settlement curves for Pipe E.

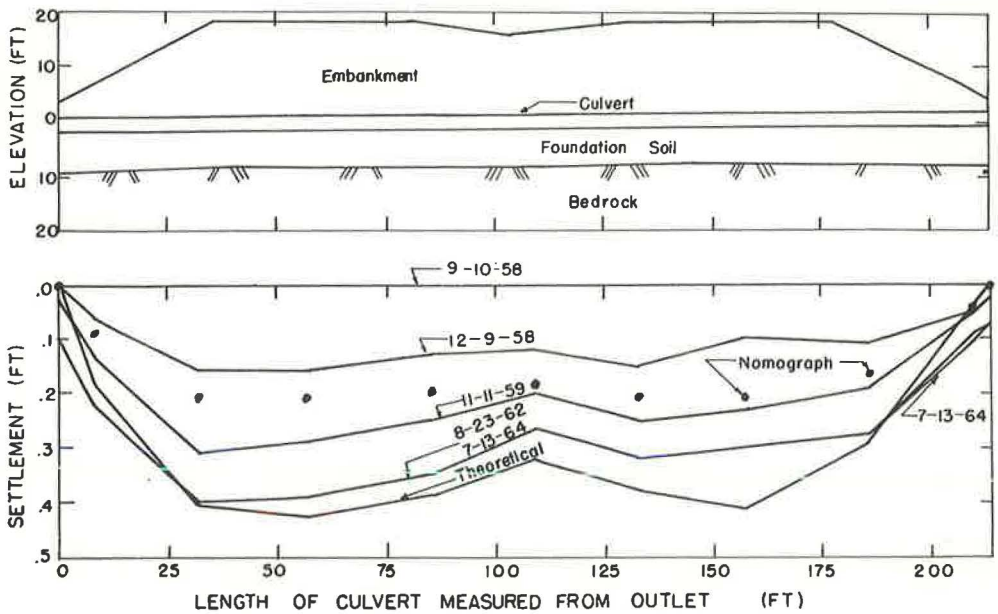

Figure 15. Actual and theoretical settlement curves for Pipe F.

was a maximum. Measurements taken on the 9-14-59 date coincided with the previous values near the center of the embankment but showed further settlement toward the ends of the culvert. This may be explained by the further addition of embankment near the inlet and the completion of the embankment covering a haul road near the outlet. A greater number of measurements was desired but could not be obtained within this 18-in. culvert because any slight sedimentation within the culvert prevented access.

Pipe B

This 24-in. culvert was installed using a B_1 bedding as called for by Kentucky Highway Department Specifications. The construction of the B_1 bedding is similar to that of the "imperfect trench" method. Loose hay was used as the compressible material in backfilling the trench. As shown in Figure 11, the measurements indicate a favorable trend—that is, the settlement curve has approached the predicted curves.

Pipe C

This culvert is under a relatively low embankment and the foundation soil is relatively shallow. It was included in the investigation because of its nearness to other culverts studied. Figure 12 shows that the inlet portion was laid close to the solid rock; camber and settlement data are shown for the outlet portion of the culvert. Significant settlement was observed at the outlet and near the centerline of survey where the culvert was close to rock. This is partially explained by the fact that earth-moving equipment passed over the culvert before the pipe was covered adequately.

Pipe D

Figure 13 reveals a good comparison between actual and predicted settlement for this 18-in. culvert which was also constructed using a B_1 bedding. It will be noted that actual settlement along the inlet portion of the culvert has already exceeded the predicted ultimate value. Again, this may be attributed to the frequent passage of heavy equipment along a haul road over the culvert immediately after construction of the backfill.

Pipe E

This culvert had the largest diameter, 36 inches, in the group and also required B_1 bedding. The foundation soil was rather shallow throughout the culvert site but was one of the more compressible soils tested. The actual settlement curves (Fig. 14) conform in a general way with the shape of the predicted settlement curve, but they do not yet agree in magnitude.

Pipe F

This 30-in. culvert, the first one constructed, was placed on a foundation soil which was rather uniform in depth. When construction was started, the resident engineer decided to remove a portion of the undesirable foundation soil and to replace it with a more suitable material. Settlement calculations were not corrected for this change, and, of course, this accounts, in part, for the fact that actual settlements have not been as great as the predicted values. This fact is illustrated by the curves in Figure 15.

CONCLUSIONS

Insofar as the soils involved in this study might be considered to be typical of many areas in Kentucky and perhaps elsewhere, it may be inferred that the camber and settlement data offered herein would provide a reasonable approximation of the settlement expected in many pipe culvert installations. In assuming the soils to be typical, it is implied that the decreases in the void ratios for each increment of load determined for these soils are more or less average. On this basis, then, the settlement of the midplane of the foundation soil, which is also taken as the settlement of the culvert, is directly proportional to the decrease in void ratio occurring within the foundation soil. A composite expression of the decrease in void ratio in terms of the fill height and depth

of foundation soil should provide the best generalization obtainable from the data available. It is believed that such a generalization is satisfied by the camber guide, presented in the form of a nomograph, since it does take into account the initial void ratio of a foundation soil produced by its own weight above its midplane and also the change in the void ratio as a result of the additional load produced by the weight of fill. The nomograph was prepared on the assumption that the foundation soil would have a submerged unit weight of 65 pcf and that the embankment material would have a unit weight of 120 pcf. More precisely, if the soils involved in this study are assumed to be typical, the nomograph satisfactorily performs the same operations as the more general settlement calculations with the exceptions that it does not allow for any stress distribution through the foundation soil, nor does it apply to a compressible layer of soil at great depths.

Of course, it is recognized that no truly average or typical soil exists and, therefore, the nomograph will yield varying degrees of accuracy (as shown in Figs. 10 through 15) depending on the variance from the so-called typical soil and its associated void ratio-pressure curve. It should be remembered that the soils encountered in this study consisted predominantly of silty clays and some clay silts and clays. Sands, gravels, and nonplastic soils would have consolidation characteristics different from the soils studied and would be obvious exceptions from the typical soil on which the nomograph is based. It is implied, moreover, that the field engineer must determine the depth of foundation soil and height of fill expected at each culvert site and make a cursory appraisal of the soil. Exceptional soils and exceptional depths of soils and fill heights may merit special investigation. Thus, use of the nomograph should be tempered with judgment.

Although the culverts studied in this project consisted of reinforced concrete pipe, it may be inferred that the guide developed therefrom would apply equally well to other situations. The nomograph has been based on Terzaghi's theory of primary consolidation, and the nomograph is thus applicable to those situations in which settlement is likely to occur by this process. There is no reason to think that the nomographic guide would not apply equally well to corrugated metal pipe culverts as well as box culverts.

It is suggested that this method of estimating settlement may find useful application in other situations involving subsidence of embankments. The differential settlement occurring between bridges and their approach embankments (see Fig. 16) is a serious problem in highway maintenance (6, 7, 8). On modern roads, this defect has become a hazard to high-speed traffic, and remedial work is expensive and causes considerable inconvenience to road users. There are, as yet, no confirming data to show whether or not the difficulty arises from consolidation within the foundation soil or to show that it can be attributed largely to volume changes within the embankment material.

A typical example of such a situation is illustrated in Figure 17. It will be noted that the abutment of the bridge is placed on piles which are bearing on firm rock at significant depth. Generally, there is a considerable depth of relatively compressible material between the rock level and the natural ground line. It is not unreasonable to expect that the placement of significant embankment material over the foundation soil will cause a differential settlement between the approach embankment and the bridge deck since the embankment can settle as a result of consolidation occurring within the original ground and the abutment cannot because it is founded on piles bearing on rock. According to the nomograph presented in Figure 8, differential settlement of approximately one foot may be expected between the approach slab and the bridge deck. This entire amount of settlement may not occur after the pavement has been completed and, therefore, may not be manifestly apparent in the final grade because some of this settlement will, of course, occur during the construction period as the embankment is placed. The differential settlements which have been noted at bridge approaches in Kentucky appear to be typically on the order of 4 to 6 inches. Although the possibility of volume changes occurring within the embankment itself should not be overlooked, it must be recognized that embankment loadings of as much as 15 or 20 feet on the natural soil may induce significant settlement. The nomograph presented in this paper might serve as a guide to estimate the order of magnitude of such settlements, and to suggest the possible need for special provisions to account for or minimize these unwanted settlements.

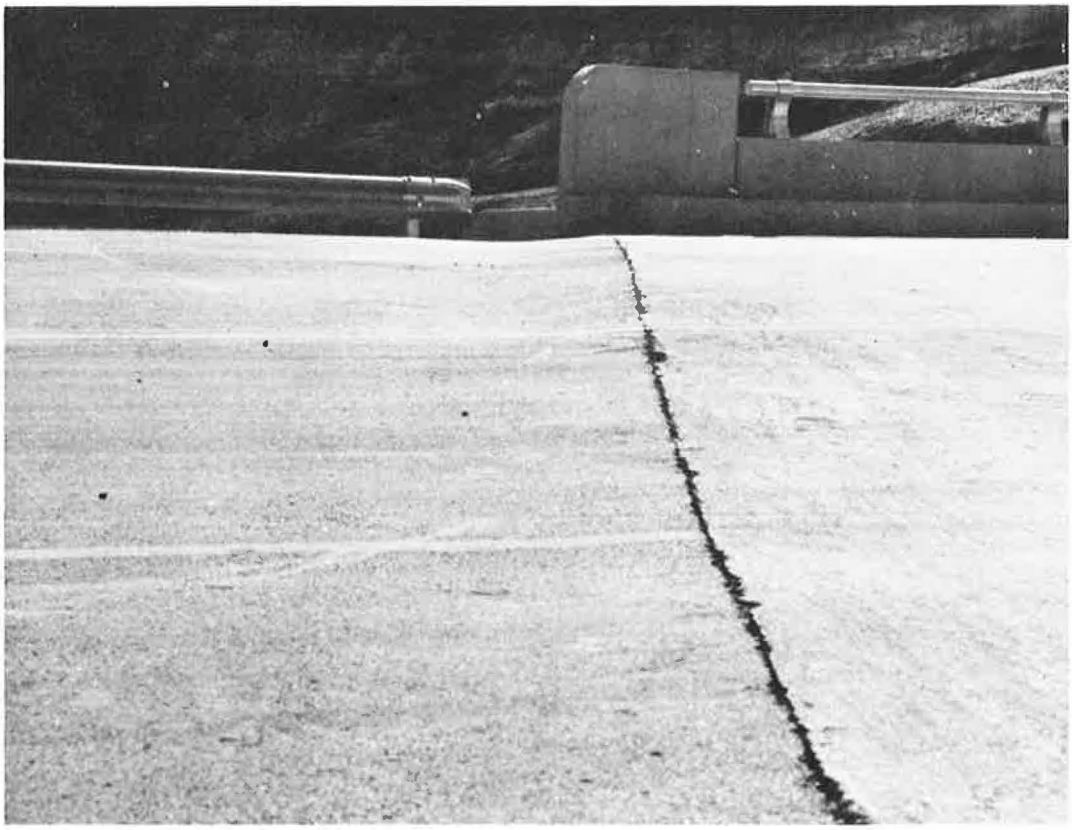

Figure 16. Settlement of bridge approach.

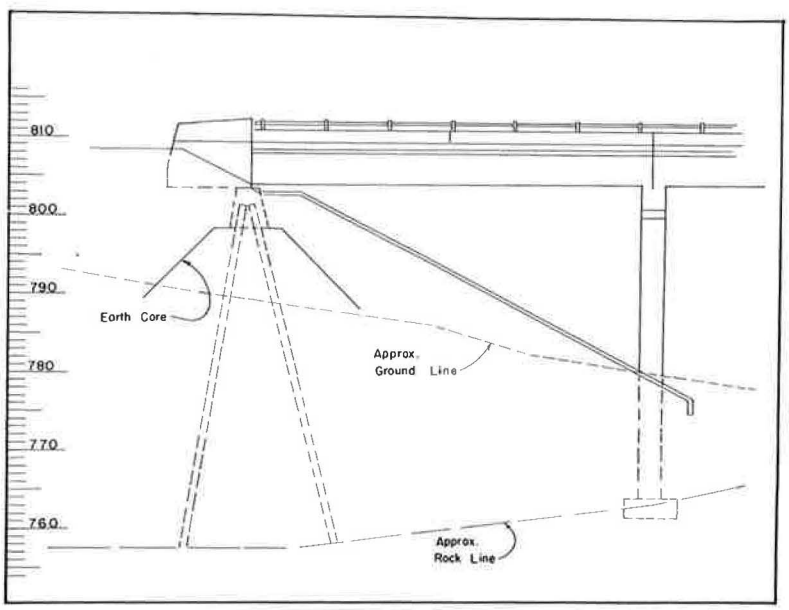

Figure 17. Example of conditions which might contribute to settlement of bridge approaches.

REFERENCES

1. Standard Specifications for Road and Bridge Construction. Kentucky Department of Highways, 1956 (Section 5.11.3).
2. Armco Drainage and Metal Products. Handbook of Drainage and Construction Products. Pp. 244-245, 436, 1955.
3. Spangler, M. G. Influence of Compression and Shearing Strains in Soil Foundations on Structures Under Earth Embankments. Highway Research Board Bull. 125, pp. 170-177, 1956.
4. Terzaghi, Karl. Theoretical Soil Mechanics. John Wiley and Sons, 1943.
5. Webber, Ray. Description of a Method of Predicting Fill Settlement Using Void Ratio. Highway Research Board Bull. 173, pp. 80-93, 1958.
6. Jones, C. W. Smoother Bridge Approaches. Civil Engineering, June 1959.
7. Peck, R. B., and Ireland, H. O. Backfill Guide. Journal of Structural Div., ASCE, Vol. 83, ST4, July 1957.
8. Margason, G. A. A Study of the Settlement of a Number of Bridge Approaches on the Maidenhead By-Pass. Chart. Mun. Engr., Institution of Municipal Engineers, England, Vol. 60, 1963.

Appendix

EXAMPLES OF CAMBER CALCULATIONS

Example 1. 2-Lane Highway

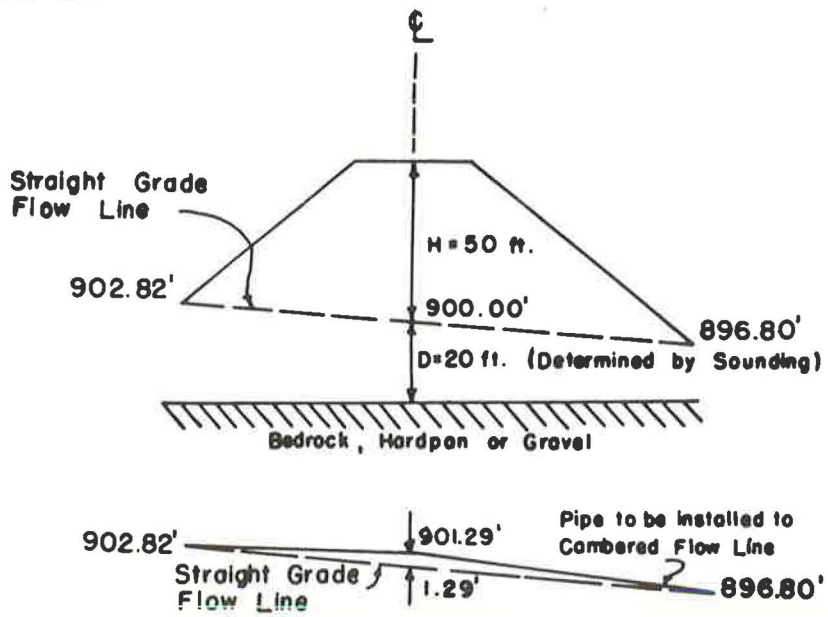

To Determine Expected Settlement:

Lay straight-edge from 20 feet on D line to 50 feet on H line and read settlement of 1.29 feet on S line (Fig. 8).

Note: In no case should camber be installed to the extent that a downstream elevation is higher than some upstream point of elevation. This problem may occur if a culvert has a small difference in inlet and outlet elevations. In such a case, the maximum camber permitted by these limiting elevations should be installed. Occasionally, the inlet portion of a culvert may have to be placed on a straight horizontal grade line at an elevation equal to that of the inlet.

Example 2. 4-Lane Divided Highway

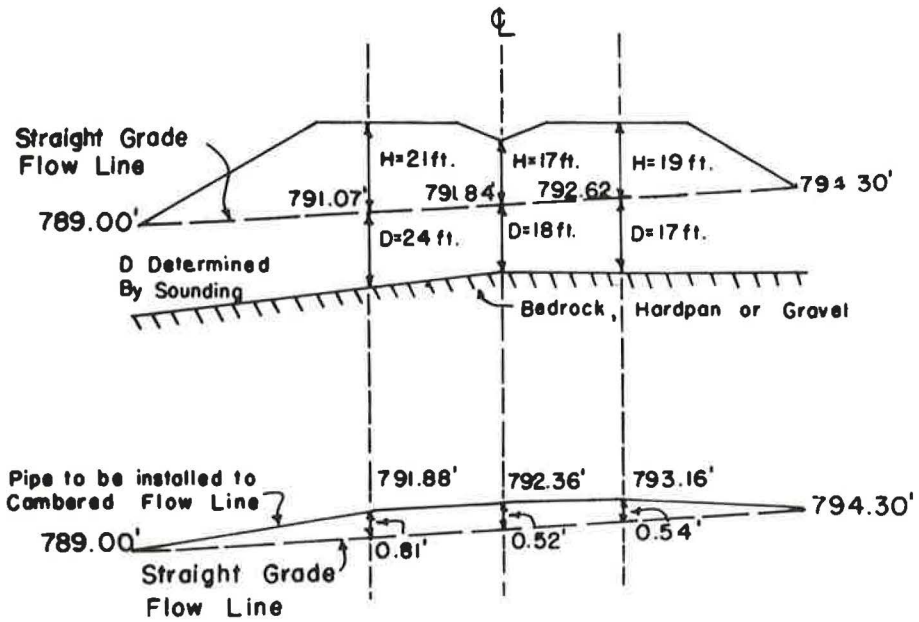

To Determine Expected Settlement:

Of centerline of roadway over outlet portion of culvert—lay straight-edge from 24 feet on D line to 21 feet on H line and read settlement of 0. 81 feet on S line.

Of median—lay straight-edge from 18 feet on D line to 17 feet on H line and read settlement of 0. 52 feet on S line.

Of centerline of roadway over inlet portion of culvert—lay straight-edge from 17 feet on D line to 19 feet on H line and read settlement of 0. 54 feet on S line.

Field Verification of Ring Compression Conduit Design

J. DEMMIN, Armco-Thyssen, Dinslaken, Germany

•IN July 1963, Armco-Thyssen, a joint venture of Armco Steel Corporation, Middletown, Ohio, and August Thyssen-Huette, Duisburg-Hamborn, Germany, carried through live-load and loading-to-failure tests. The test structure was a 7-gage multi-plate pipe arch of 20-ft 7-in. span and 13-ft 2-in. rise, Armco's largest structure of this shape on record.

The live-load test was conducted to prove to the German Federal Railway that large corrugated steel structures are safe for use as conduits and underpasses in railway embankments. Therefore, the live-load test was to be conducted under the severest possible loading conditions required by the German Federal Railway design criteria, considering a safety factor of 3. The loading-to-failure test was conducted to provide scientific data on the behavior of corrugated steel structures under loading conditions, especially to determine under what load the structure would finally collapse and how this collapse developed. Both tests were conducted on the same test structure. Only the cover height and the positioning of the load were varied according to the different test purposes.

Size and gage of the structure were primarily designed for practical considerations suggested by the test purposes. For general acceptance of corrugated steel structures by the Federal Railway, it had to be proved that even the largest structure designed, of the most unfavorable shape, would satisfy performance requirements. Pipe arches, in particular, were considered statically unfavorable. Therefore, Armco's largest pipe arch was chosen as a test structure. Since the cover was low and the live load was fairly small, the wall thickness was not determined by ring-compression methods, but by empirical data applying to the structure during backfilling. Therefore, the wall thickness was designed by the "flexibility factor."

The suggested maximum flexibility factor is 5.0×10^5; $FF = D^2/J$. Since the periphery of this pipe arch is 20 ft 7 in. × 13 ft 2 in. = 207π (see Armco Catalog MP-1663), for the pipe-arch structure D = 207. In addition, the moment of inertia of multi-plate wall for 7-gage thickness is given by $J = 0.1080$ in.^{4}/in. and for 8-gage thickness by $J = 0.0961$ in.^{4}/in. Therefore, the 7-gage flexibility factor $FF = 207^2/0.1080 = 3.97 \times 10^5$ (o.k.), and the 8-gage flexibility factor $FF = 207^2/0.0961 = 4.46 \times 10^5$ (o.k.). With a special view to the loading-to-failure test and since the same structure was to be used for both tests, a wall thickness of 7 gage was chosen.

TEST SETUP

Test Structure and Backfilling

The pipe-arch structure—20-ft 7-in. span and 13-ft 2-in. rise—to which loads were to be applied, consisted of two rings, each of 8-ft length, which could freely deflect (Fig. 1). This 16-ft long test structure was completely within the pressure area of the applied load under the selected cover heights. Additional pipe sections were attached to this central body. The section at the open end was also made up of two rings bolted together, whereas only one ring section was added to the rear which was closed by a wooden cover and backed up with earth. The pipe sections adjacent to the central body were only to serve for widening the upper grade surface, thus reducing the danger of subgrade failure. They were separated from the center body by 4-in. wide gaps to

NOTE: In this paper kp (kilopond) is equivalent to kilogram (kg).

Paper sponsored by Committee on Culverts and Culvert Pipe.

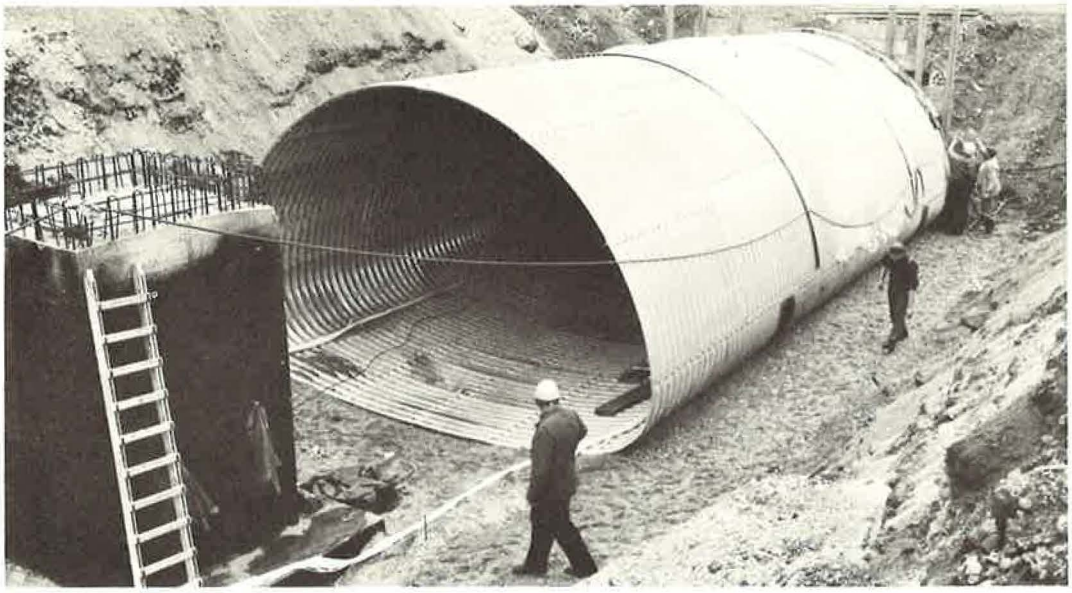

Figure 1. Test structure before backfilling.

Figure 2. Placement and compaction of backfill.

permit independent deflection of the actual test structure. Only the lower corner plates of all sections were firmly connected. To prevent soil seepage, the gaps between the pipe sections were covered with 10-gage corrugated metal strips of 1.5-ft length.

Backfill material was placed in lifts of 8 in., with each layer tamped separately (Fig. 2). Gravel was used as backfilling material and surface vibrators were employed for compaction. Tamping operations were continuously checked by drop-penetration testing. A laboratory Proctor test showed a soil density of 107 percent of single Proctor density (see Appendix).

The test was carried out in the works area of the August Thyssen-Huette plant. An excavated site that was to accommodate heavy column foundations served as a trench. The test structure was installed between two strong concrete pillars.

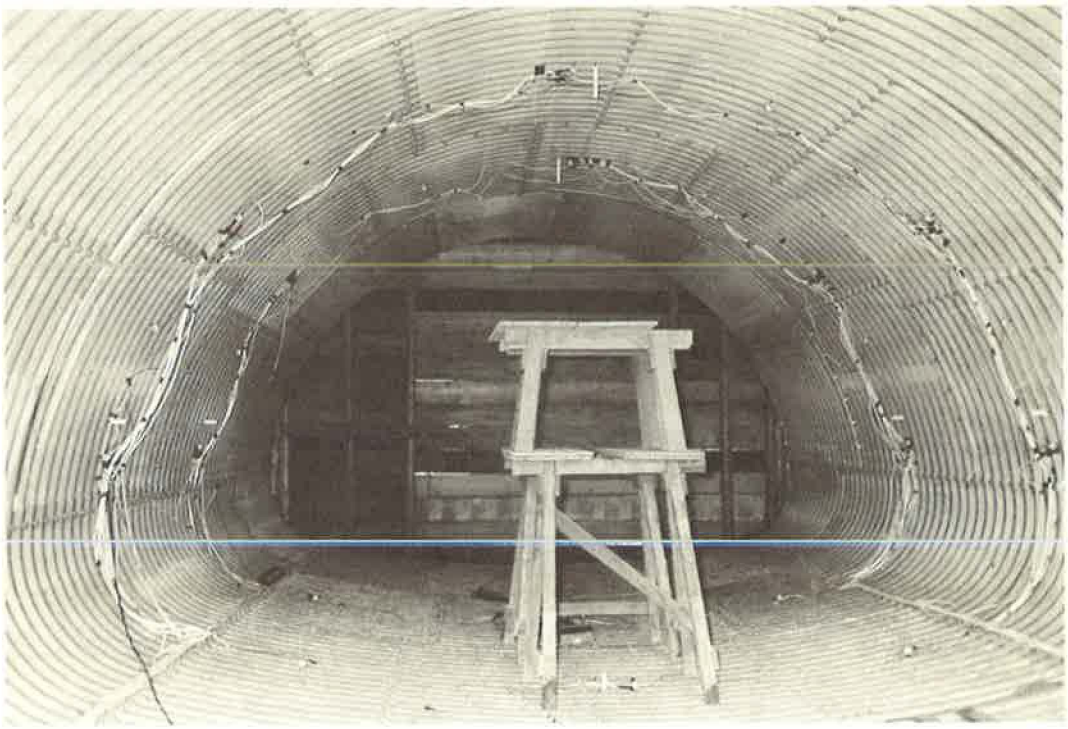

Figure 3. Inside view of structure.

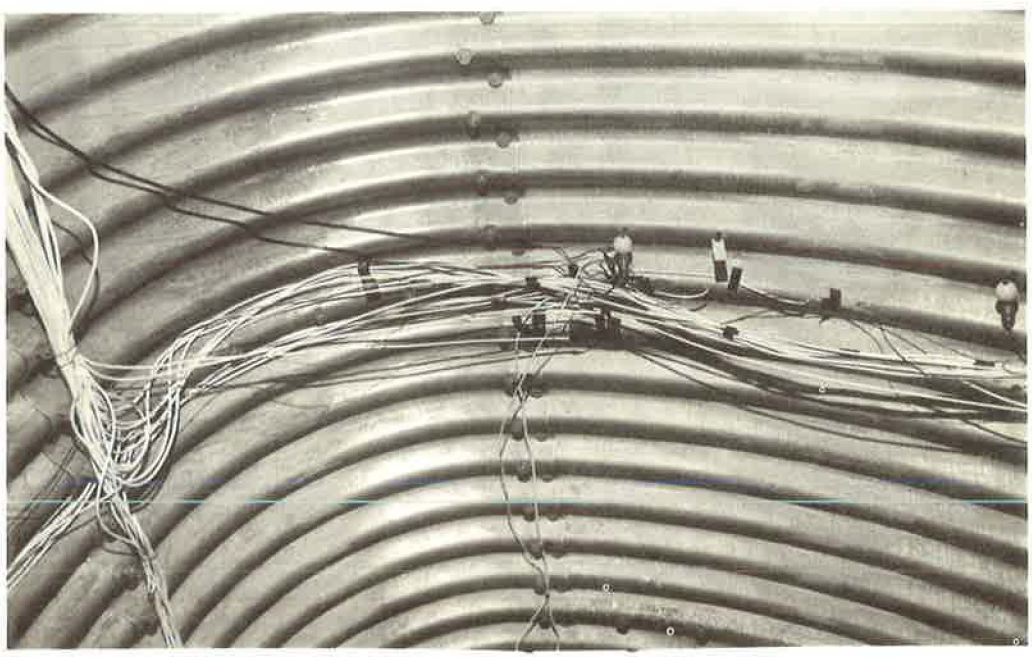

Figure 4. Partial view with measuring elements.

Measuring Instruments

Strain measurements were taken with strain gage strips. Three gages were installed at each of six measuring points (in the trough, and the crest of the corrugation and near the axis through the center of gravity of the corrugated profile) in two sectional planes. They were glued on with the special X-60 adhesive. To compensate for the influence of thermal expansion, compensation strips were placed near the gage points. To accomplish this, gages were stuck into small test coupons of the pipe-arch material. These were attached to the pipe arch so that they would undergo the same thermal expansion as the test structure without suffering any strain through the imposed load. The actual

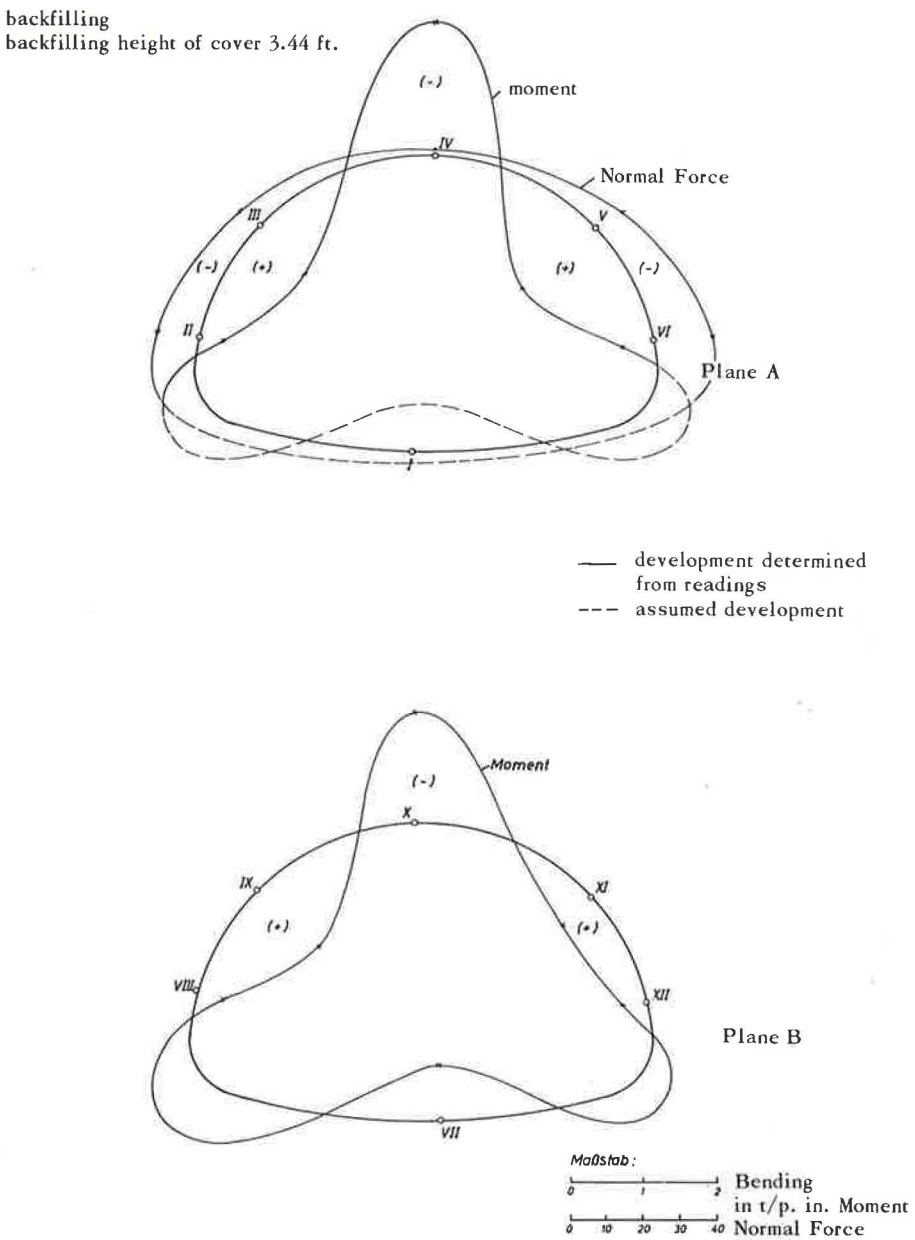

Figure 5. Development of normal forces and bending moments from reading taken.

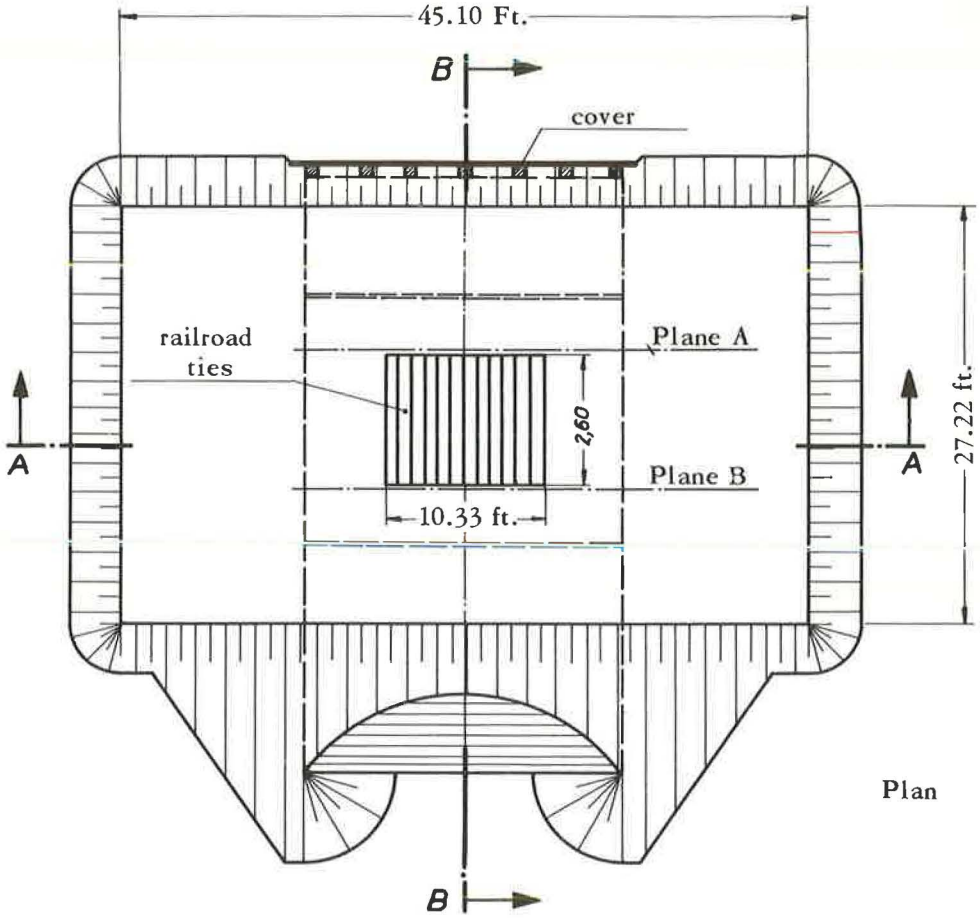

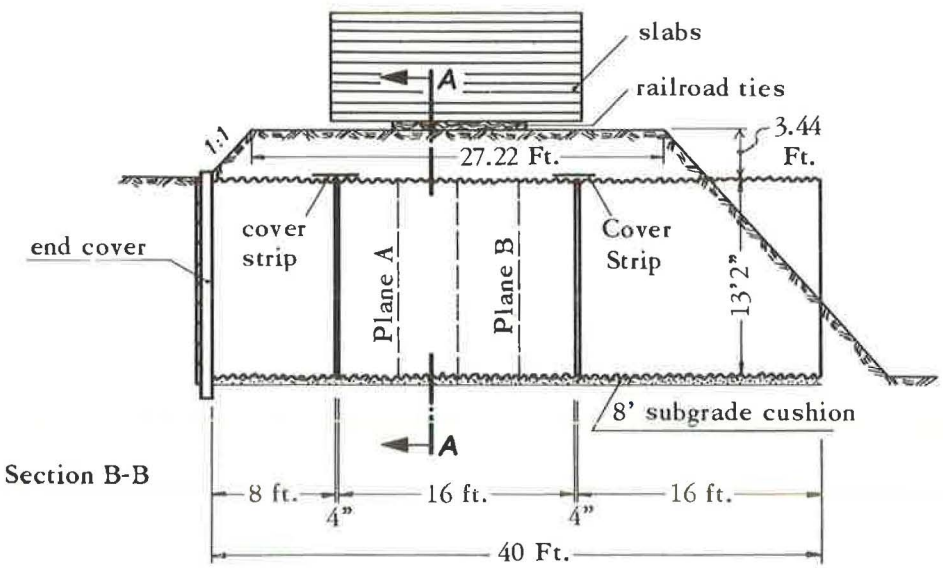

Figure 6. Setup for live-load-test.

Symmetrical Loading

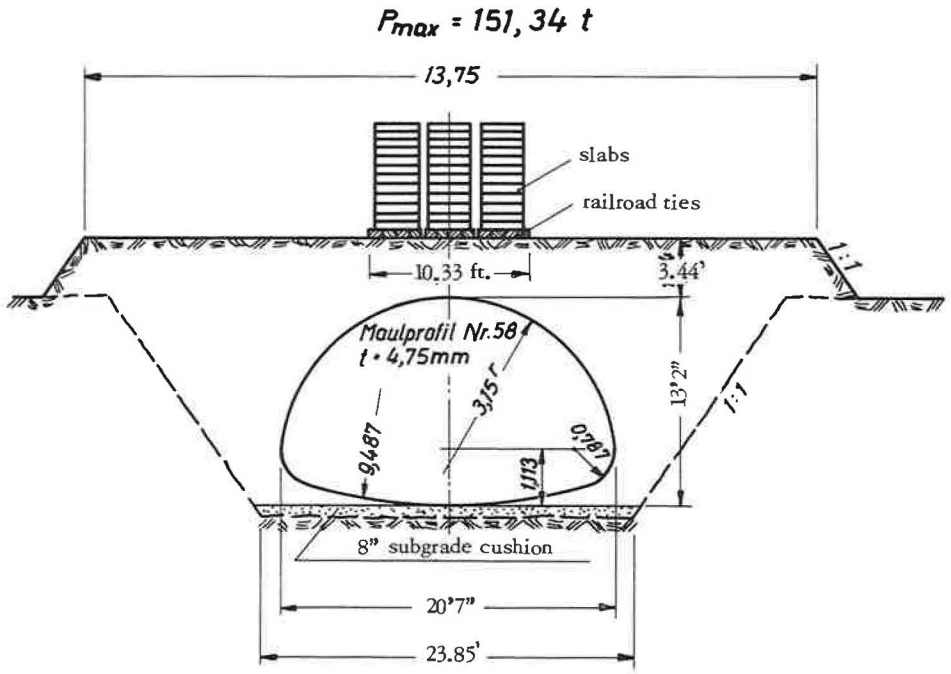

Section A-A

Off-center Loading

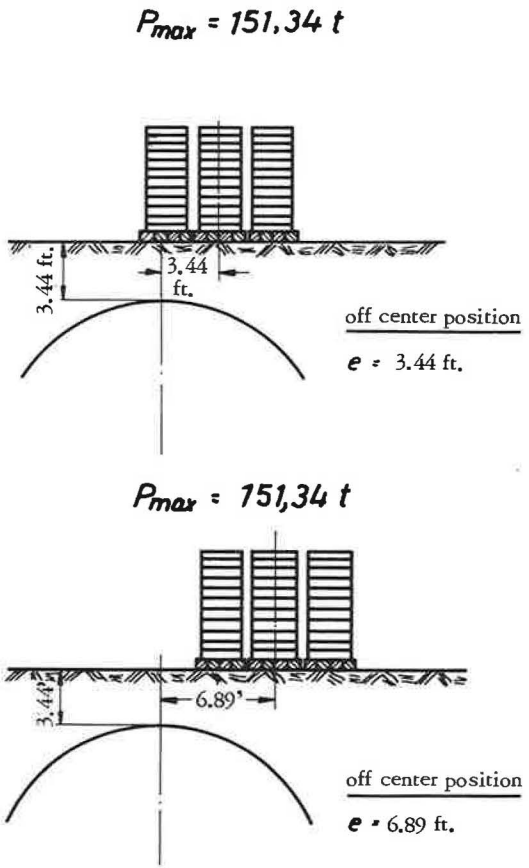

Figure 6. Continued.

strain was determined by establishing the difference between the measured value and a base reading taken before loading (Figs. 3 and 4).

Deformation was measured photographically. Measuring lights, with a black dot in the middle of each bulb, were installed next to and between the strain gage points. Zeiss-Jena phototheodolites registered the displacements of the dots so that the magnitude and direction of the displacements could subsequently be determined from the photographs by a stereocomparator. This procedure permitted indication of the movement of measuring points with an accuracy of 0.02 in. To be able to determine pipe-arch deformation on the spot at any time, additional gage pins were placed in the crest, the invert and on the side walls. By means of a theodolite, the displacement of the leveled points could then be read off immediately.

LIVE-LOAD TEST

After installation of the instruments required for strain and deformation measurements, backfilling and covering operations were begun on June 18, 1963. During backfilling and earth tamping, considerable vertical deflection of the pipe arch was noted. With 3.44 ft of cover, the horizontal diameter had decreased by 2.64 in., and there was an elongation of 3.86 in. in the vertical diameter; i.e., the crest was pushed up by 3.62 in. while the invert settled 0.24 in. (zero reading: pipe free in trench). At the same time, there was a considerable increase in the extreme fiber strains and, consequently, the extreme fiber stresses.

Extreme fiber stresses due to backfilling and cover of 3.44 ft over pipe center (Fig. 5) were in crest point IV $\sigma_1 = +31,931$ psi, $\sigma_3 = -39,299$ psi, and in crest point X $\sigma_1 = +28,759$ psi, $\sigma_3 = -30,466$ psi. To support the load, 8.53-ft long railway ties were placed side by side on the surface grade parallel to the pipe-arch axis, covering a

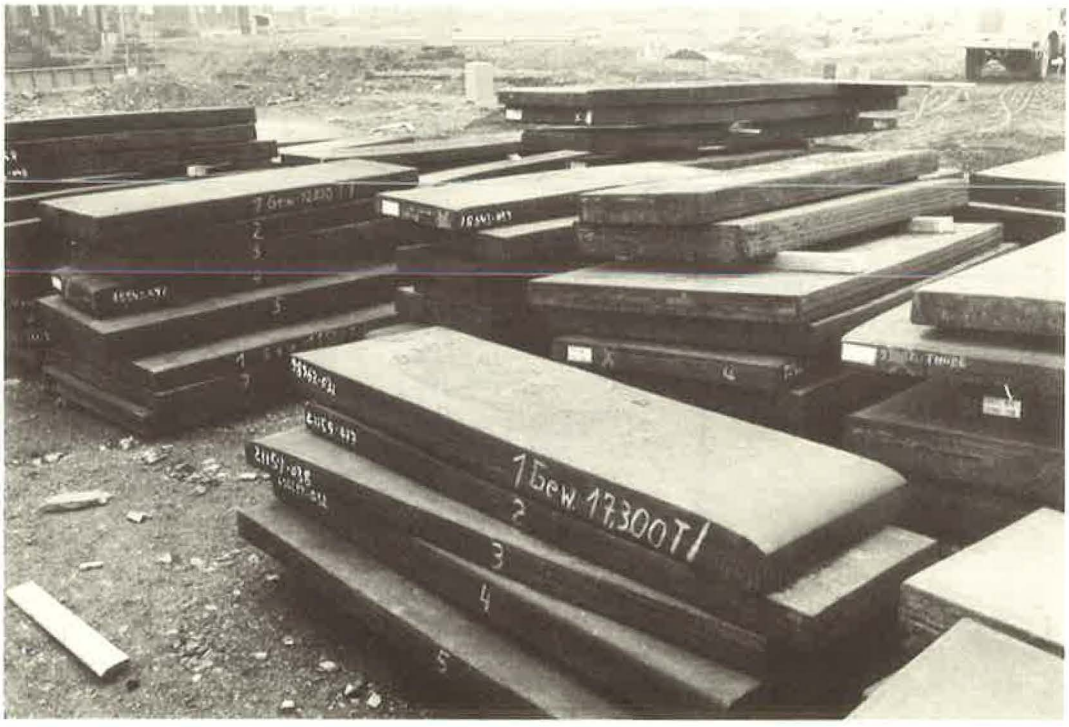

Figure 7. Slabs ready to be placed on structure.

width of 3 × 3.44 = 10.33 ft, or about half the clear span of the pipe arch. Thus, the supporting area was 8.53 × 10.33 ft = 88.11 sq ft (Fig. 6).

Steel slabs from the August-Thyssen steel mill were used as a load (Fig. 7). For the live-load test, the Munich Central Office of Federal Railways had determined that 50 tons was the most severe load a structure of similar span might have to carry. This represents the load transmitted by a two-axle railway car, each axle weighing 25 tons. Considering a safety factor of 3, the total load for the live-load test was to be 150 tons. This load was to be applied by three independent slab piles placed axially on the pipe arch and also on one side only, since for arched supporting structures, off-center loading will often constitute the severest condition. For the loading-to-failure test the steel slabs were also used as a load. As the actual carrying capacity was unknown, a maximum load of 1,000 tons based on a computation with the ring compression formula was planned to be applied for this test. With a supporting area of 88.11 sq ft, this load could be imposed only by piling the slabs crosswise.

On June 21, 1963, a cover height of 3.44 ft, or one-sixth the span, was reached, so that loading could begin. The steel slabs weighing between 5 and 10 tons, weighed in advance, were positioned on the ties by a crane. Strain and deformation were measured at 25-ton load increments. These measurements showed that deflections and strains resulting from the overhead load were small in comparison to those that had resulted from backfilling and acted in the opposite direction. To start with, a load of 151.32 tons was applied axially over the pipe arch (Fig. 8). Until then, no marked changes in deflections and strains appeared. Results from application of this load (Fig. 9) were as follows:

Plane 1—downward deflection in crest 0.374 in.;
Plane 2—downward deflection in crest 0.339 in.;

Figure 8. Live-load test, test structure with 151.32-ton axial load.

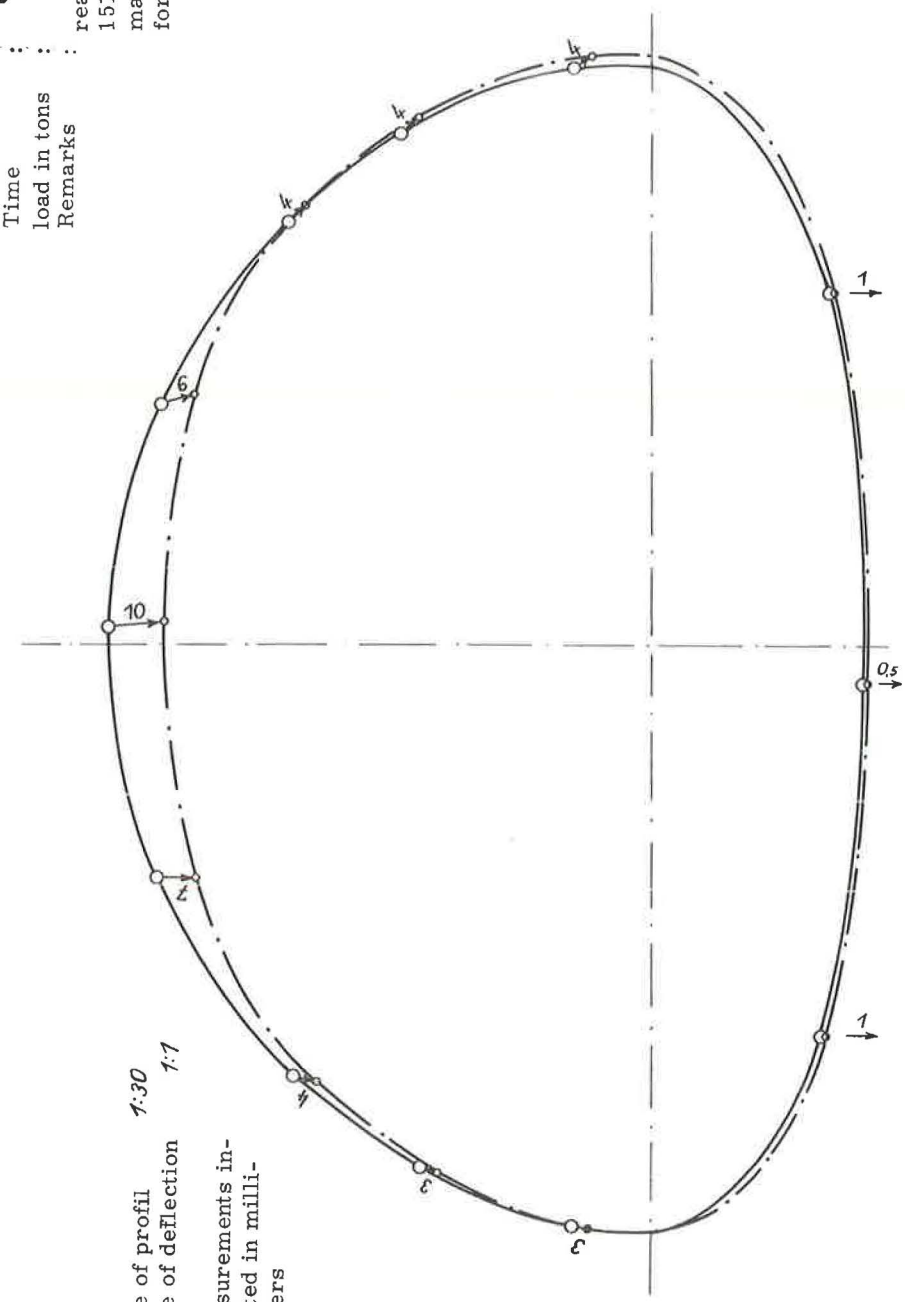

Figure 9. Live-load test, deformation measurement.

live-load-test
applied load P = 151, 32 t
readings 6 to 12

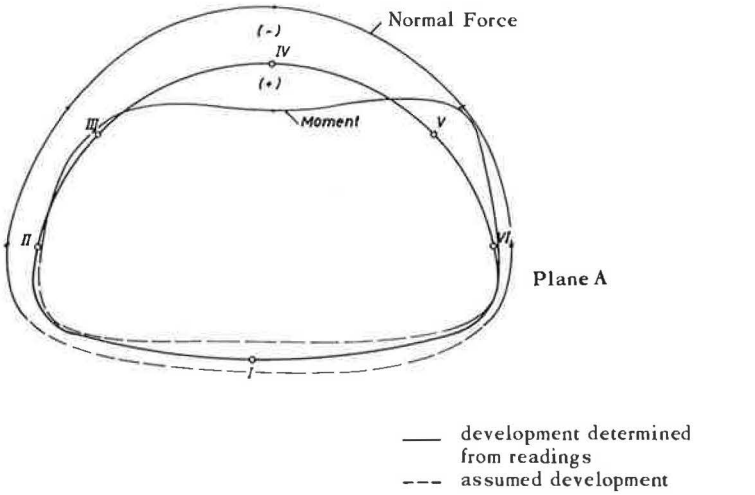

—— development determined from readings
--- assumed development

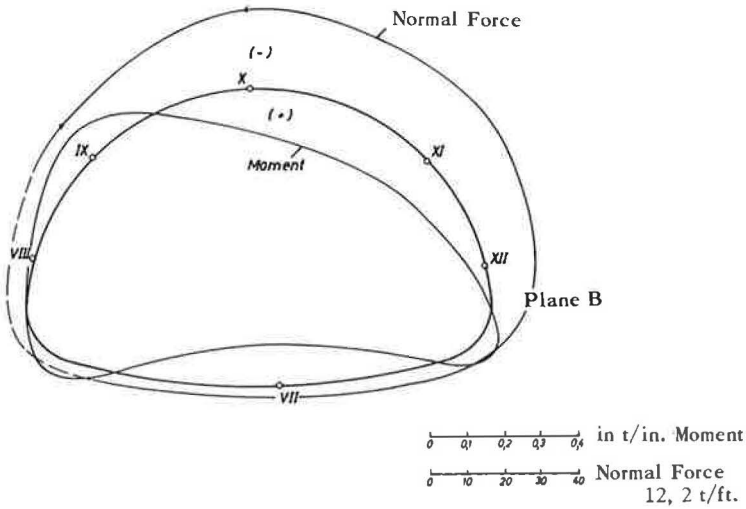

Figure 10. Development of normal forces and bending moments from reading taken.

Changes in extreme fiber stresses (Fig. 10) in crest point IV σ_1 = -6,088 psi, σ_3 = -626 psi; and in crest point X σ_1 = -7,353 psi, σ_3 = -2,717 psi.

The load of 151.32 tons was left in place for 6 days, and readings were taken each day. Both the strain and deflection measurements varied at different times. During the 6 days and, indeed, during loading operations, there was a shift in soil pressures which, however, died away after a few days. Thus, practically no further change in deflection could be noted on the third day. It was also observed that deflections and strains were not symmetrical, although the gage points were located symmetrically and

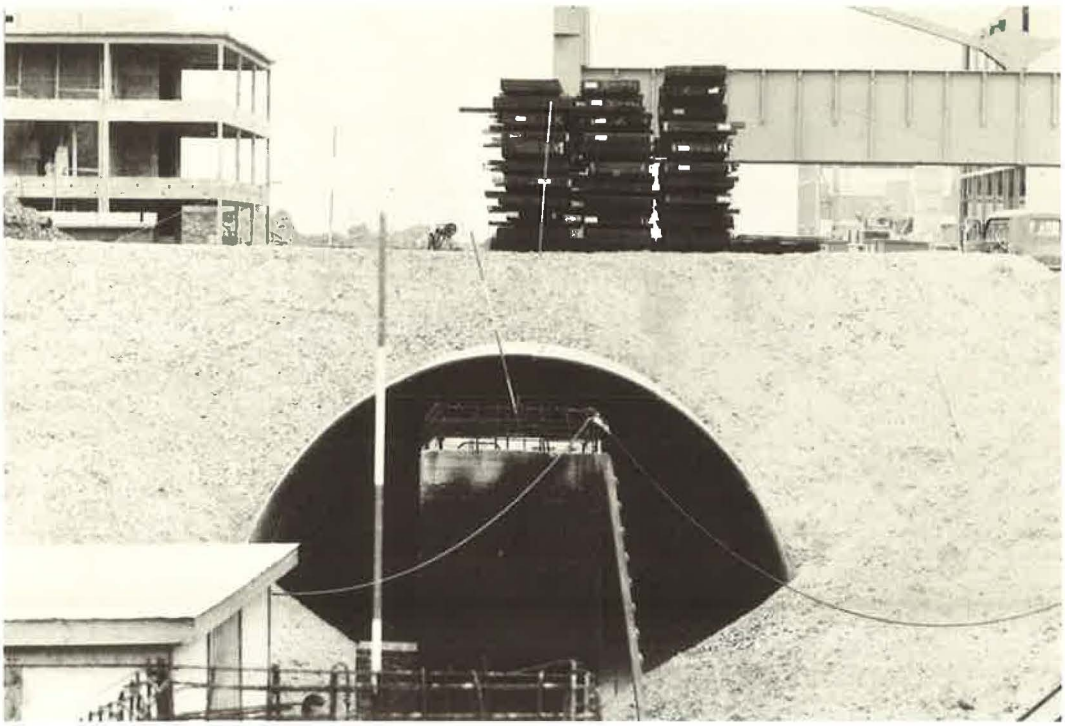

Figure 11. Test structure under load of 151.32 tons applied in 3.44-ft off-center position.

Figure 12. Test structure under load of 151.32 tons applied in 6.89-ft off-center position.

care had been taken to place the load as near as possible over the center. Apart from inevitable off-center loadings, this development may be traced primarily to non-uniform backfill material. The deflections caused by backfilling were only slightly diminished under this load.

After 6 days the load was removed to one side by shifting the slabs (Fig. 11). First one of the outer piles was moved to the other side, and after that the center pile. Loading was then 6.89 ft off-center (Fig. 12). Only very slight strains and deformations

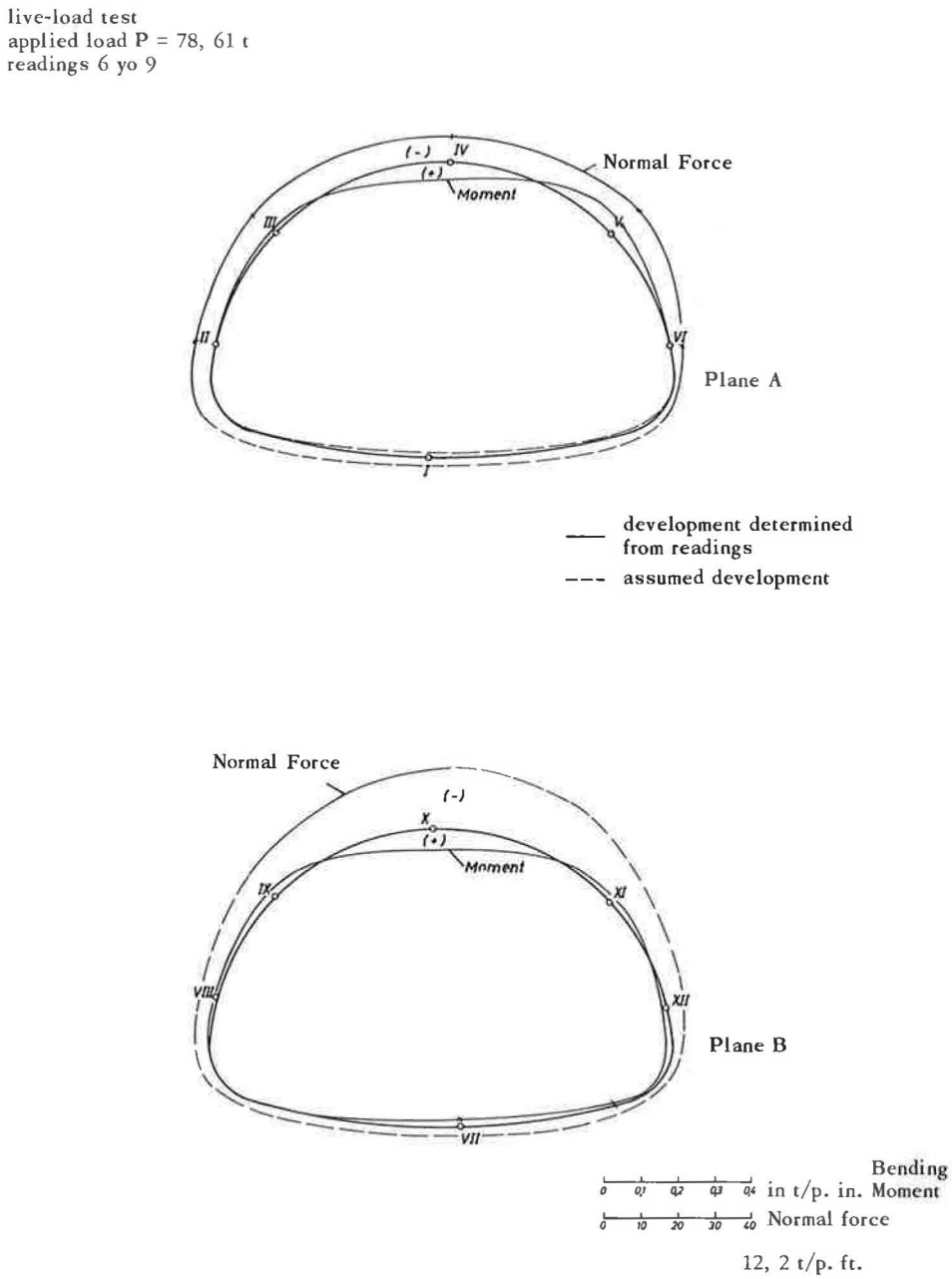

Figure 13. Development of normal forces and bending moments from reading taken.

were caused by this load shifting. The pipe-arch crest which had moved to the right by 0.04 in. under the axial load, moved back 0.12 in. to the left with the load in the off-center position.

Results of Strain Measurements

Figures 5, 10, and 13 show the results of the strain measurements made in the course of the live-load test. In some gage points several readings reveal that strain development along the section height is not linear. This is not in agreement with Euler-Benouilli's hypothesis that sections will remain even, which generally is considered true enough also in the plastic sphere. This strain pattern deviating from linearity may be explained in that the pipe-arch wall of corrugated metal sheet represents a plane load-bearing structure consisting of curved half-sections of a cylinder. Since the rigidity of the pipe arch along the centerline is very small as compared with that across the axis, the load will be primarily distributed along the ring, and the supporting structure may be regarded as a curved beam with a corrugated cross-section. Under concentrated pressures induced by rock in the backfilling material, however, the metal wall may in places react as a plane load-carrying structure, thus developing localized strains opposed to the hypothesis of linearity of strains along the section height.

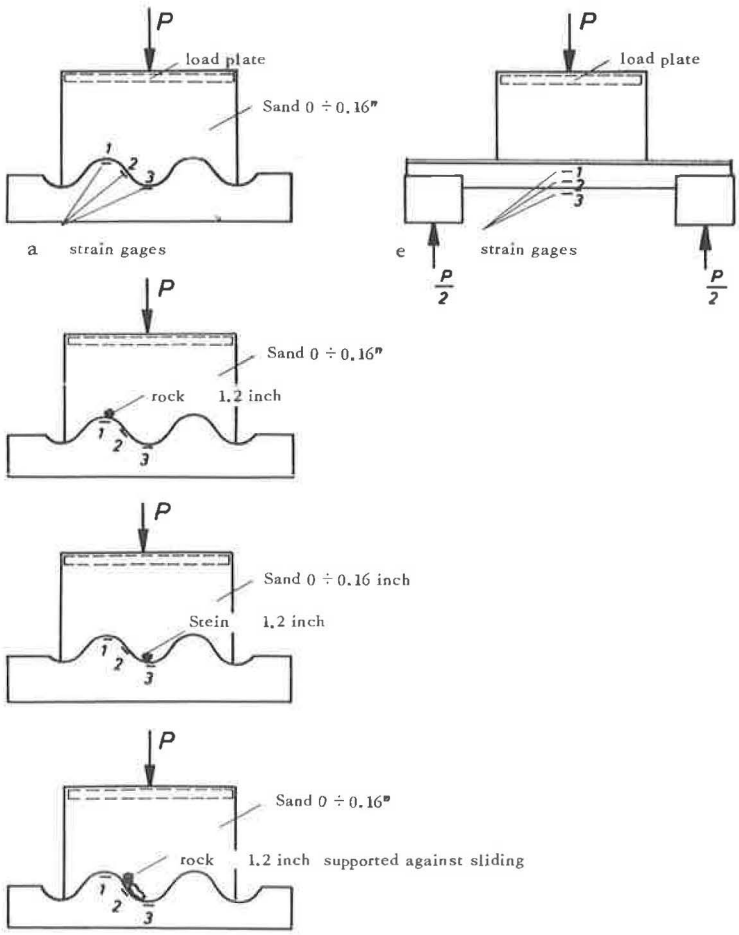

Figure 14.

The same effect also became apparent in tests conducted at the Institute for Statics and Steel Construction, for the purpose of clarifying this question. An Armco-Thyssen corrugated metal sheet was submitted to bending stress in a manner shown in Figure 14. These tests proved that the constantly acting lateral pressure, resulting from the corrugated profile, cannot possibly be the reason for the nonlinear strain development when using uniform granular material.

Although even localized pressures in the wave crest or the wave trough hardly affected the linearity, lateral pressures resulting from the presence of rock in the backfilling material would cause strain developments opposed to linearity.

For the determination of stresses and sectional forces from the strains, it was assumed that all strains were within the range of elasticity. Due to the low bending strength of the pipe arch, the acting bending moments will produce high extreme fiber strains which may exceed the yield point. Particularly during the placement of fill, considerable bending moments will be encountered in the absence of support by surrounding soil. Since the instruments for strain measuring were not installed until erection was completed, the yield development in the respective places could not be registered. During backfilling and loading operations, stresses induced on the pipe arch changed several times. Changes of this kind occurring in the plastic sphere will generate residual stresses that are superposed on the load stresses. It is not possible to study the stress pattern accurately, since stresses during erection are unknown and, furthermore, the stress curve will fluctuate as various loads are being applied or removed. The best results are obtained when the stresses are derived independently from the strains introduced at each individual load increment without considering initial stresses. This procedure was followed when evaluating the measurements. Even if it were possible to register all the influences affecting the strain measurements, a summation of strains or stresses would not provide much clarity inasmuch as the effects of the individual load increments would be concealed.

The computed stresses and sectional forces shown in the tables as "stresses from readings" and "sectional forces from readings" will, therefore, only approximately represent the forces to which the pipe arch was subjected but will permit qualitative conclusions as to the behavior of the structure under loading conditions.

In addition to the sectional forces resulting from backfilling and loading, which are shown in the tables, a rough estimation may indicate the range of sectional forces developing by erection. The pipe arch was erected by attaching and bolting together pipe elements of differing curvature, starting from the invert and continuing toward the sides. Due to inevitable production tolerances when curving the plates, and as a result of the weight of the structure, the rings consisting of individual sections can be closed only by pulling the open ends together or by parting overlapping ends.

Since it is impossible to determine the necessary amount of adjustment after assembly has been completed, the rough estimate of stresses during erection of the pipe arch will be based on an empirical adjustment value of $C_2 = \pm 1.64$ ft. In the most unfavorable instance, this adjustment and the effect of the pipe-arch weight will cause the following bending moments to arrive at the points marked (Fig. 15):

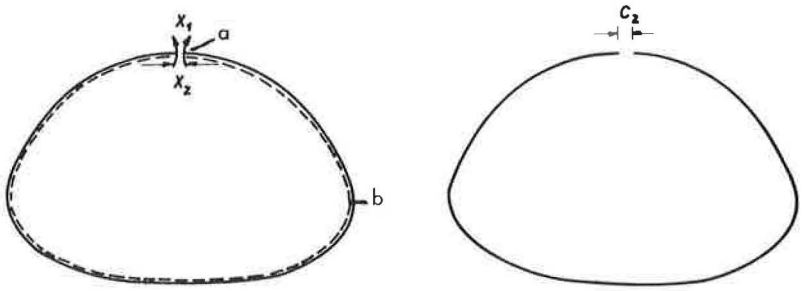

Figure 15. Sectional forces resulting from adjustment of ring ends.

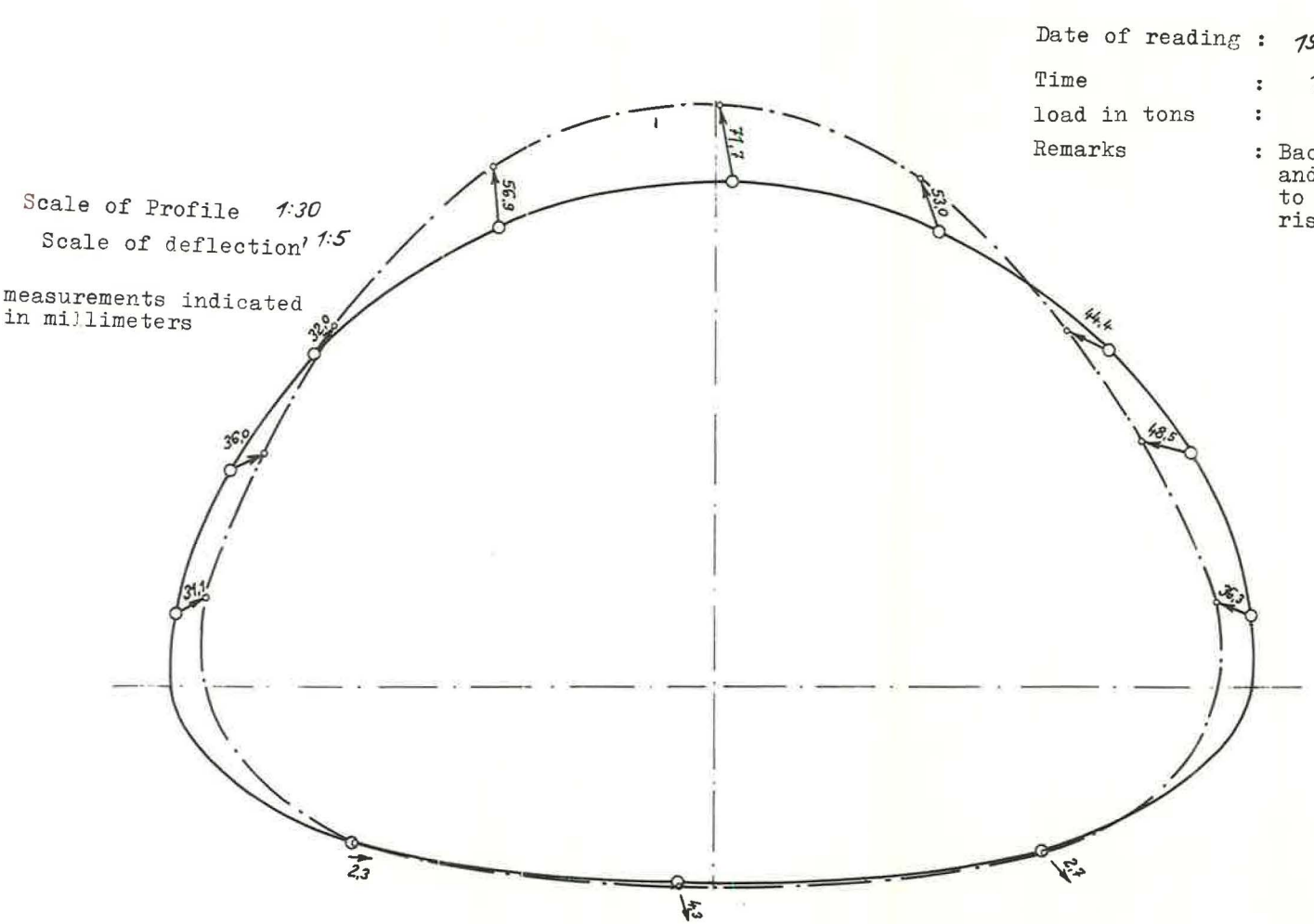

Figure 16. Live-load test, deformation measurement.

Date of reading: 21. Juni 1963

Time : 8⁰⁰

load in tons: 0

Remarks : Base reading prior for loading test

Scale of Profil 1:30

Scale of deflection 1:5

measurements indicated in millimeters

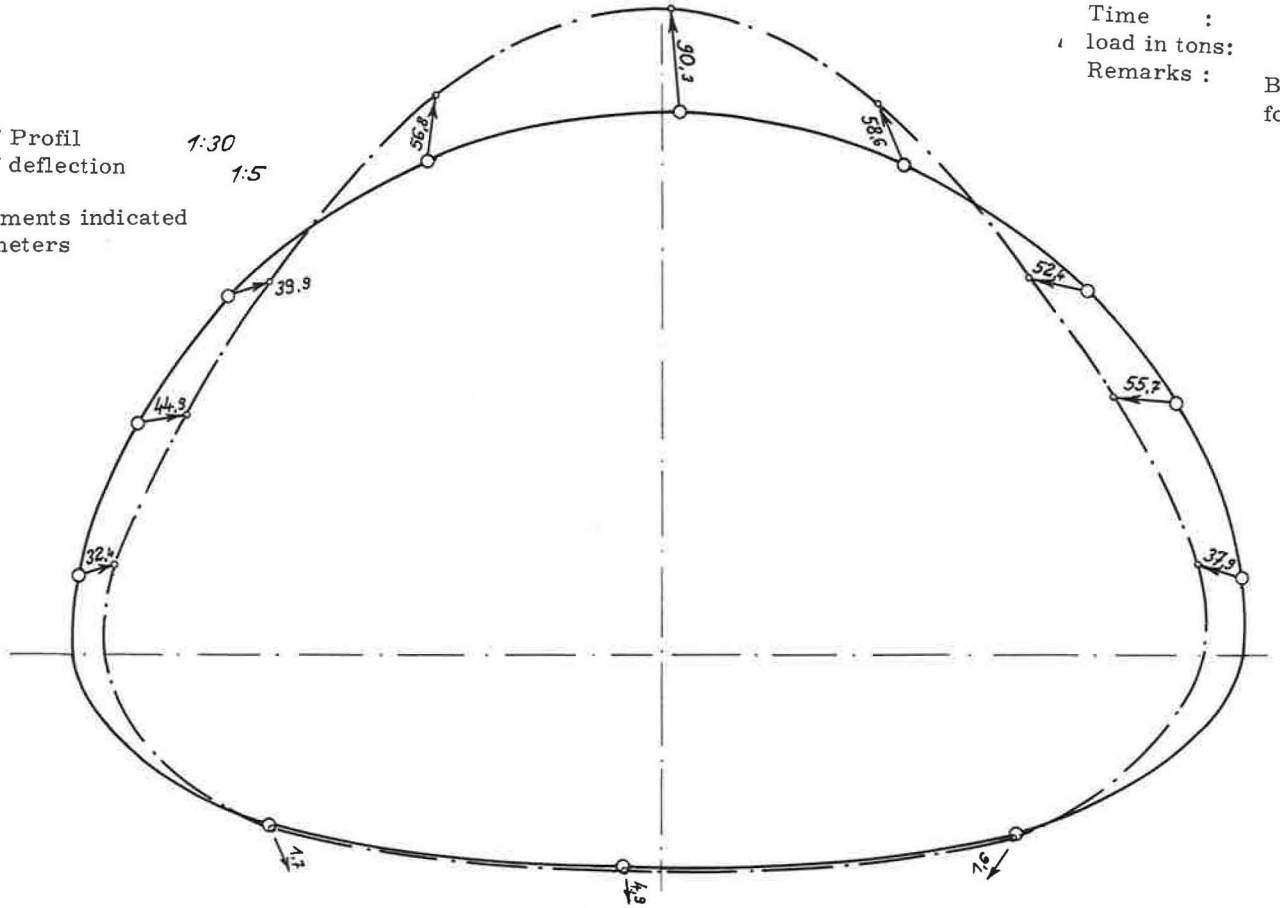

Figure 17. Live-load test, deformation measurement.

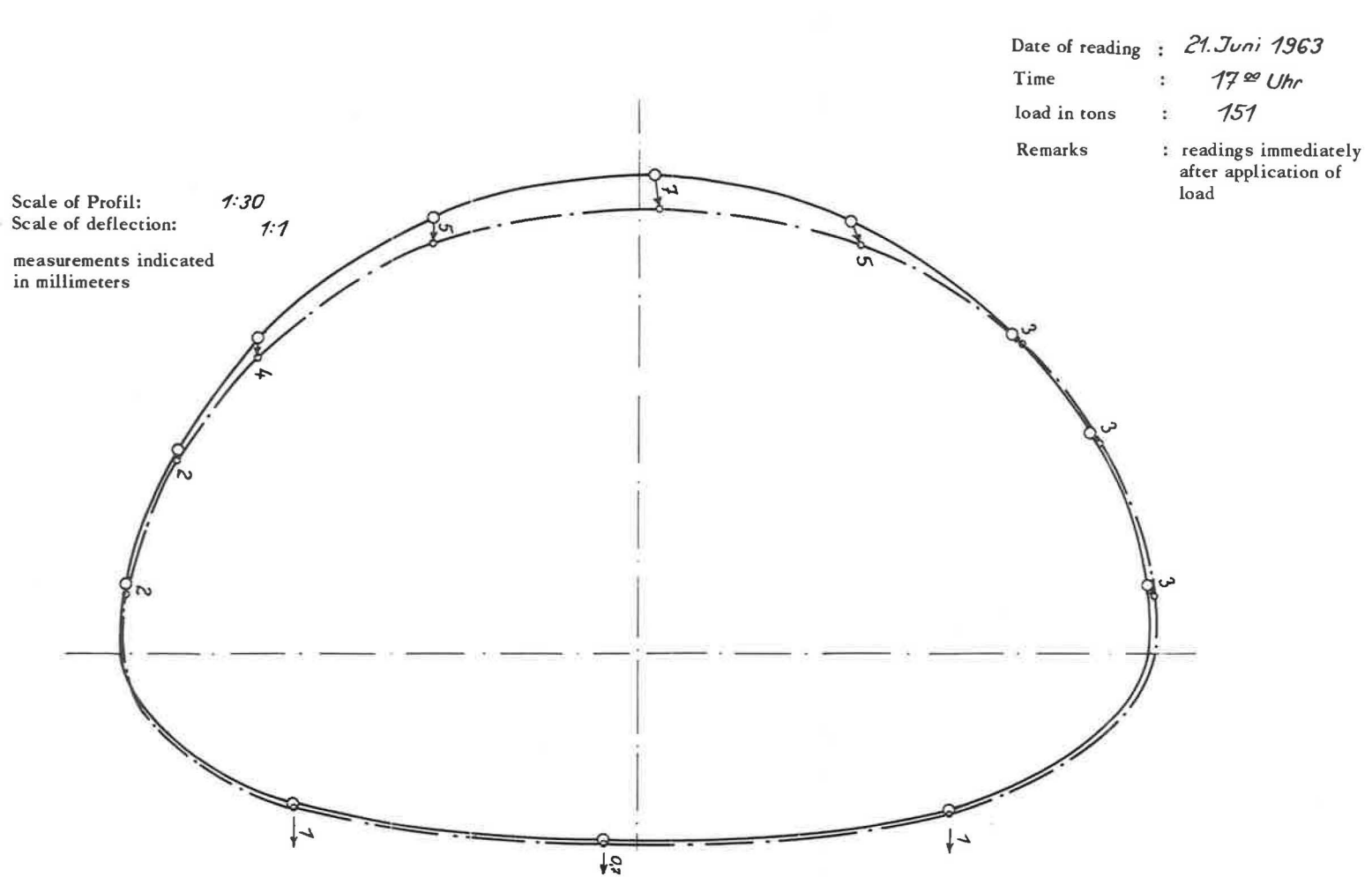

Figure 18. Live-load test, deformation measurement.

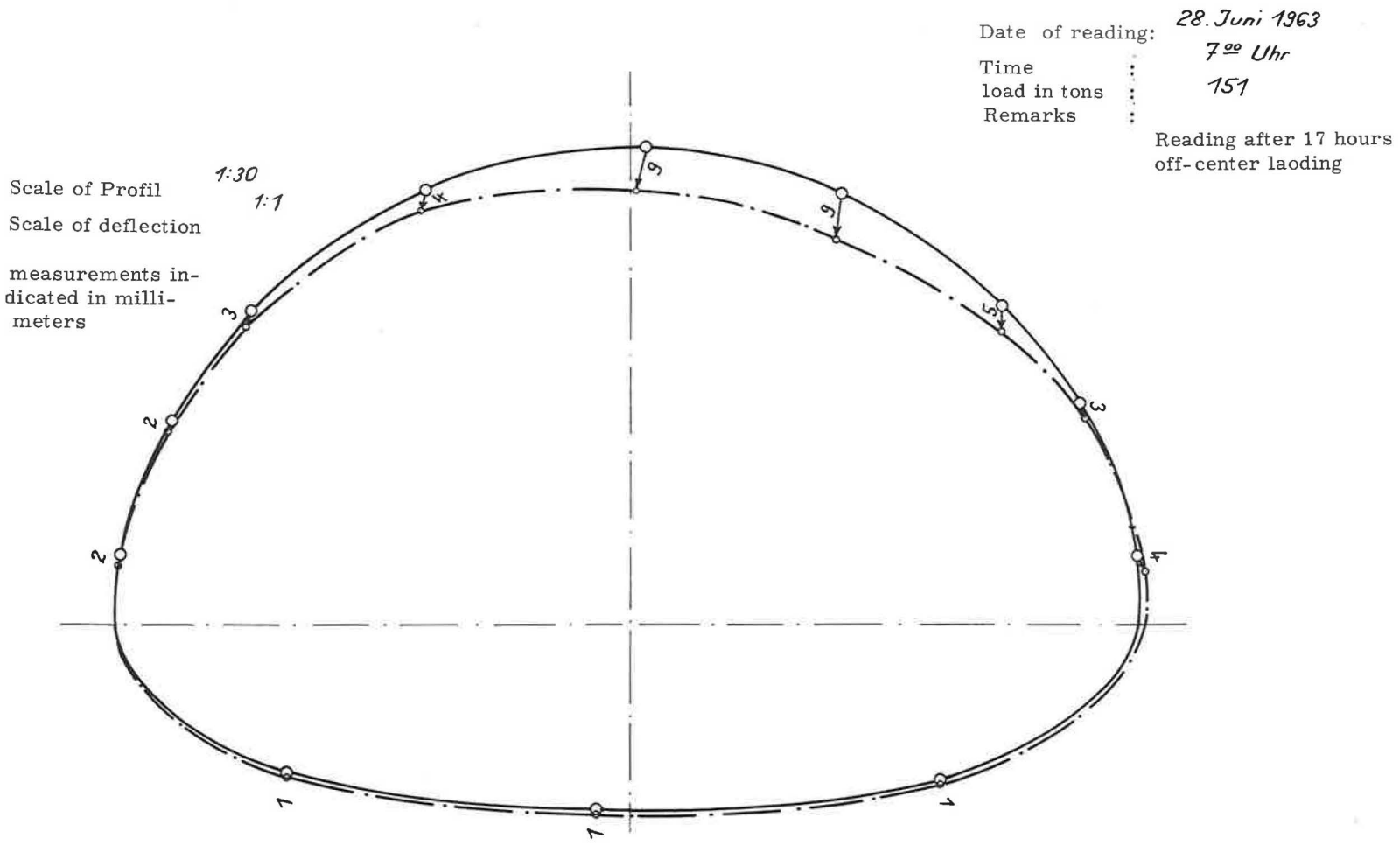

Figure 19. Live-load test, deformation measurement.

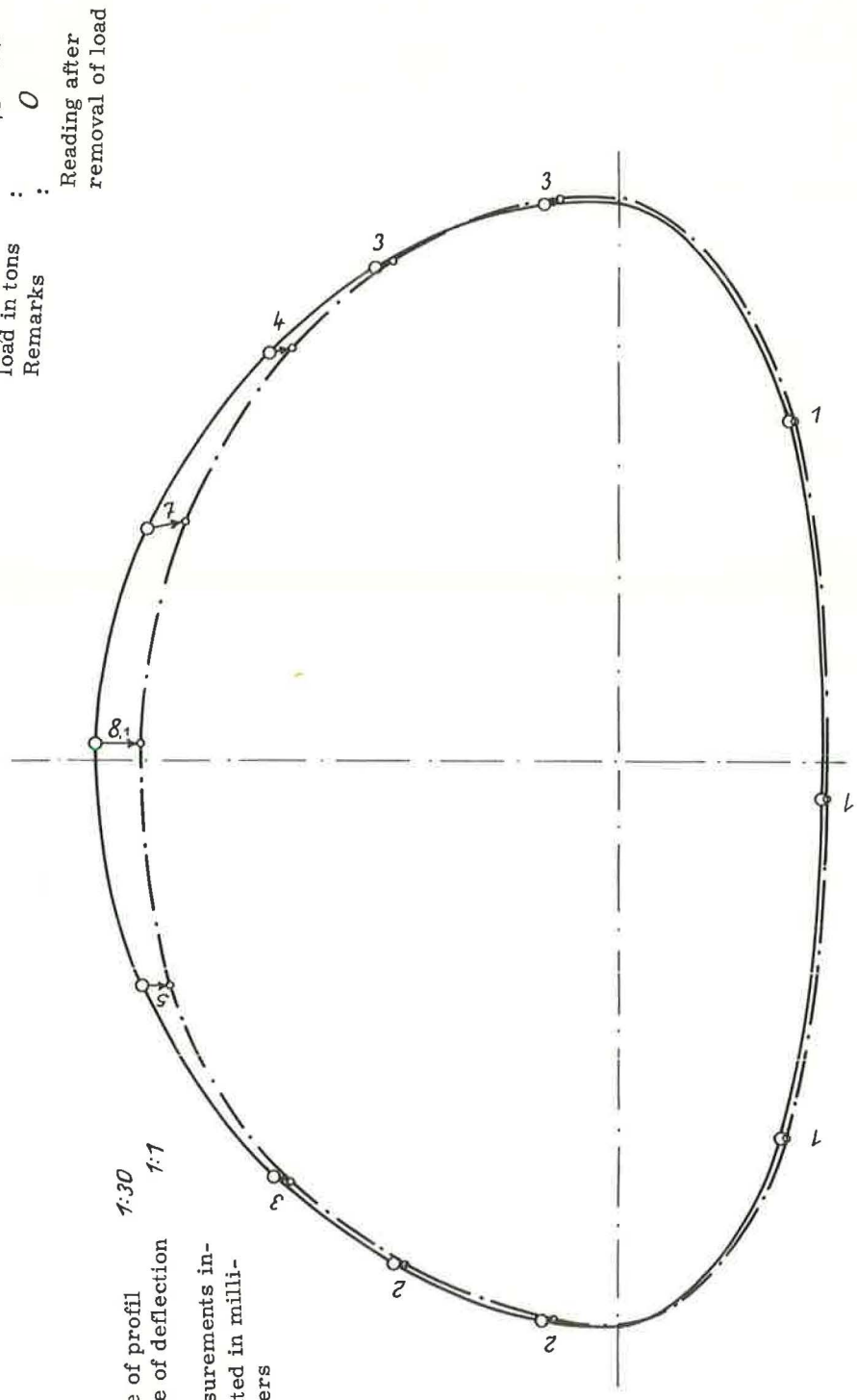

Figure 20. Live-load test, deformation measurement.

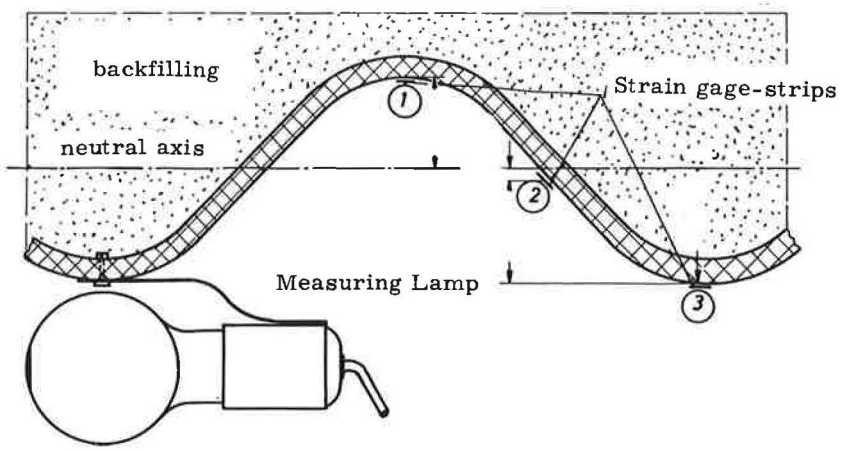

Figure 21. Positioning of strain gage strips and measuring lamp.

Point a

$$M_a = \pm 2,470 \text{ lb-in./in.}$$

Point b

$$M_b = \pm 1,367 \text{ lb-in./in.}$$

The stresses thus developed are as follows (the effect of normal force having been neglected as insignificant):

Point a

$$\begin{matrix}\text{min.}\\ \text{max.}\end{matrix} \sigma_a = \pm\frac{2,470}{0.0989} = \pm 24,975 \text{ psi}$$

Point b

$$\begin{matrix}\text{max.}\\ \text{min.}\end{matrix} \sigma_b = \pm\frac{1,367}{0.0989} = \pm 13,822 \text{ psi}$$

This rough estimate shows that the stresses in the load position "assembly" may become so large that they must be taken into account together with the loading stresses under the service load, when considering the stresses effective in the structure.

Deformation measurements are shown in Figure 9 and Figures 16 through 20. The positioning of the strain gage strips and measuring lamp for this test is shown in Figure 21.

LOADING-TO-FAILURE TEST

On June 28, 1963 preparations began for the loading-to-failure test. The slabs were removed and the pipe arch uncovered to the crest. The unloading caused a slight vertical rise of the crest of 3.47 in. The upper layers were removed for the purpose of conducting the crushing test with undisturbed and unpreloaded soil in the area of largest soil pressures, i.e., directly underneath the applied load. Before the new material was placed, three Heierli pressure cells were installed in backfill in a horizontal place above the pipe arch (Fig. 22). The center cell was placed 4 in. above the crest underneath the center of the loaded area, and the other two were installed at distances of

Figure 22. Installing Heierli pressure cells.

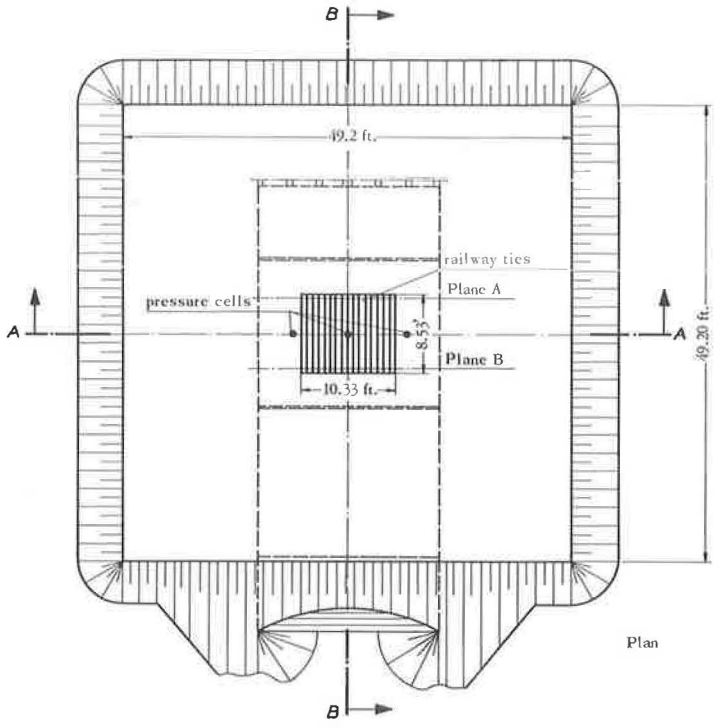

Figure 23. Setup for loading-to-failure test.

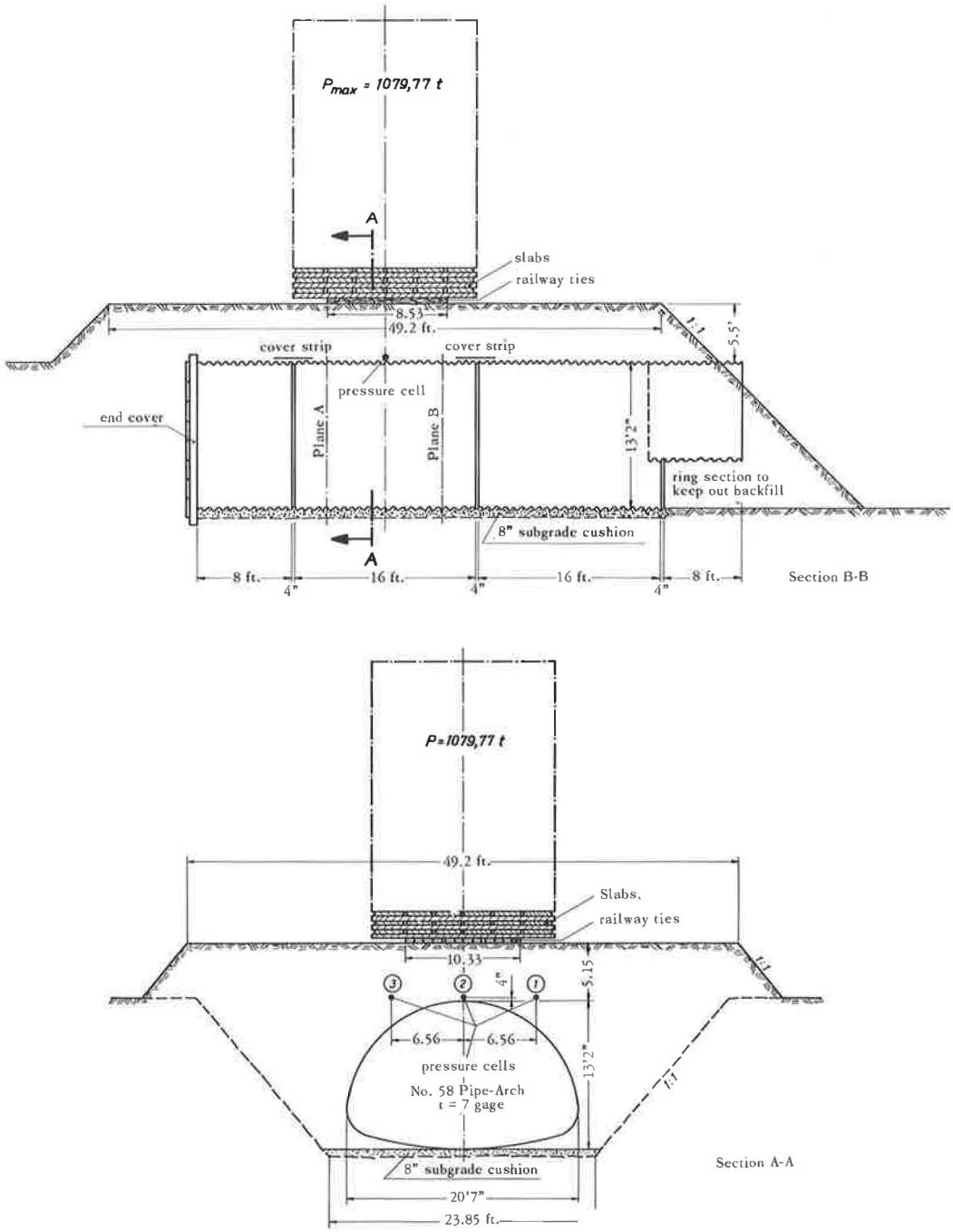

Figure 23. Continued.

6.56 ft left and right of the crest. Measurements are made by pressure gage strips incorporated in pressure cells. For the crushing test, the backfill was extended at the shoulders as a further precaution against subgrade failure. This required the addition of another ring section at the open end of the structure. After the cover height of 5.15 ft for the crushing test was reached, loading was started on July 2, 1963. For higher

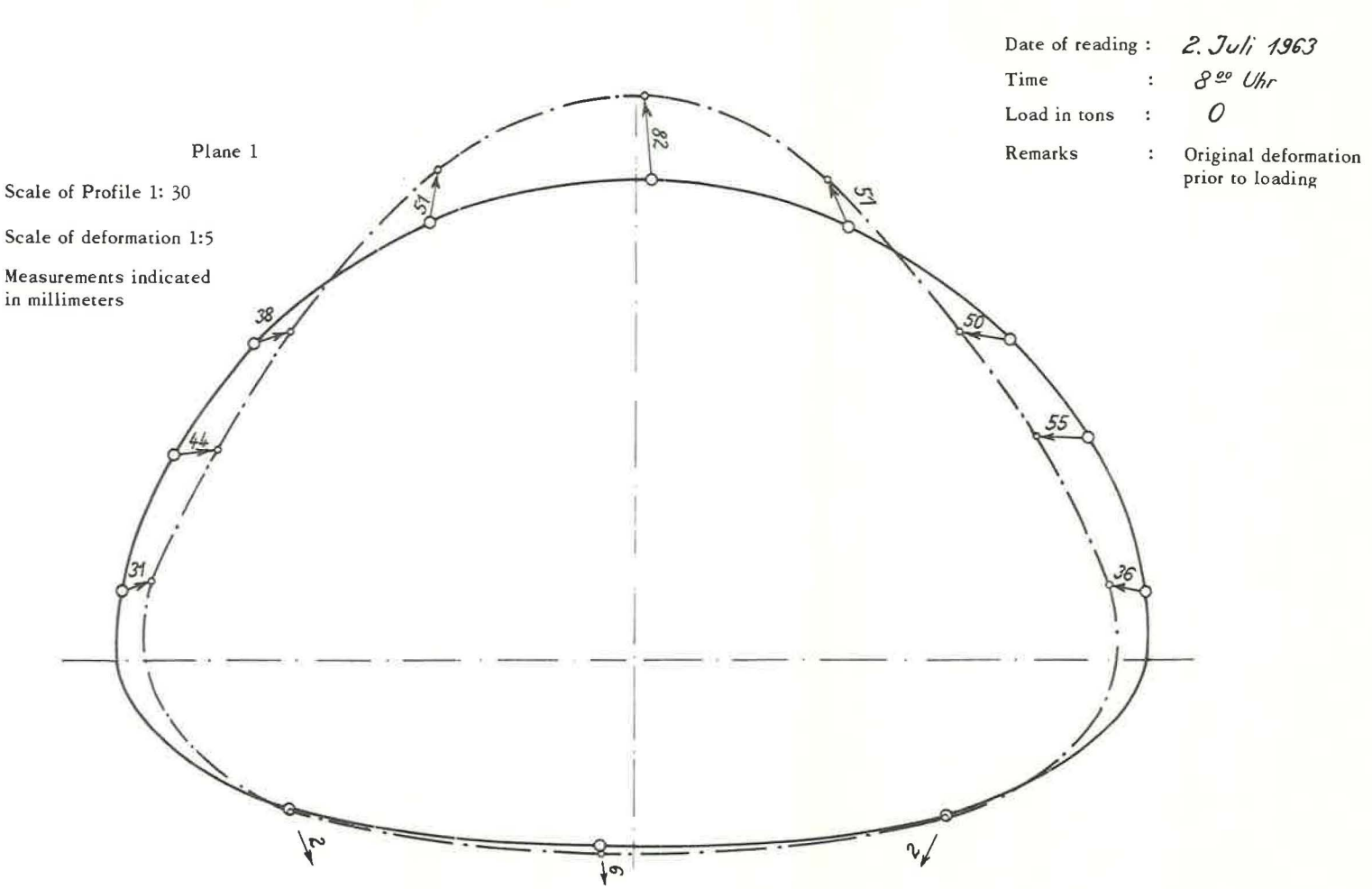

Figure 24. Loading-to-failure test, deformation measurement.

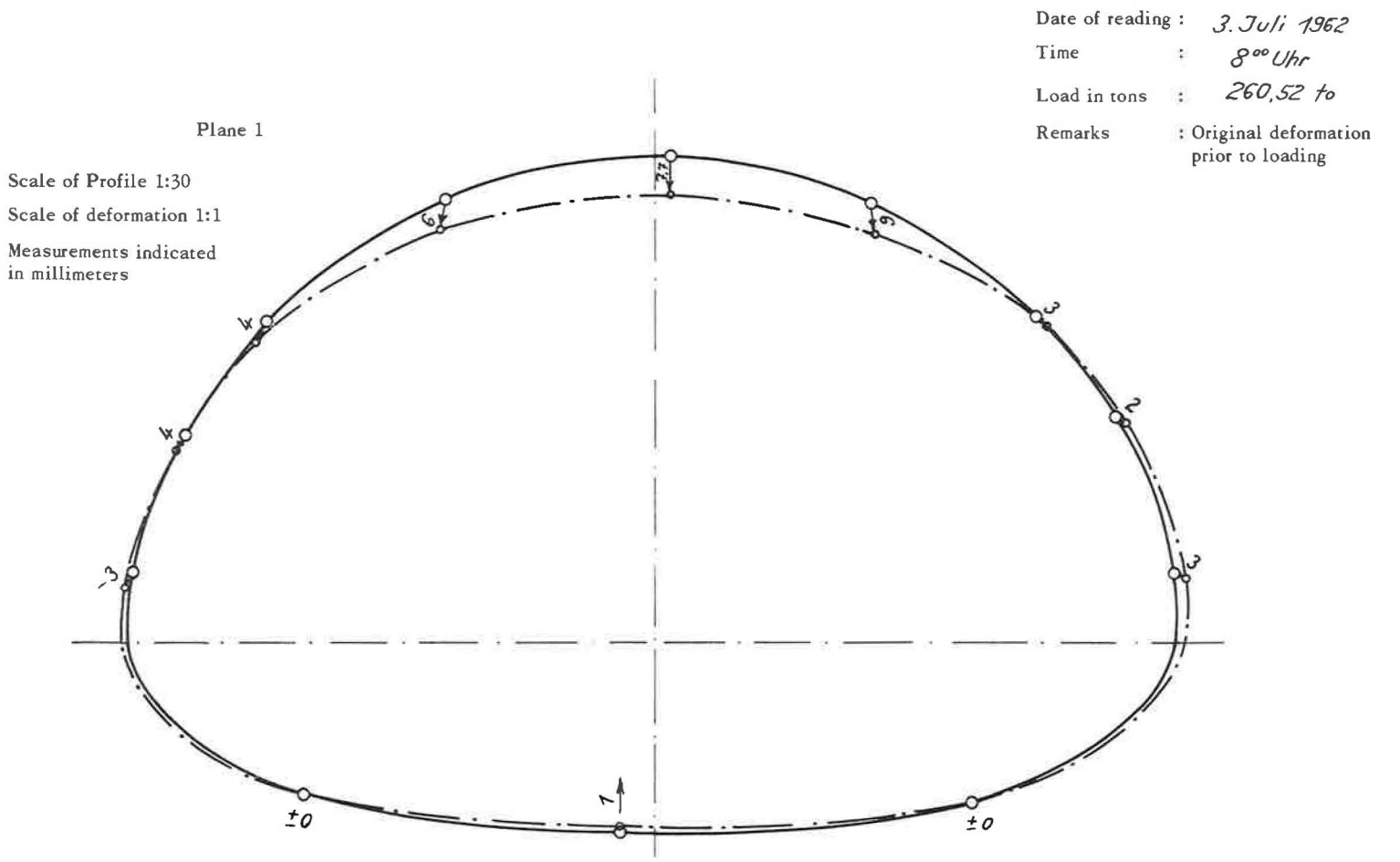

Figure 25. Loading-to-failure test, deformation measurement.

stability of the slab pile, slabs were placed crosswise for this test, using the same supporting area of railway ties as in the live-load test. The setup for the loading-to-failure test is shown in Figure 23.

At the end of the first day, a 260.52-ton load had been applied. As was the case during the live-load test, only slight deflections and strains were introduced by this load. As compared to the conditions before the application of this load (Fig. 24) the following values (Fig. 25) were noted for the most important deformations, stresses and soil pressures at P = 260.52 tons:

Plane 1—0.26-in. vertical deflection in crest;
Plane 2—0.27-in. vertical deflection in crest;

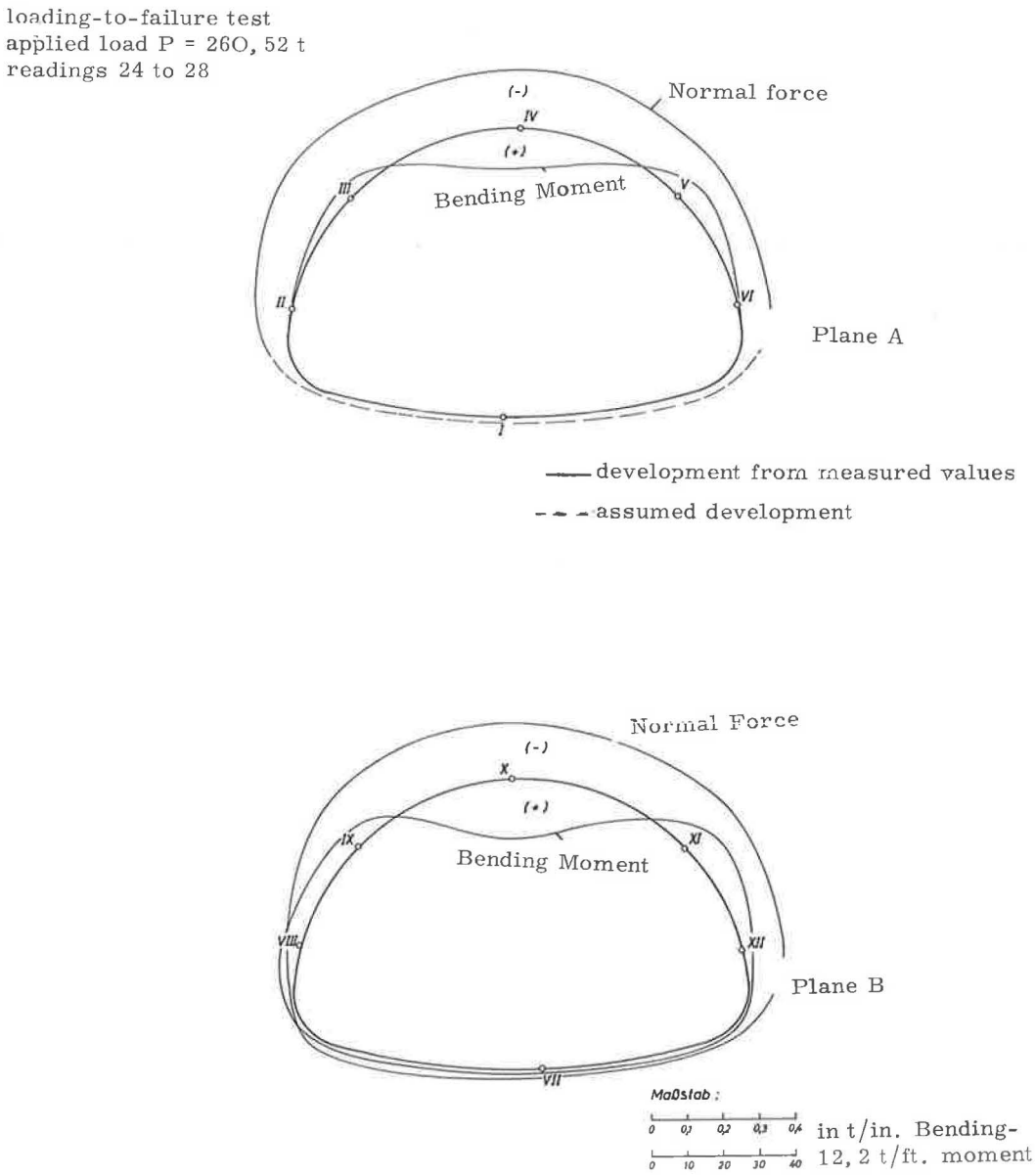

Figure 26. Development of normal forces and bending moments from reading taken.

Change of extreme fiber stresses (Fig. 26) in crest point IV = -6,159 psi = -1,309 psi; in crest point X = -6,841 psi = +28.4 psi; and
Soil pressure at 4 in. above crest—p_2 = 19.34 - 5.83 = 13.51 psi.

The 260.52-ton load was left unchanged overnight. The following morning, a reading revealed the following slight changes under the same load:

Plane 1—0.30-in. vertical deflection in crest;
Plane 2—0.31-in. vertical deflection in crest;

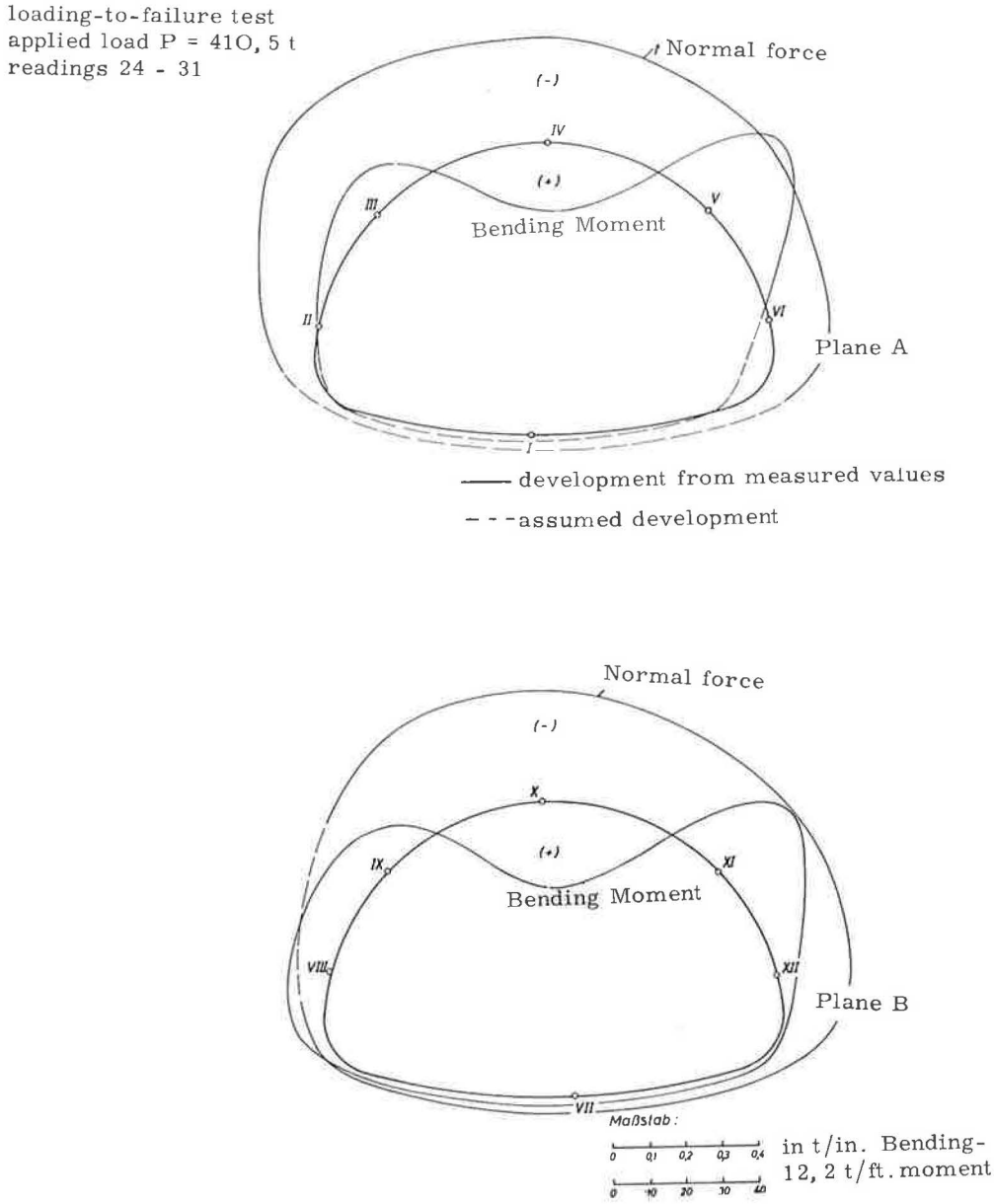

Figure 27. Development of normal forces and bending moments from reading taken.

Date of reading: 4. Juli 1963
Time : 14.22 Uhr
Load in tons : 561,70 to
Remarks : Original deformation prior to loading

Plane 1

Scale of Profile 1:30
Scale of deformation 1:5

Measurements indicated in millimeters

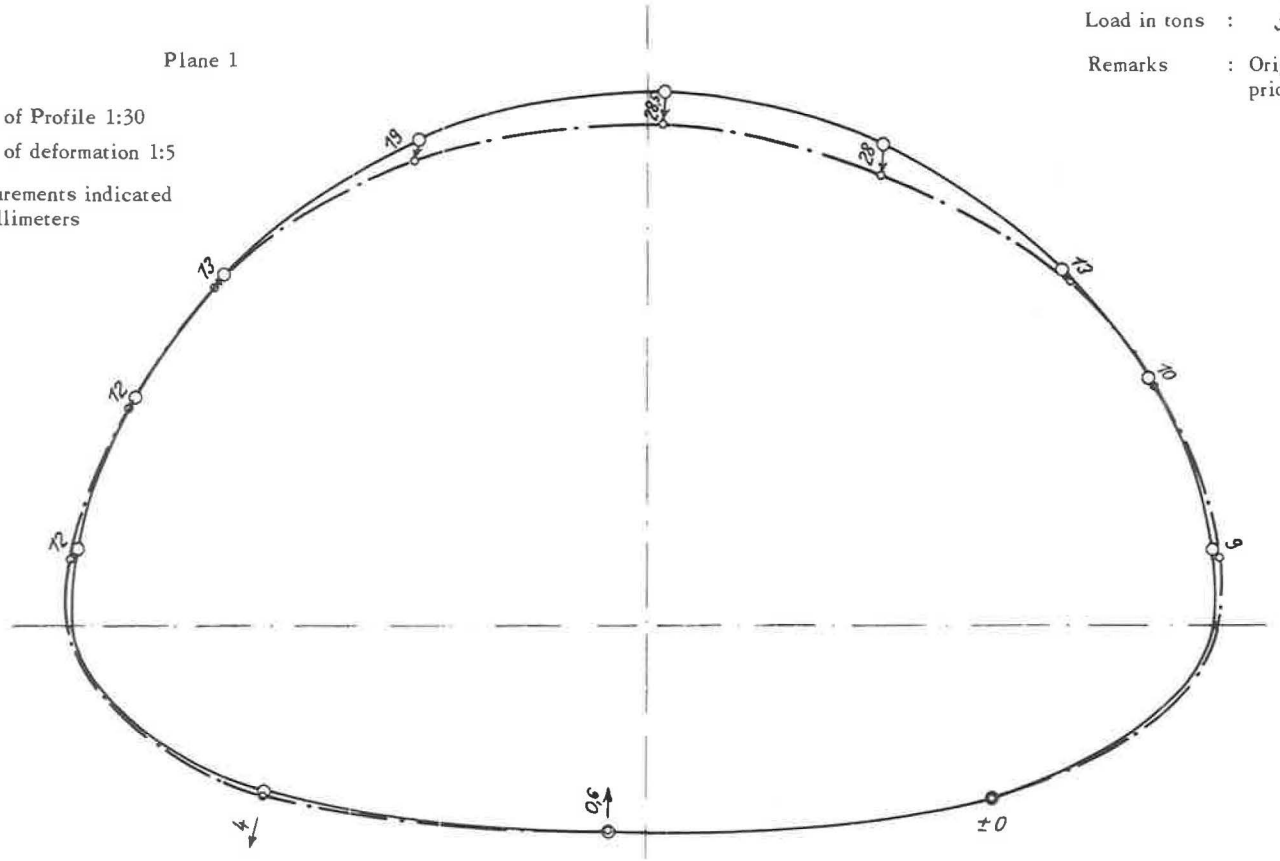

Figure 28. Loading-to-failure test, deformation measurement.

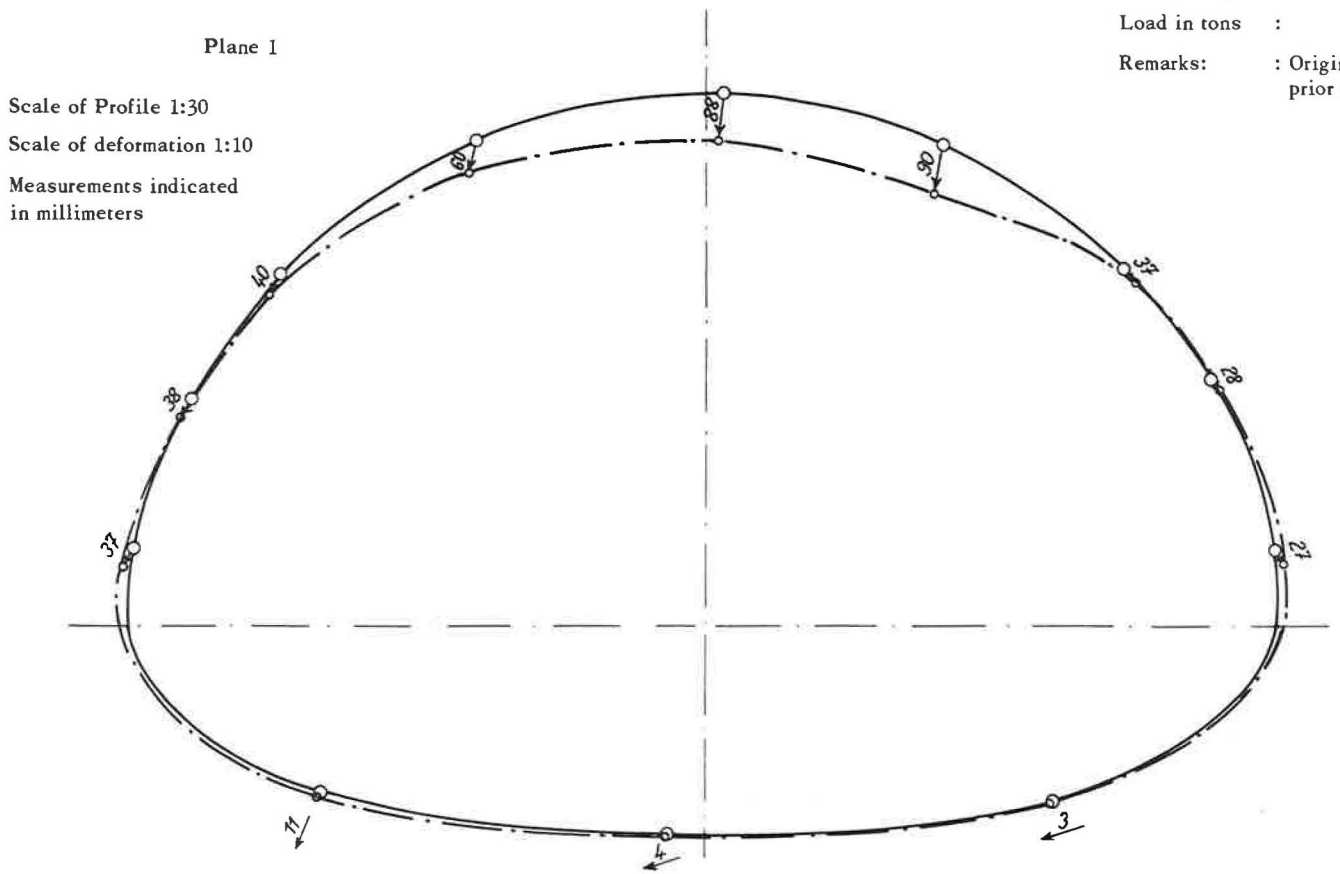

Figure 29. Loading-to-failure test, deformation measurement.

Date of reading : 5. Juli 1963
Time : 17¹⁵ Uhr
Load in tons : 1079,77 to
Remarks : Crushing test was stopped at this point

Plane 1

Scale of Profile 1:30

Scale of deformation 1:10

Measurements indicated in millimeters

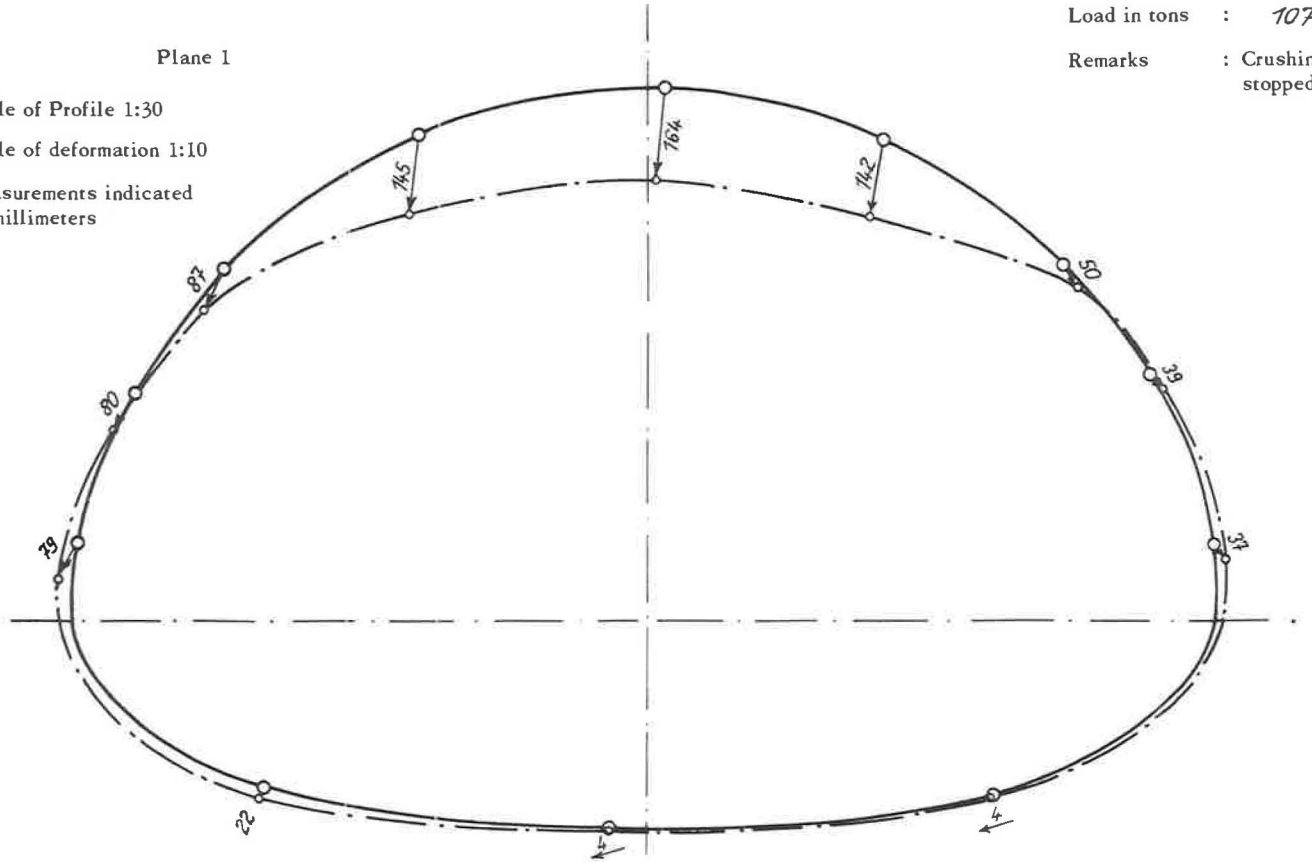

Figure 30. Loading-to-failure test, deformation measurement.

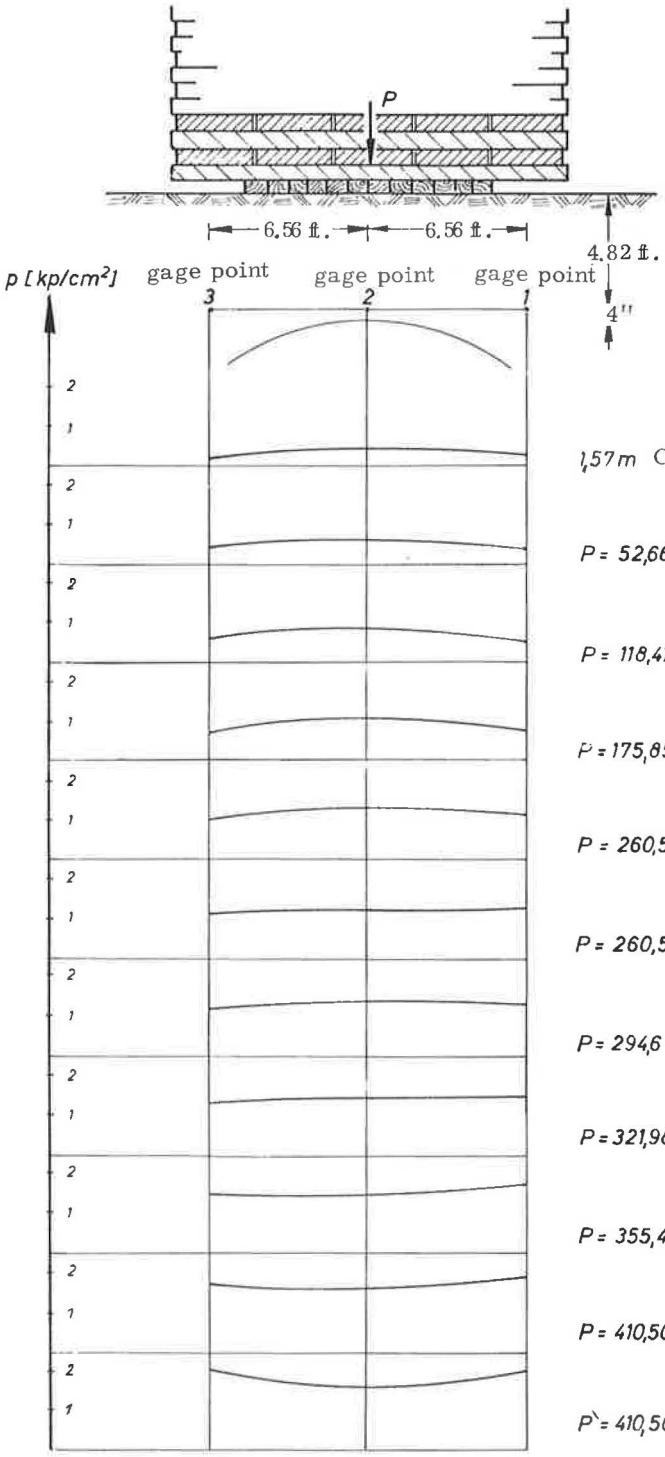
P
6.56 ft.
6.56 ft.
4.82 ft.
4"
p [kp/cm²]
gage point
gage point
gage point
3
2
1
1,57 m Over height
P = 52,66 to
P = 118,41 to
P = 175,85 to
P = 260,52 to
P = 260,52 to after 13 hrs.
P = 294,6 to
P = 321,98 to
P = 355,48 to
P = 410,50 to
P = 410,50 to after 15,5 hrs.

Figure 31.

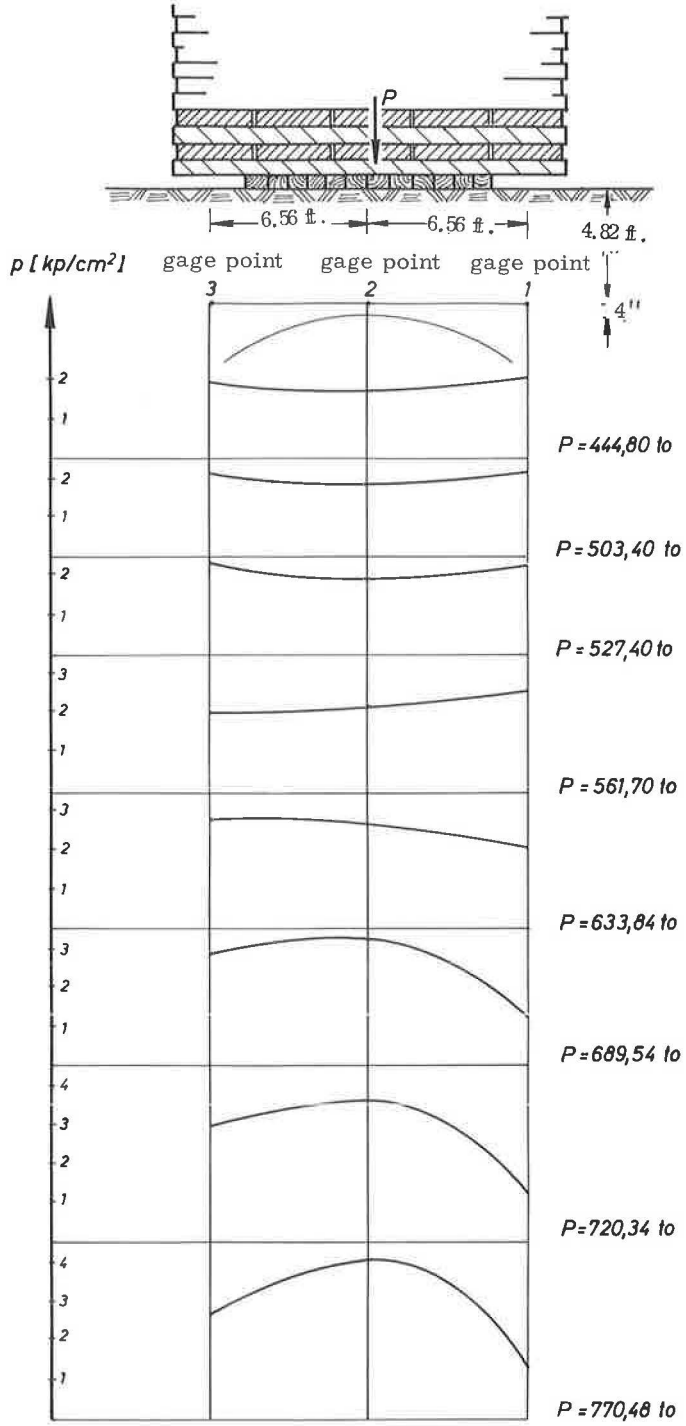
P
6.56 ft.
6.56 ft.
4.82 ft.
p [kp/cm²]
gage point
gage point
gage point
3
2
1
4"
P = 444,80 to
P = 503,40 to
P = 527,40 to
P = 561,70 to
P = 633,84 to
P = 689,54 to
P = 720,34 to
P = 770,48 to

Figure 32.

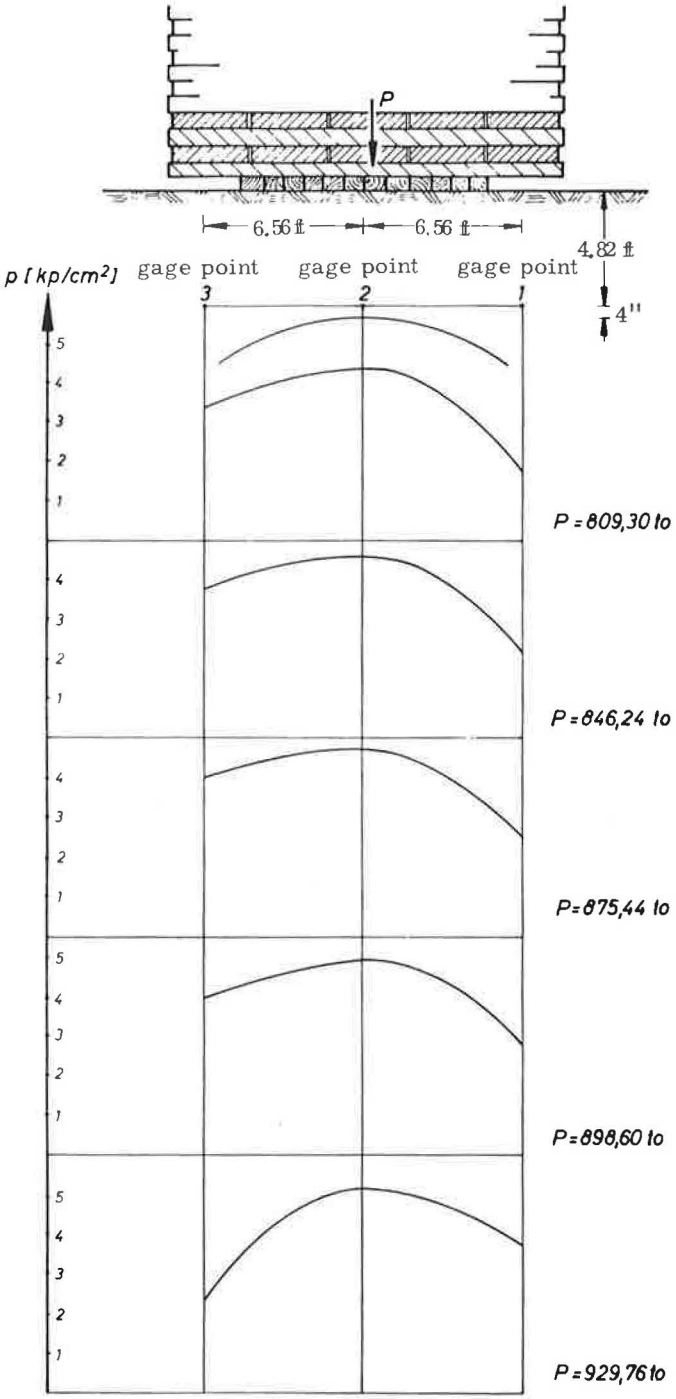
P
6.56 ft
6.56 ft
4.82 ft
4"
p [kp/cm²]
gage point
gage point
gage point
3
2
1
P = 809,30 to
P = 846,24 to
P = 875,44 to
P = 898,60 to
P = 929,76 to

Figure 33.

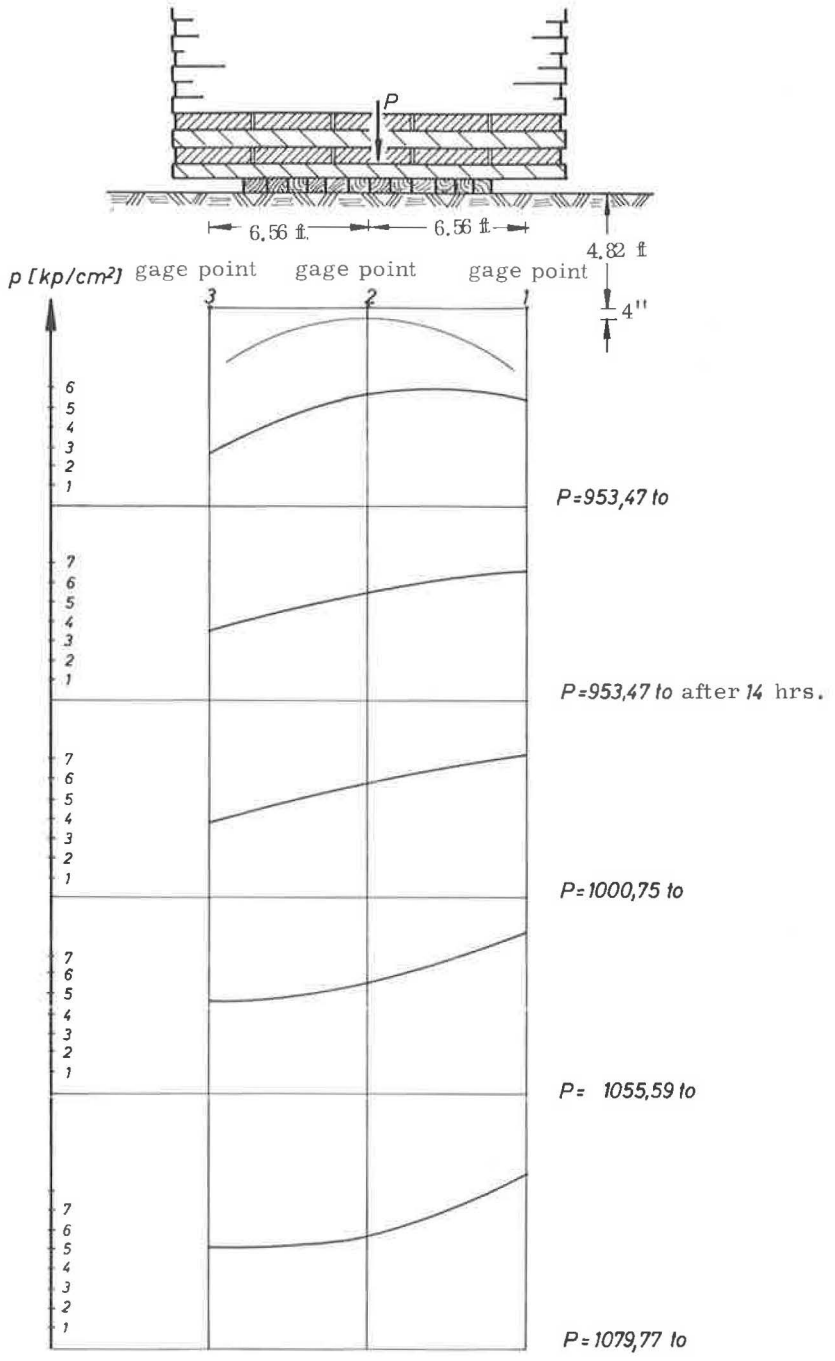

Figure 34.

Extreme fiber stresses in crest point IV = -5,021 psi = +156 psi; in crest point X = -6,600 psi = +484 psi; and

Soil pressure at 4 in. above crest—p_2 = 18.35 - 5.83 = 12.52 psi.

These changes may be ascribed to consolidation of the soil. Although reduced soil pressure was measured at the central gage point, pressures at the other point (p_1 and p_3) had increased.

On July 3, 1963, the load was increased to 410.5 tons. Measurements showed the following changes, as compared to the condition at P = 0:

Plane 1—0.59-in. vertical deflection in crest;
Plane 2—0.60-in. vertical deflection in crest;
Extreme fiber stresses (Fig. 27) in crest point IV = -10,184 psi = -3,001 psi; in crest point X = -11,734 psi = -2,205 psi; and
Soil pressure at 4 in. above crest—p_2 = 23.90 - 5.83 = 18.70 psi.

The gage pins observed by the theodolite and the measurements of soil pressure revealed a slight eccentricity of the load, which again had to be ascribed to inevitable off-center loading and nonuniform soil. As the slab pile became higher (approximately 2.46 ft/100 tons), the danger of inclination increased. Throughout the test, however, direct deformation measurements and soil pressure readings evaluated on the spot permitted an estimate on the amount of eccentricity, which could then be offset, as required, by stacking the slabs accordingly.

On July 4, 1963, the load was increased from 410.5 to 953.74 tons. From above 510 tons, deformations increased considerably (Figs. 28-30). Whereas a 0.31-in. deflection in the crest had been measured under a load of P = 260.52 tons, the deflection increased to as much as 1.12 in. under a 561.70-ton load and to 3.43 in. at 820 tons. Up to a 561.70-ton load, soil pressures in the plane 4 in. above the crest showed a larger increase at the outer measuring points 1 and 3 than at the central point 2 (Figs. 31 and 32). From 561.70 to 929.76 tons, soil pressure at the central gage point increased faster than on the sides. Soil pressures at points 1 and 3 indicated and unstable behavior of the slab pile (Figs. 33 and 34). As it was expected that the pipe arch would soon collapse and there was a danger of the high stack destroying the measuring instruments when falling down, the strain gages were removed at P = 689.54 tons, so that after that no strain readings were taken.

With P = 689.54 tons, readings were as follows:

Plane 1—2.06-in. vertical deflection in crest;
Plane 2—3.11-in. vertical deflection in crest;
Extreme fiber stresses (Fig. 35) in crest point IV = -18,874 psi = -5,291 psi; in crest point X = -23,084 psi = -7,766 psi; and
Soil pressure at 4 in. above pipe-arch crest—p_2 = 47.22 - 5.83 = 41.39 psi.

Under a load of 850 tons, two inward bulges began to develop on each side of the crest (Fig. 36). At that stage, the one on the right was about 11.8 in. and the one on the left 5.9 in. deep, as measured radially. When darkness set in, loading had to be interrupted at P = 953.74 tons. Since a collapse seemed imminent on account of the inward bulging, the pipe was watched throughout the night so that the development of a possible collapse might be studied closely. The large increase in deformations noted toward the evening, which caused the pipe arch to continue deflecting for a short while even after loading had been stopped, came to a standstill in the course of the night.

On the next morning, it was noted that the first layer of slabs was resting firmly against the soil as a result of settling of the ties and sagging of the slabs. Through this, the loaded area had increased from 8.53 × 10.33 = 88.11 sq ft to approximately 16.4 × 9.84 = 161.4 sq ft. These and the earlier consolidations may be regarded as the reason why settlements and deformations died down during the night after a period of sharp rise. When loading was continued on July 5, 1963, the influence of the enlarged loaded area was notable. Although the soil pressure at gage point 2 remained unchanged under a load increase from 1,000.75 to 1,055.79 tons, it rose on both sides. Under a load of P = 561.70 tons, an irregular increase of pressures had already been observed, particularly at the outer gage points. By the time 1,079.77 tons had been applied, this development had reached such unfavorable effects that the soil pressure

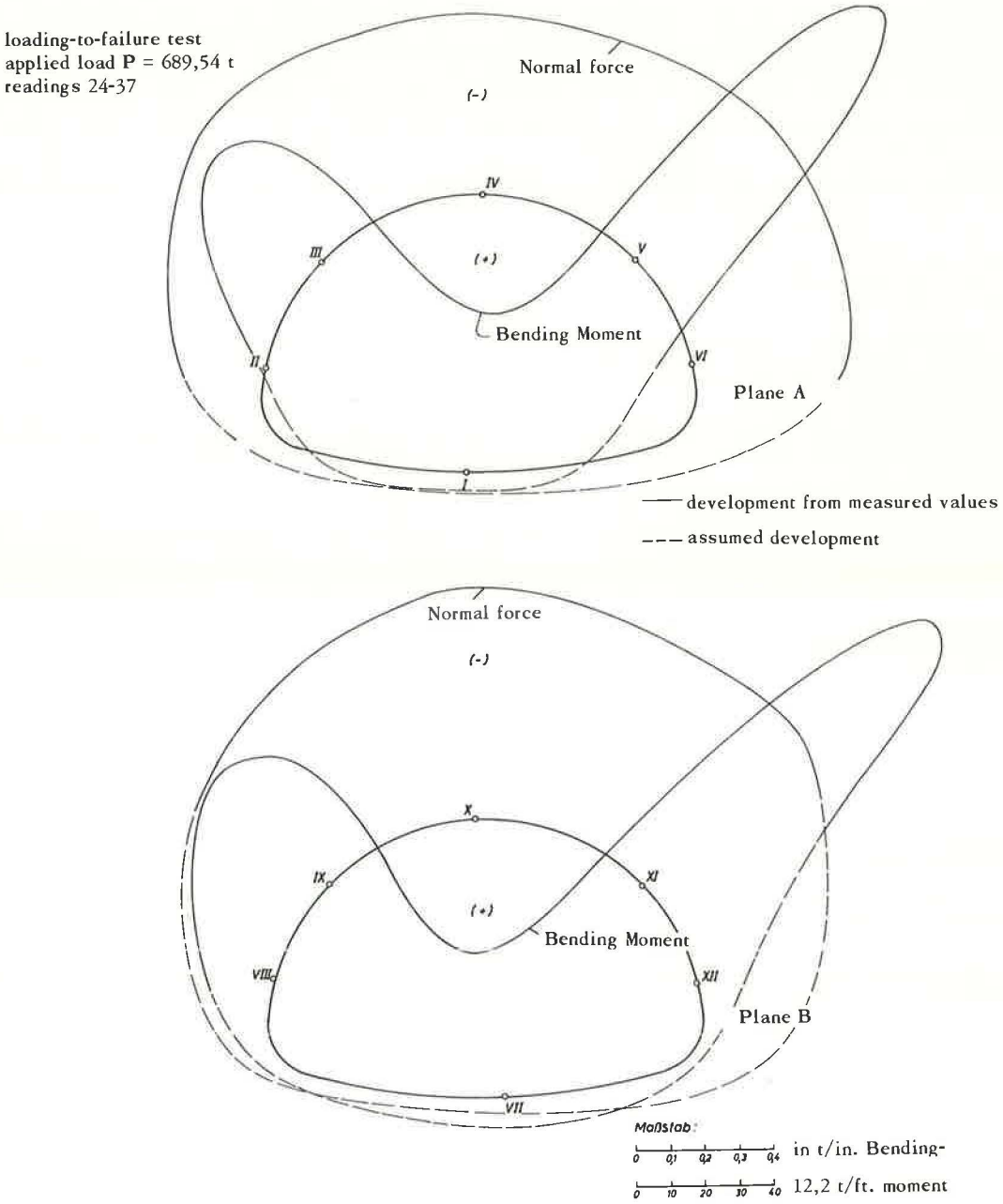

Figure 35. Development of normal forces and bending monents from reading.

at gage point 1 was nearly double that at point 3, which suggested a further loss of symmetry. Deformation measurements, however, gave no indication of imminent collapse. Even the bulge-shaped deformations did not increase much. Thus, there was a risk that the slab pile, which had reached a height of approximately 28 ft and was about 5.25 ft above the surrounding terrain, would tumble down before the utmost carrying capacity of the pipe arch could be reached. This would probably have damaged the two cranes employed for stacking the slabs (Figs. 37 and 38). The applied

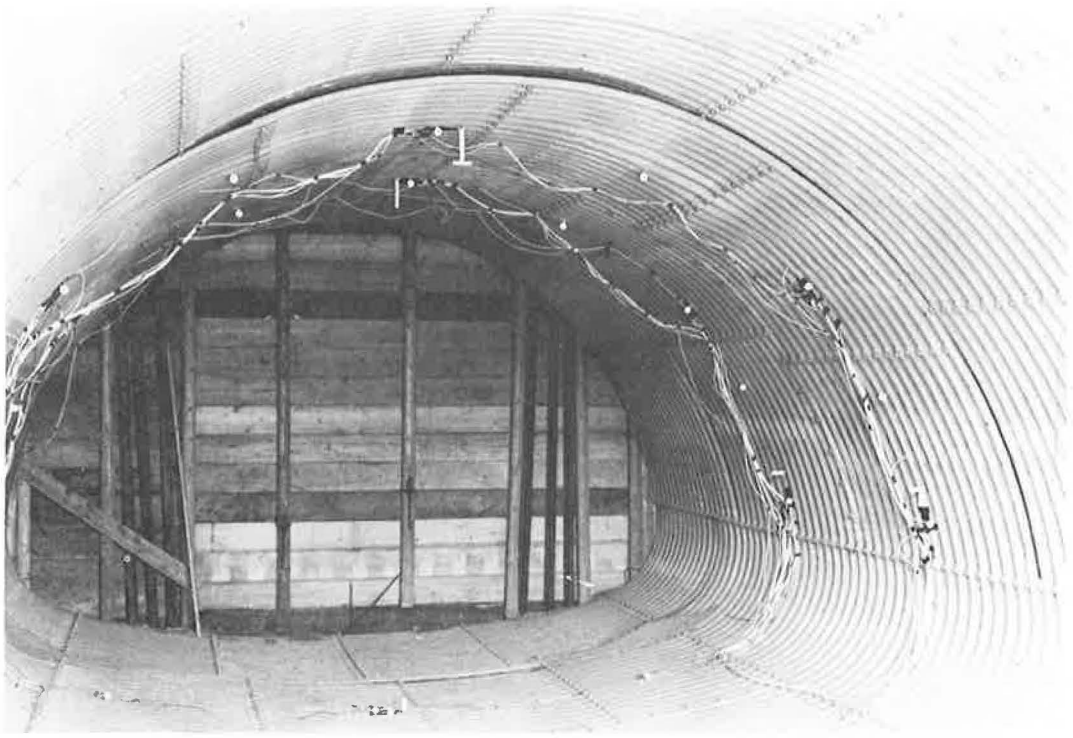

Figure 36. Inside of pipe arch with bulge-shaped deformations on either side of crest. Center section of structure clearly deflected against adjacent rings.

load of p_{max} = 1,079.77 tons and measurements taken so far seemed to give ample evidence; therefore, it was considered not necessary to continue loading until the pipe arch collapsed, which would have been dangerous under the high load.

On July 6, 1963, the slab pile was removed by the cranes and on July 7, the uncovered pipe arch was examined (Fig. 39). The bulge-shaped deformations observed from 850 tons upward were of a plastic nature (Fig. 40), as was the deflection in the crest line parallel to the axis.

Although the center section of the structure was free to move independently from the outer parts and its length of 16 ft had been so selected that it should be completely within the pressure area of the load, plastic deflection near the center was much larger than toward the ends. The bulges always followed the longitudinal seams, even where these were staggered in the two rings of the center section. Near these bulges the ring sections were bent and the plates shifted against each other. The connecting bolts were deformed to an extent that some had been sheared off.

Results of Strain Measurements

Figures 26, 27, 35, 41 and 42 show the normal forces and bending moments for the various load increments as measured by the strain gages. As was done accordingly when measuring deflection, the strains existing after backfilling were disregarded; in other words, base readings of strains were taken as loading began.

Results of Deformation Measurements

Deflection readings have been shown separately for the structure after backfilling and for the loading conditions, as was done for the live-load test. Figure 24 shows

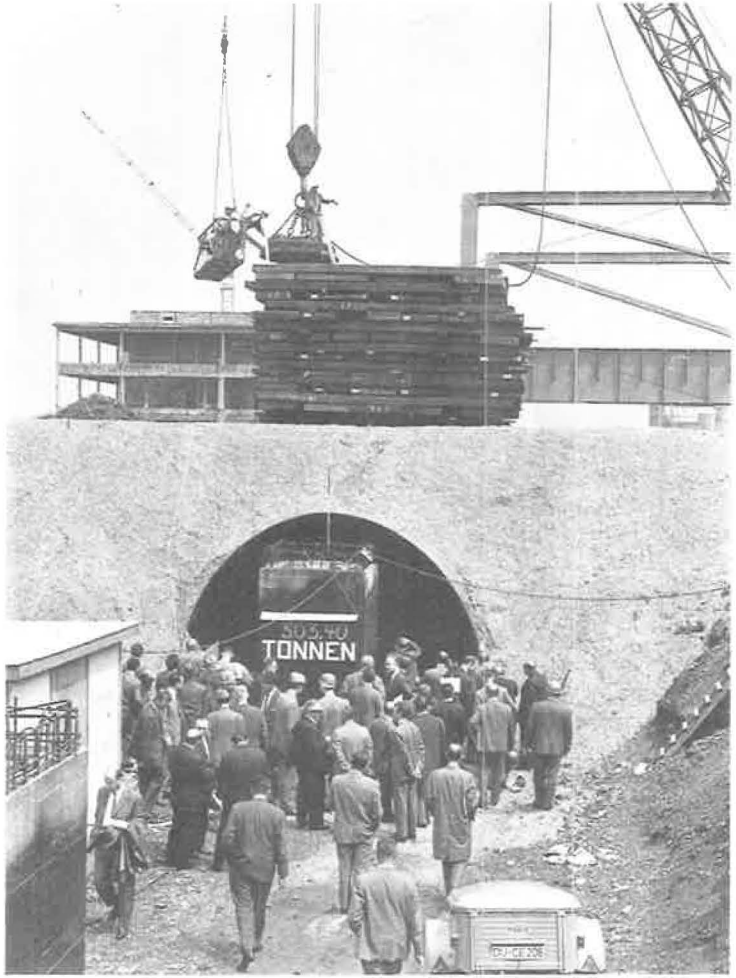

Figure 37. Loading-to-failure test, application of load by magnetic crane.

Figure 38. Loading-to-failure test with P = 1,000 tons.

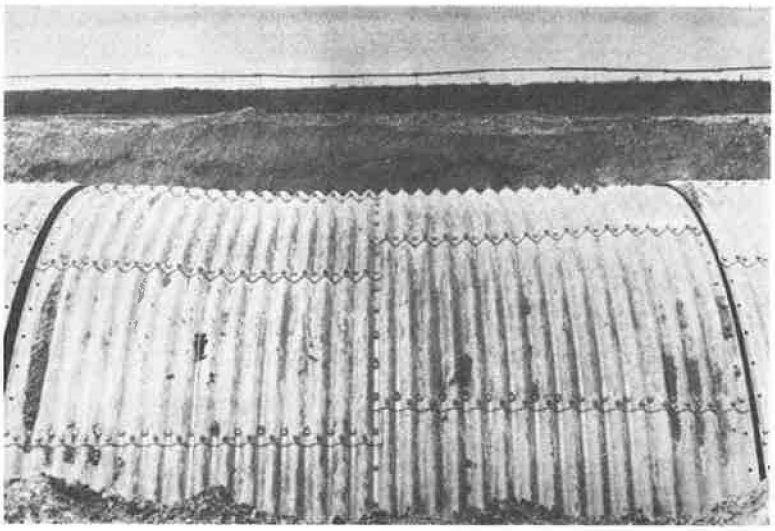

Figure 39. Test structure uncovered after maximum loading of p_{max} = 1,079.77 tons.

Figure 40. Plastic deformations apparent in uncovered structure.

Loading-to-failure test
applied load P = 175.85 t
readings 24-27

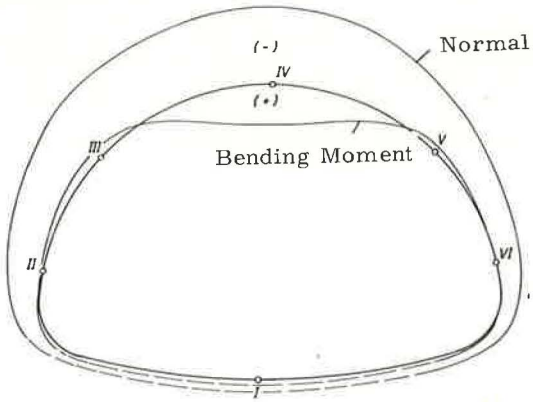

— development from measured values

--- assumed development

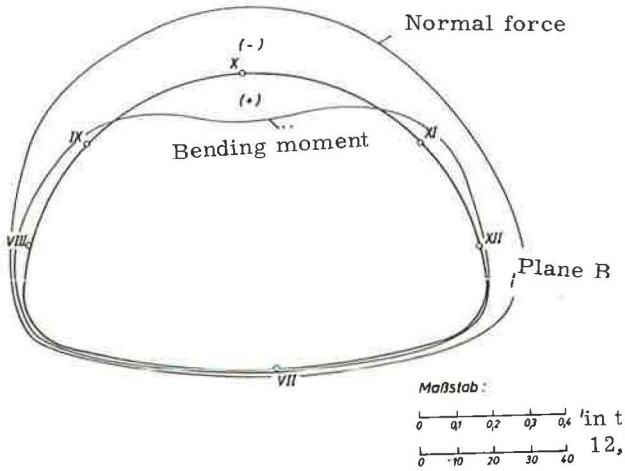

Figure 41. Development of normal forces and bending moments from readings taken.

deflections during placement of fill and new cover up to a height of 5.5 ft above center. Figures 25, 28, 29 and 30 represent the newly introduced deformations for the various load increments. As for the live-load test, these readings do not include the deflections resulting from backfilling. The actual total of deflections from the beginning of backfill placement becomes evident when superposing these deflection figures on Figure 24.

Results of Soil Pressure Measurements

Soil pressures were measured at three gage points on a plane 4 in. above the crest. One of the gage points was located in the load center directly above the pipe-arch crest,

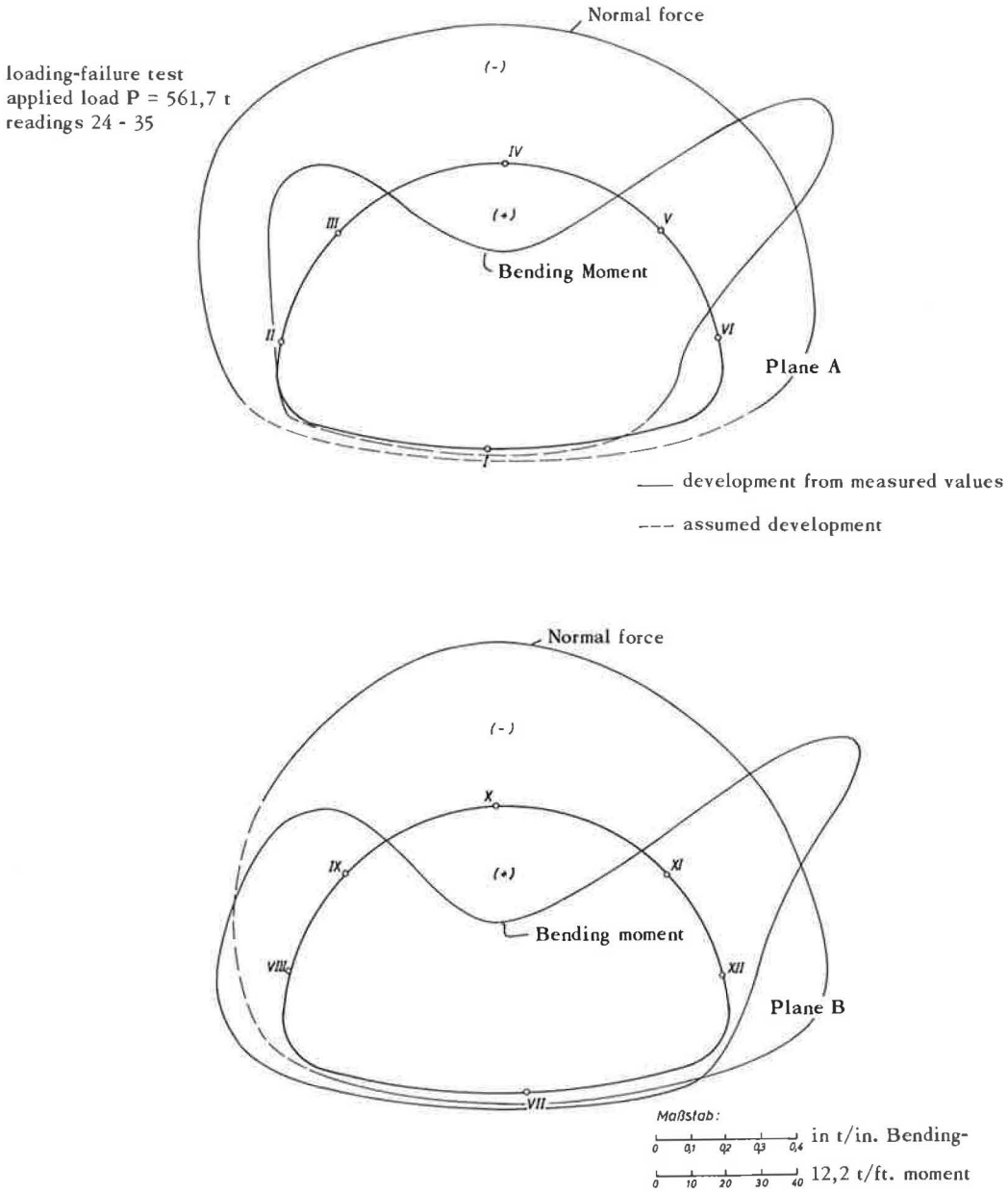

Figure 42. Development of normal forces and bending moments from reading.

and the others at a distance of 6.56 ft on either side of the center. Soil pressure readings are shown in Table 1 and have also been represented in a graph for further clarity. The pattern of soil pressures at the outer gage points, which shows higher values sometimes on the right and sometimes on the left sides, resulted from different loading according to the measured soil pressure. As soon as readings at one of the outer gage points showed higher values, more load was applied on the other side to prevent inclination of the slab pile. Values shown are metric measures.

Computation of Average Distribution of Soil Pressures. —The soil pressure distribution is assumed linear along the height h = 4.82 ft. From the determined values p_o and p_u the pressure distribution is given by:

TABLE 1

SOIL PRESSURE

Applied Load (t)	Soil Pressure (kg/sq cm)		
	Point 1	Point 2	Point 3
1.57 m[a]	0.32	0.41	0.25
52.66 = P	0.45	0.73	0.49
118.41 = P	0.65	0.97	0.63
175.85 = P	0.81	1.15	0.78
260.52 = P	1.15	1.36	1.07
260.52 = P[b]	1.24	1.29	1.17
294.60 = P	1.36	1.39	1.27
321.98 = P	1.48	1.45	1.37
355.48 = P	1.68	1.54	1.46
410.50 = P	1.92	1.68	1.76
410.50 = P[c]	1.97	1.64	1.85
410.50 = P[d]	1.98	1.63	1.95
444.80 = P	2.12	1.75	2.05
503.40 = P	2.31	1.98	2.24
527.40 = P	2.45	2.07	2.39
561.70 = P	2.67	2.23	2.05
633.84 = P	2.10	2.73	2.80
689.54 = P	1.40	3.32	2.90
720.34 = P	1.23	3.68	3.00
770.48 = P	1.48	4.17	2.64
809.30 = P	1.75	4.41	3.37
846.24 = P	2.15	4.68	3.83
875.44 = P	2.55	4.80	4.07
898.60 = P	2.83	4.98	4.00
929.76 = P	3.80	5.24	2.34
953.47 = P	5.52	5.58	2.64
953.47 = P[e]	6.97	5.58	3.63
1000.75 = P	7.59	5.88	3.88
1055.59 = P	8.63	5.88	4.77
1079.77 = P	9.29	5.92	5.34

[a] Cover height.
[b] After 13 hr.
[c] After 4.5 hr.
[d] After 15.5 hr.
[e] After 14 hr.

$$p_o = \frac{P}{F}$$

where

P = applied load,
F = loaded area 8.53 × 10.33 = 88.11 sq ft, and
p_u = measured value.

CONCLUSIONS

The test described in this report conducted on an Armco-Thyssen multi-plate pipe-arch conduit of 20-ft 7-in. span, 13-ft 2-in. rise and 7-gage wall thickness, showed the following results:

1. With a cover height of one-sixth the span = 3.44 ft and a loaded area 8.53 ft wide and 10.33 ft long = 88.11 sq ft, the pipe-arch-soil structure proved capable of carrying a load of P = 151.32 tons applied both axially and off-center showing but slight deformation (0.386 in. = 1/640 of span).

2. With a cover height of one-fourth the span and the same axial loaded area a load of 953.75 tons was applied and, with an enlarged loaded area of approximately 16.4 × 9.84 = 161.4 sq ft resulting from settlement, a load of 1,079.77 tons could be reached in this test without the pipe arch being crushed.

A comparison with the ring compression method may seem of interest in this connection. As is known, the determination of load-carrying capacity by this theory is based alone on compression in the ring and the seam strengths, as derived from actual test data on bolted seams. For 7-gage multi-plate and 4 bolts/ft the seam strength is 93,000 lb/ft (see Armco Catalog MP-1663). The maximum load is determined as follows:

Table 2 shows the determination of average pressure distribution at the outer and centrally located pressure cells. The pressure drop at the outer cells was 68 percent, that at the center cell 66 percent, the average being

$$\frac{68 + 66 + 68}{3} = 67.33\ \%.$$

On the basis of this load distribution, the loaded area above the pipe-arch crest may be determined.

TABLE 2

COMPUTATION OF AVERAGE PRESSURE DISTRIBUTION

P (to)	p_0 (kp/sq cm)	p_{u1} (kp/sq cm)	p_{u2} (kp/sq cm)	p_{u3} (kp/sq cm)	$p_{ur} = (p_1 + p_3)/2$	$\Delta p_{outer} = p_0 - p_{ur}$	$\Delta p_{center} = p_0 - p_{u2}$	$\frac{\Delta p_{outer}}{p_0}$	$\frac{\Delta p_{center}}{p_0}$
175.85	21.5	5.1	7.4	5.3	5.2	16.3	14.1	0.75	0.65
294.0	35.9	10.4	9.8	10.3	10.3	25.7	26.1	0.71	0.73
410.5	50.0	16.0	12.7	15.1	15.5	34.5	37.3	0.69	0.75
503.0	61.5	20.0	15.7	19.9	20.0	41.5	45.8	0.67	0.75
633.8	77.5	18.0	23.2	25.5	21.8	55.7	54.3	0.72	0.70
720.0	88.0	9.1	32.7	27.5	18.3	69.7	55.3	0.79	0.62
809.0	99.0	14.3	40.0	31.2	42.7	56.3	59.0	0.56	0.59
929.8	113.0	34.8	48.3	20.9	27.8	85.2	65.0	0.75	0.58
1055.0	129.0	83.1	54.7	45.2	64.2	64.8	74.0	0.50	0.57
Average value								0.68	0.66

$$F_1 = 10.33 \times 8.53 = 88.11 \text{ sq ft}$$

$$F_2 = \frac{F_1}{1 - 0.6733} = \frac{88.11}{0.3267} = 269.70 \text{ sq ft.}$$

Furthermore,

$$F_2 = (8.53 + 2x) \times (10.33 + 2x) = 269.70 \text{ sq ft}$$

following

$$x = 3.51 \text{ ft at } 4.82\text{-ft depth.}$$

At crest level or 5.15 ft below surface,

$$x' = \frac{3.51}{4.82} \times 5.15 = 3.75 \text{ ft.}$$

The total loaded length of the structure is

$$L = 8.53 + (2 \times 3.75) = 16.03 \text{ ft.}$$

This shows that the test structure of 16-ft length is completely within the loaded area.

According to the seam strength chart, the maximum load the structure can carry will be 1,273 tons (metric tons), derived as follows:

$p_{max} = 93,000 \times 16 \times 2 \times 2,976,000$ lb; less dead load of $20.56 \times 16 \times 5.15 \times 100 =$ 169,414 lb — leaving for the imposed load, 2,806,586 lb, or 1,273 metric tons.

With 1,079-ton loading, this ultimate load was nearly reached in the test. The safety factor of 4 recommended for the determination of wall thickness by the ring compression method is thus fully insured for the safety of the structure against collapse.

When 850 tons had been imposed, the first signs of overloading appeared. Should

TABLE 3

AVERAGE VALUES FROM TENSION TEST

Wall Thickness	Test Taken from	Yield Stress °F (lb/in.)	Tensile Stress °B (lb/in.)	Elongation (%)
1 gage	Crest	54,447	61,302	17.5
	Flank	44,694	53,252	29.5
5 gage	Crest	52,228	58,443	23.5
	Flank	47,221	55,115	35.6
7 gage	Crest	55,442	64,360	21.4
	Flank	45,870	58,600	29.7
8 gage	Crest	51,460	58,785	22.2
	Flank	49,639	61,018	30.0

ARMCO MULTI-PLATE PROFIL NR. S 32

FOR COUNTRYSIDE ROADS
STANDARD CLEARANCE PROFILE
WIDTH OF CARRIAGEWAY = 16'5"

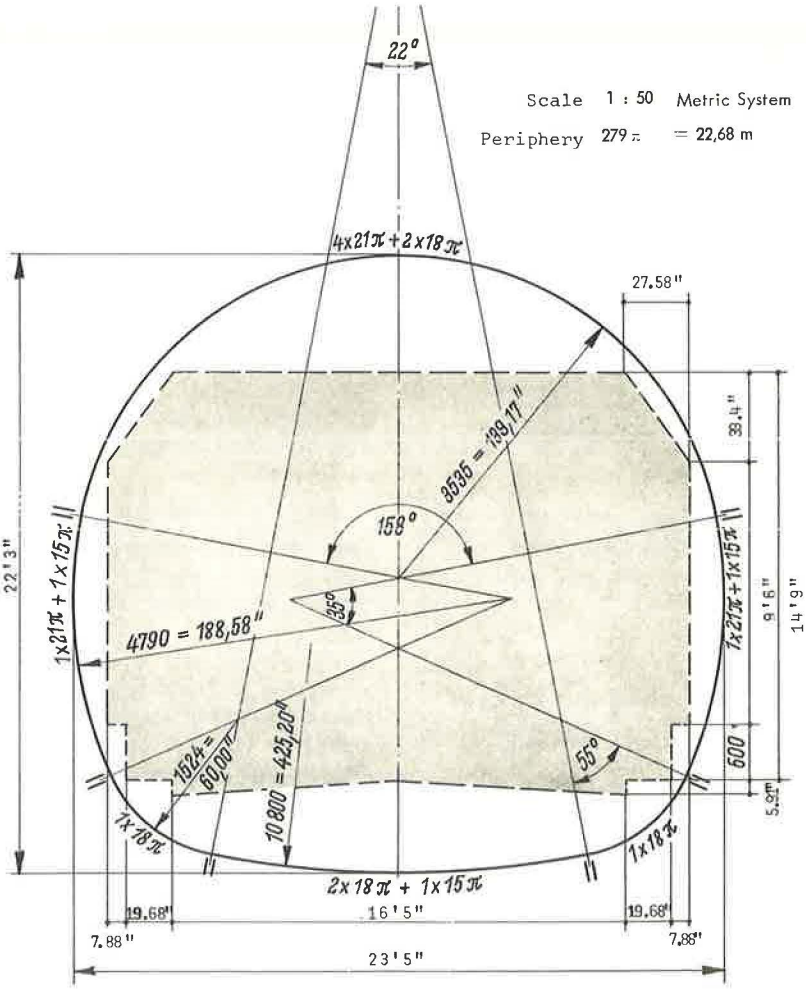

Figure 43.

Figure 44. Special profile S 32 during construction.

these be eliminated, this would leave an actual safety factor of SF = 4 - 1,273/850 = 4 - 1.5 = 2.5. Thus the loading-to-failure test proved again that the ring compression method is well suited for designing corrugated steel pipe.

In consequence of this test result, a 213-ft long king-size multi-plate pipe arch of 23.42-ft span, 22.30-ft rise and 279π circumference could be successfully installed in Germany under the Autobahn between Butzbach and Siegen. This is believed to be Europe's largest corrugated pipe to date (Table 3, Figs. 43, 44).

ACKNOWLEDGMENTS

This test was conducted under the scientific direction of Professor Dr.-Ing. Dr.-Ing. h.c. Kloeppel, Darmstadt Technical University, Germany. This report is based on the test report made by him. The computations and measuring results contained in this paper were taken from that report. All strain measurements and tension tests were conducted by the Institute of Statics and Steel Construction headed by Professor Kloeppel.

Deformation was measured by Dipl.-Ing. E. Jacobs, Essen Engineering College.

Measurements of soil pressures were made by the Weil/Rhein branch of Ernst-Mach Institute.

Tests on backfilling material were made by the Institute of Soil Mechanics headed by Professor Dr.-Ing. H. Breth, Darmstadt Technical University.

Operations were responsibly directed by Armco-Thyssen, Dinslaken.

The test setup was designed in conjunction with the German Federal Railway Authorities.

Appendix

TESTING OF MATERIALS USED

Backfilling Material

Sandy gravel was used as backfilling material for the pipe arch. Its single Proctor density at an optimum moisture content of 6.8 percent was determined to be 120 pcf. The results of the three axial pressure tests indicate a friction angle of 37.5 deg for the sandy gravel at this density.

During backfilling the compactness obtained at the 7 points was determined by the calibrated sand method. This showed an average dry density of 128 pcf, which means that by compaction of fill in 8-in. lifts with Losenhausen AT 200 surface vibrators, a compactness of 107 percent of the single Proctor density was obtained. The results of the drop-penetration test with 70 to 90 blows for 8 in. of penetration depth also indicate the good compaction of the fill.

Tension Tests on Conduit

Test Specimen. —Corrugated multi-plate sheet of different gages as per the company's delivery program, but not curved vertical to the direction of corrugations.

Material. —MU St 34-2 steel plate, cold worked by pressing the rolled shape and hot-dip galvanized consequently.

Tension Test. —Six proportional test bars from each specimen, i.e., four from the corrugation crest and two from the flank.

Discussion

M. G. SPANGLER, Research Professor of Civil Engineering, Iowa State University, Ames—This is an excellent paper; a scholarly and well-written report on a well-conceived and conducted full-scale experimental demonstration project in the field of loads and supporting strengths of underground conduits. It is a particularly noteworthy contribution in this field because it chronicles the change in shape of a pipe-arch structure acted upon by vertical loads and lateral earth pressures. Quantitative data are presented which show that the deformation of a pipe arch under vertical load follows the same general pattern as that of a circular flexible conduit; that is, the vertical dimension shortens and the horizontal dimension lengthens, thereby mobilizing the lateral support of the side columns of soil. The writer has always assumed this to be true but this is the first documentation of the facts which he has seen.

The author states that the live-load test was conducted under severest possible conditions as regards the railroads' desires for loading on the structure and considering a safety factor of 3. However, from the standpoint of structural performance of the conduit, it is the writer's opinion that the installation was unusually favorable. It is difficult to imagine an environment for a flexible conduit installation which could be more favorable with respect to deformation of the pipe, the performance characteristic most frequently in evidence when a structure of this kind gets into structural difficulty.

Flexible conduits, particularly those of larger radius, derive their ability to sustain vertical load almost wholly from the restraining influence of the soil backfill at the sides. The more strain-resistant the sidefill soil, the less will be the deflection of the conduit and vice versa. To visualize this fact, imagine a structure of the type and size used in these experiments, installed in such a way that there was no soil in contact with the sides, and therefore no lateral pressures acting on the conduit (Fig. 45). Obviously this imaginary structure could carry only the merest fraction of the vertical load which the actual structure successfully carried.

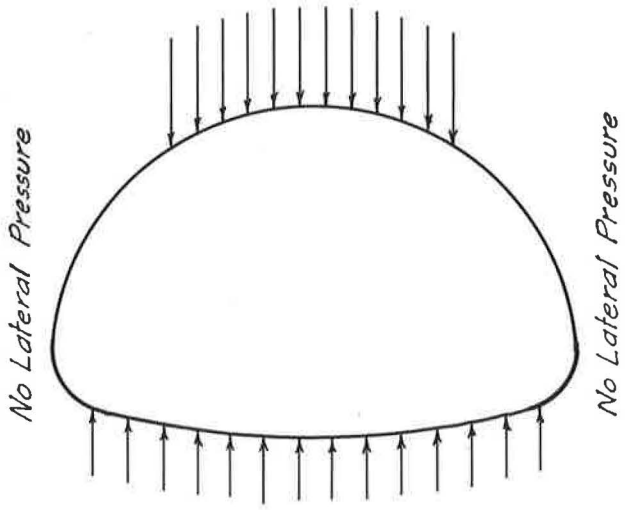

Figure 45. Imaginary pipe arch with no lateral pressure.

Now imagine further that the sidefill soil consisted of a highly compressible low-density material such as a uniform grain-size silt of high moisture content. The deflection of the structure would be nearly as great and its ability to carry vertical load nearly as limited as in the imaginary no-lateral-pressure case illustrated. These imaginary situations are cited to emphasize the fact that the structural performance of a flexible conduit is directly dependent on the strain-resistant quality of the sidefill soil, and there is a tremendous range of soil quality between this very poor imaginary material and the very excellent sandy gravel used in the experiments. The physical properties of the conduit wall—that is, the gage of metal, depth and spacing of corrugations, modulus of elasticity, etc.—are relatively minor contributors to resistance to deformation and ability to carry vertical load. The structural performance of flexible conduits cannot be predetermined without a reasonably precise statement concerning the kind, quality and extent of the side columns of soil which play such an important role in supporting the structure. It is not sufficient to say merely that the sidefill soil should be "of good quality" or "thoroughly compacted" or some similarly vague description.

The quality of soil from the standpoint of its effectiveness in minimizing deformation of flexible conduits can be expressed in terms of the "modulus of soil reaction" (3, 8), whose units are lb/sq in. It is somewhat similar to modulus of elasticity of elastic materials, except that it appears to involve a size-factor. Present knowledge, still very imperfect, indicates the following relationship:

$$E' = er$$

in which

E' = modulus of soil reaction, psi;
r = radius of conduit wall, in.; and
e = modulus of passive resistance of soil, psi/in.

The modulus of passive resistance is a quantitative expression of the relationship between strain of the soil and pressure exerted by a body pushing against it. This modulus is similar to Westergaard's (6) modulus of subgrade reaction, in his analysis of stresses in concrete pavement slabs; and to Cummings' (2) modulus of foundation, in his analysis of the stability of foundation piles against buckling under axial load.

The backfill soil used in Dr. Demmin's experiments was of extremely high quality for the purpose of minimizing deformation of the conduit. It consisted of a sandy gravel

material which was placed in lifts of 8 in. and each layer compacted with surface vibrators. Laboratory and field tests indicated an average dry density of 128 pcf or 107 percent of single Proctor density. The angle of friction was 37.50 deg; a very high-strength material. It is apparent that this backfill material is closely comparable to that placed at the sides of the classical Cullman County, Alabama (5) installation of 84-in. circular metal pipes wherein the pipe deflection was negligible. It is a kind of material which is completely unavailable in many areas, or if available, only at very high cost.

The modulus of reaction of the Cullman soil has been estimated to be in the neighborhood of 7,980 psi (4). In contrast, several installations of circular pipes have been observed in which the estimated modulus of soil reaction was less than 300 psi (4). This illustrates the wide range of sidefill soil restraint which may actually develop depending on the quality of soil and the manner of its placement and compaction. There is also evidence to indicate that even where high quality soil sidefills are provided, they must extend laterally for a considerable distance to be fully effective. A number of situations have developed in which excessive deflection of circular flexible pipes could be attributed to the fact that the side columns or berms of soil were very limited in lateral extent. A rule of thumb in this regard relative to actual field installation is to provide side columns of good quality, well-compacted soil for a distance on each side of the structure equal to at least twice its horizontal dimension.

The wide range of possible values of the modulus of soil reaction encountered in actual flexible conduit construction, accounts very largely for the wide range of performance of these structures with reference to deflection under load. A survey of 239 corrugated steel culverts (4), conducted in 1943 by a leading manufacturer of this type of structure, indicated a range in deflection from -5.0 to +12.1 percent of nominal diameter. Other observers have noted similar results, though on a less extensive scale. This characteristic of structural performance points up the need for research in this area to evaluate and identify the strain-resistant characteristics of soil materials in terms of determinable properties, such as mechanical analysis, Atterberg limits and density. Watkins (9) has contributed a great deal to our knowledge in this area by his work with the Modpares Device, but additional studies of the actual performance of structures in relation to sidefill soil environment are sorely needed. It is suggested that much value would accrue from an extensive detailed record of flexible conduit installations which would include not only the physical details of the conduits, but also facts concerning their installation, such as the character of bedding, and the manner of placement and lateral extent of the sidefills. The soil should be carefully identified in each case and its density determined. Then accurate records of conduit deflections over a period of several years would make it possible to determine empirically an appropriate value of the modulus of soil reaction for a variety of soils within a practical range of densities. The manufacturers of flexible metal pipes and pipe arches would be ideal agencies for collecting such information because of their worldwide contacts with installation of these kinds of structures.

An important phenomenon reported in the paper is the initial deformation of the structure as the sidefill soil berms were built up and compacted. During this stage of construction, the deflection of the pipe arch was opposite in direction to that caused by vertical load in later phases of embankment construction and, in effect, was a "prestressing" operation. The amount of reverse deflection was nominal in this instance and well within that which the structure could tolerate. The relatively low magnitude of this initial reverse deflection is thought to be associated with the very high strain-resistant quality of the sandy gravel sidefills. If the material had been a compacted clayey material, the reverse deflection probably would have been much greater. Instances are known in which it has been necessary to inhibit this initial reverse deflection by the installation of diagonally oriented tie rods inside the structure, or by piling sand bags or loose soil on top as the sidefills were built up, to prevent reverse curvature of the sides of the conduit and "barnroofing" of the top.

These experiments provide information which appears to conflict with the fundamental tenets of Whites' (7) Ring Compression Theory. This theoretical approach begins with the assumption that all loads on a flexible underground conduit act normal to the pipe wall and that the effective load system is similar to hydrostatic pressure acting

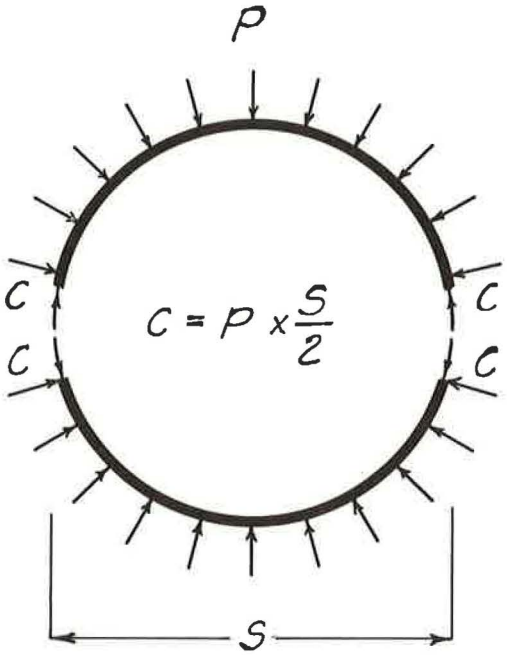

Figure 46. Basic concept of the ring compression theory.

on the outside of a cylindrical vessel. Therefore, it is postulated that the only stresses of consequence in the pipe wall are tangential compressive stresses; hence the name Ring Compression Theory. Figure 46 (1) illustrates this basic concept. Bending moment and deflection of the pipe are completely ignored in the theory.

Dr. Demmin's measurements clearly indicate that there were bending moment stresses of considerable magnitude in the experimental structure. During placement and compaction of the sidefills, the sides of the pipe arch were pushed inward and the top moved upward. This caused prestressing of the pipe wall in tension on the inside face at the sides and bottom, and on the outside face at the top and at the lower corners. At the completion of 3.44 ft of cover, prestressing was reversed to some extent, but there was a residual moment which produced a maximum outer fiber stress in the crown of nearly 40,000 psi. Graphs of the normal force and bending moment at 2 transverse planes through the structure at this load are shown in Figure 5 of the report.

As the live-load slabs were placed at the embankment surface, prestressing was counteracted to the extent that the bending moment became essentially zero at an applied load of 78.62 T, as shown in Figure 13. Then as further load was added up to 151.32 T, the bending moment increased in the opposite sense as shown in Figure 10. These bending moments, like the deflection, were probably much less in this installation than would have been the case if a more usual and less strain-resistant backfill material had been used. That the bending moments keep on increasing as loads are increased is shown by the moment diagrams in Figure 35 which were measured when the applied load was at 689.54 T. The failure to recognize bending moments and deflections and failure to relate these phenomena with the quality of the sidefill soil material constitute serious shortcomings in the Ring Compression Theory, in this writer's opinion.

In reference to the diagrams showing bending moments and normal forces around the periphery of the pipe arch: Values of these functions developed from instrument measurements are shown in solid lines, whereas dashed lines are used to indicate assumed values in regions where the instruments apparently did not yield firm information. It is noted that most of the diagrams shown assumed values in the bottom of the structure between the corners and that these assumed values are consistently relatively low.

This writer has never seen a pipe arch which has developed structural difficulty. However, he has been told by some who have observed such phenomena that there is a tendency for the bottom of the structure to bend upward near the longitudinal centerline, which would seem to indicate a fairly high positive moment in this region. This tendency is in evidence where measured values of bending moment are shown in Figures 5 and 10. However, most of the estimated values of moment are negative in direction and relatively low in magnitude.

Furthermore, the estimated normal forces on the bottom of the arch are very low in magnitude, while the measured values on the top surface are relatively high. Since action must equal reaction it is difficult to accept the estimated values as shown. At least it is suggested that here is a fertile field of needed research to determine more

accurately the actual magnitude and distribution of normal forces on the bottom of an arch and bending moment stresses in this region and in the vicinity of the bottom corners.

There is a great deal of value in demonstration projects such as this, but there are dangers associated with them also. One danger is that readers may not fully realize the favorable aspects of the demonstration and thus gain the impression that all such structures will perform equally satisfactorily. This of course is far from true, as evidenced by the fact that failures of underground conduits do occur. And all too often such failed structures are merely replaced and potential lessons which might be learned are not made available to the engineering profession.

It is this writer's contention that engineers can learn more from one failure situation, if it is thoroughly studied and the causes determined, than can be learned from a dozen or more successful installations. One difficulty in the development of knowledge in this manner is the reluctance of owners and installers of conduits to permit publication of the facts when failures occur. Typical of attitudes in this regard is that of a member of the staff of a certain state highway department. Knowing the writer's interest in underground conduits, he told of a failure of a large-size highway culvert in his state. It had been investigated and a report made to the chief engineer. When asked for a copy of the report, including the photographs which accompanied it, he hesitated, then agreed to send the report, but with the understanding that it be held confidential. He remarked, "We are not very proud of this installation." In another state a series of culverts under an interstate highway got into trouble and the writer was asked to investigate the situation, but before even going on the job, was sworn to secrecy by the chief engineer of the department. There is heartening evidence that this attitude may be changing for the better, but it has been all too prevalent in the past.

Much of our knowledge in engineering practice has resulted from the study of failures of structures and publication of the results. Early in this century the failure of the great Quebec cantilever bridge stimulated research relative to the carrying capacity of latticed steel columns, with the result that column design is now on a much more reliable basis than formerly. Later the failure of the Ft. Peck dam led to tremendous advances in the art of foundation exploration and interpretation of sub-soil materials. Still later, study of the failure of the Tacoma Narrows suspension span resulted in the development of a vast body of knowledge of aerodynamic forces on suspension bridges, and adequate design of this type of structure is much more sure than formerly.

In each of these instances, extensive and detailed studies of the causes of failure were made by teams of experts, and the results of their studies were published so that the whole engineering profession could read and profit thereby. It is this writer's plea that the same type of high-level engineering statesmanship be applied in the culvert industry so that structural distress and failures of this small, but important type of structure may be reduced to a minimum.

References

1. Armco Steel Corporation, Drainage Products Division. Ring Compression Report, 1964.
2. Cummings, A. E. The Stability of Foundation Piles Against Buckling. Proc. Highway Research Board, Vol. 18, Pt. II, pp. 57-65, 1938.
3. Spangler, M. G. The Structural Design of Flexible Pipe Culverts. Iowa Eng. Exper. Sta. Bulletin 153, Iowa State Univ., 1941.
4. Spangler, M. G. Discussion of Structural Considerations and Development of Aluminum Alloy Culvert, by A. H. Koepf. Highway Research Board Bull. 361, pp. 55-64, 1962.
5. Timmers, John H. Load Study of Flexible Pipes Under High Fills. Highway Research Board Bull. 125, pp. 10-11, 1956.
6. Westergaard, H. M. Computation of Stresses in Concrete Roads. Proc. Highway Research Board, Vol. 5, Pt. I, pp. 90-112, 1925.
7. White, H. L., and Layer, J. P. The Corrugated Metal Conduit as a Compression Ring. Proc. Highway Research Board, Vol. 39, pp. 389-397, 1960.

8. Watkins, Reynold K., and Spangler, M. G. Some Characteristics of the Modulus of Passive Resistance of Soil: A Study in Similitude. Proc. Highway Research Board, Vol. 37, pp. 576-583, 1958.
9. Watkins, R. K. Development and Use of the Modpares Device. Proc. ASCE, Vol. 90, PL 1, Jan. 1964.

J. DEMMIN, Closure—The writer is very happy that such a well-known expert on underground conduits as M. G. Spangler was prepared to discuss the paper presented. His comments are sincerely appreciated.

It certainly cannot be stressed too much that the structural performance of flexible pipe to a great extent depends on the quality of the backfill material and the way it has been compacted. It is also very true that from one failure situation one can learn more than from a dozen successful installations. However, systematic examination of the reasons for structural failure will be possible only if preceded by tests that were conducted under known conditions. The test was to contribute to the task of collecting fundamental theoretical data that might help to indentify the causes for structural failure.

Professor Spangler mentioned in his discussion that the author has never seen a pipe arch which had developed structural failure; this is true. But the author knows more than 2,000 structures installed in Germany which have never caused major troubles so far.

Being an expert of great renown, Professor Spangler will be asked to investigate all structural failure situations, and it may therefore seem understandable that, from this point of view, the ability of the test pipe to sustain vertical loads should have been qualified. In the meantime, however, the results of this experiment have been substantiated in the field, and it has become evident that structures will not collapse if installed under similar conditions as was the test pipe. These conditions normally are to be met quite easily.

Professor Spangler has indicated that the backfill soil was of extremely high quality and that everything had been done thereby to minimize deformation. It is a fact that the backfill material was selected by the Federal German Railways, and compacted in lifts with commercial vibrators, as is recommended by our company in our installation instructions. For the test, a sandy gravel was used which had been taken from a gravel pit without further processing. This material, naturally, will not be available on every jobsite at an economically justifiable price. In case material of poorer quality is used, greater deformation will develop, and the carrying capacity would be reduced accordingly. As may be recalled, however, the test showed that a twentyfold load could be applied when using good quality soil. There is ample reserve, therefore, to warrant sufficient safety even where poorer quality backfill soil is used. By this, the writer acknowledges that the quality of backfill soil must be regarded as a factor when predetermining the carrying capacity of flexible pipe. To express this quality in terms of determinable factors, it will be necessary to know the "modulus of soil reaction." This modulus of soil reaction, together with an examination of the stability of a pipe section, should provide reliable information on its structural performance. In Germany, Professor Kloeppel is conducting research work in this field.

White's Ring Compression Theory has never claimed to be a scientific basis of structural performance, and therefore a comparison between the ring compression theory and the measured bending moments does not seem appropriate. However, the ring compression theory at present provides the best approximation to the actual structural performance of flexible pipe. This is evidenced by the fact that hundreds of structures designed by this method are operating quite satisfactorily. As shown in the paper, the author calculated a maximum load of 1,273 tons for the test structure on the basis of the ring compression formula disregarding bending moments. The fact that the test had to be stopped at 1,079 tons without complete failure, shows that the ring compression formula gives astoundingly good approximations for determining load capacity.

It is certainly just appropriate to ascribe too much value to the measured bending moments, since the bending moment stresses already developing during assembly and prior to backfilling are so high that they could cause the steel to yield. It must also be expected, that as the sidefill berms are built up to the crest, bending moment stresses might develop in other places, which might approach the yield point of the steel. From a conventional point of view, therefore, the pipe has been "overloaded" several times even before the top cover is placed. Despite this, we know that these bending moments have not much influence on the ability of a flexible structure to carry loads. This fact will justify, disregarding the bending moments, as is the case in the ring compression theory.

Even if the assumed values of bending moments and normal forces developed on the bottom of the pipe are not based on strain gage readings, they were estimated with good reliability on the basis of deformation on the pipe invert. Unfortunately, the strain gages installed on the bottom of the pipe arch were damaged beyond use. As deformations of the bottom of the pipe arch were very low in magnitude, the corresponding bending moment would likewise be very low. The possibility of an inaccurate estimate, as indicated by Spangler, would therefore seem unlikely. Further, it was stated that the small normal forces acting in the bottom area of the pipe arch, did not conform to the relatively high values in the top of the structure. In the writer's opinion, this fact may be explained by the great frictional forces acting around the pipe periphery, which would bring about an equilibrium.

Finally, the writer would like to stress that this one large-scale experiment will naturally not answer all the questions pertaining to the determination of the load-carrying capacity of flexible pipe. Convincing evidence was provided, however, that when using good quality backfill soil which was carefully compacted, a large pipe arch was capable of carrying twenty times the load desired by the railroad authorities. This provides for a sufficient safety margin even in cases where lower quality soils are used.